

Monolithic Colliding Pulse Mode-Locked Quantum Well Lasers

by

Joaquim Ferreira Martins Filho

A Thesis submitted to the Faculty of Engineering,
Department of Electronics and Electrical Engineering
of the University of Glasgow for the degree of
Doctor of Philosophy

June 1995

© Joaquim Ferreira Martins-Filho, 1995.

ProQuest Number: 13818452

All rights reserved

INFORMATION TO ALL USERS

The quality of this reproduction is dependent upon the quality of the copy submitted.

In the unlikely event that the author did not send a complete manuscript and there are missing pages, these will be noted. Also, if material had to be removed, a note will indicate the deletion.



ProQuest 13818452

Published by ProQuest LLC (2018). Copyright of the Dissertation is held by the Author.

All rights reserved.

This work is protected against unauthorized copying under Title 17, United States Code
Microform Edition © ProQuest LLC.

ProQuest LLC.
789 East Eisenhower Parkway
P.O. Box 1346
Ann Arbor, MI 48106 – 1346

Theris
10181
Copy 1

GLASGOW
UNIVERSITY
LIBRARY

Acknowledgements

The following people and organisations were essential to the realisation of this project.

The CNPq, Conselho Nacional de Desenvolvimento Científico e Tecnológico (Brazilian Research Council), is gratefully acknowledged for the financial support.

The University of Glasgow is acknowledged for providing excellent facilities to develop the project in the Department of Electronics and Electrical Engineering, as well as for the refreshing and stress releasing exercise sections in the Stevenson Building, and the helpful English language classes in the Hetherington Building.

I thank the members of the academic, technical and administrative staff, as well as research students of the Department of Electronics and Electrical Engineering of the University of Glasgow who contributed directly or indirectly to the completion of this project. Special thanks to my supervisor Charles Ironside and to Efim Portnoi, Eugene Avrutin, Stewart M^cDougall, Richard De La Rue, Kadhair Al-Hemyari, Stephen Ayling and Vitor Moreira for the encouragement, help, guidance and hours of useful discussions.

I also thank John Roberts from the SERC III-V Semiconductor Growth Facility at Sheffield University for supplying excellent material.

I would like to thank all my friends in Glasgow and at home, in Brazil, for their company, help, understanding and support. In special to Carol, Janine, David and Paul Barnett, Larissa Chermont, Justine Cosgrove, Andre and Ana Santos, Vitor Moreira, Cheryl Campbell, Hermano and Rose Moura, Adela Saavedra, Bartolomeu Uchoa Filho, Catarina Gomes, Ian Penny, Øyvind Gillingsrud and the whole of the Brazilian community in Glasgow, for their complicity at relaxing and memorable moments at parties, nights out, ceilidhs, trips, football games (specially the World Cup), dinners, lunch breaks at the refectory of the Western Infirmary, talks through the e-mail system, and etc.

And finally, my relatives, my brothers and my parents for their invaluable moral support.

Abstract

The design, fabrication and characterisation of monolithic passive colliding pulse mode-locked (CPM) quantum well lasers are described. Firstly, a standard configuration of CPM laser is realised and mode-locking is obtained at repetition rates in the range of 73 to 129 GHz. These are the first published results on monolithic CPM quantum well laser at short wavelength, i. e. GaAs/AlGaAs based material. This device presented a previously unseen output laser polarisation dependence with the applied reverse bias to the absorber section of this laser. The generation of TE and TM polarised light from the CPM laser is analysed and discussed.

A novel configuration of CPM laser, the multiple colliding-pulse mode-locked (MCPM) laser is realised. This multi-section device can have 1, 2, or 3 monolithically integrated saturable absorber sections in the cavity, inducing the laser to operate at the first up to the fourth harmonic of the repetition rate. This is the first observation of geometry dependent switchable change of harmonics in mode-locked lasers. The different regimes of operation of the MCPM laser are investigated, comprising single mode, multimode, Q-switched and first to fourth harmonic mode-locking, generating pulses of around 1 to 3 ps width at up to 375 GHz repetition rate. Studies of the range of mode-locking at 240 GHz show that mode-locking occurs at two distinct regions of current and reverse bias. This previously unseen feature may represent an indication of the contribution of excitonic nonlinearities to the ultra-fast operation of the device.

A monolithic CPM ring laser with two saturable absorbers in the cavity is described. Frequency domain measurements indicate mode-locking operation at 28 GHz repetition rate. The use of two saturable absorbers in colliding pulse configuration in the ring cavity showed improvements on the device operation.

The design and fabrication of a CPM laser based device which is intended to perform clock recovery at high repetition rates, above 100 GHz, is described. This device consists of a standard CPM laser which has an extra waveguide in side-injection configuration. This extra waveguide amplifies and guides the optical signal from which the clock is to be recovered to the absorber section of the laser. To achieve clock recovery this signal should contribute to the saturation of the absorber section of the CPM laser, synchronising its saturation with the injected data signal. Preliminary characterisation and tests showed that the CPM laser part of the device works as a standard CPM laser, as expected.

Table of Contents

Chapter 1: Introduction	1
1.1. - Quantum Well Lasers	2
1.2 - Short Pulse Generation in Semiconductor Lasers	6
1.3 - Applications	9
1.4 - Outline of the Thesis	10
1.5 - References to Chapter 1	11
Chapter 2: Review of Mode-Locked Semiconductor Lasers	14
2.1. - Simple Description of Mode-Locking	14
2.2 - Methods and Configurations of Mode-Locking	17
2.3 - Passive Mode-locking	19
2.3.1 - Pulse shortening effect	19
2.3.2 - Conditions for mode-locking	20
2.3.3 - Techniques for producing saturable absorption	21
2.3.4 - Pulse broadening effect	23
2.4 - Colliding Pulse Mode Locking	26
2.5 - Mode-Locking Stabilisation	28
2.6 - Conclusions	29
2.7 - References to Chapter 2	31
Chapter 3: Device Fabrication	36
3.1 - Material Structure and Characterisation	37
3.2 - Waveguide Structure	40
3.3 - Fabrication Technique	41
3.4 - Discussions and Conclusions	47
3.5 - References to Chapter 3	51
Chapter 4: Device Characterisation Techniques	52
4.1 - Mode-Locked Laser Test Set-up	52
4.2 - Linear Cross-Correlator	53
4.3 - Simulations of the Linear Correlator	59
4.4 - Conclusions	66
4.5 - References to Chapter 4	68

Chapter 5: Experimental Results	69
5.1 - GaAs/AlGaAs CPM Quantum Well Lasers	69
5.2 - Multiple Colliding Pulse Mode-Locked Lasers	76
5.3 - Monolithic CPM Ring Lasers	89
5.4 - CPM Bow-tie Lasers	92
5.5 - Clock Recovery Device	96
5.6 - Conclusions	101
5.7 - References to Chapter 5	103
Chapter 6: Summary and Conclusions	109
Appendix 1: General Equations for the Linear Correlator	114
Appendix 2: References	117
A2.1 - Publications and conference contributions arising from this work	117
A2.2 - Alphabetical list of references to the thesis	118
Appendix 3: Journal Publications	129
A3.1 - J. F. Martins-Filho, C. N. Ironside and J. S. Roberts, "Quantum well AlGaAs/GaAs monolithic colliding pulse mode-locked laser", <i>Electron. Lett.</i> , vol. 29, pp. 1135-1136, June 1993.	129
A3.2 - J. F. Martins-Filho and C. N. Ironside, "Multiple colliding pulse mode-locked operation of a semiconductor laser", <i>Appl. Phys. Lett.</i> , vol. 65, pp. 1894-1896, Oct. 1994.	131
A3.3 - J. F. Martins-Filho, E. A. Avrutin, C. N. Ironside and J. S. Roberts, "Monolithic multiple colliding pulse mode-locked quantum well lasers: experiment and theory", <i>IEEE Journal of Selected Topics in Quantum Electronics</i> , vol. 1, no. 2, pp. 539-551, Special Issue on semiconductor lasers, June 1995.	134

Chapter 1: Introduction

Research and development on new materials and material processing for electronics and optics, along with the understanding of the physical processes related to these materials in the past 50 years are leading mankind into the information age. Discrete electronic devices firstly, and then electronic integrated circuits (microelectronics) have transformed the world, changing the concepts of communication, work and life that had persisted almost intact for centuries. The ever increasing demand for these transformations are pushing electronic devices and systems to their limits, in terms of speed and functionality. However, associated to electronics, the development of semiconductor lasers and optical fibres as compact, high performance and low cost means of optical signal generation and transmission boosted the development of optoelectronics in general. This combination of the already developed electronics with the large bandwidth (high speed) and parallelism (high interconnectivity) of optics is capable of changing the limits of the systems, setting a much higher standard for their services. And as in the evolution of electronics, the development of optoelectronic integrated circuits (OEICs) and photonic (all-optical) integrated circuits (PIC) is expected to trigger a new technological revolution. This "microoptoelectronics" will launch us all deep into the information age, when machines will have much higher levels of functionality, as well as much higher levels of machine-machine and machine-man interactivity.

Within the context of the development of microoptoelectronics for the information age, this thesis is concerned with the design, fabrication and characterisation of high speed optoelectronic devices, namely monolithic passive colliding pulse mode-locked quantum well lasers for high speed short pulse generation. As an introduction to the thesis this first chapter presents a general outlook of quantum well lasers, short optical pulse generation and their applications. Section 1.1 gives an introduction to quantum well structures and quantum well lasers, which are key elements for the realisation of OEICs. Section 1.2 presents an overview of the field of short pulse generation in semiconductor lasers. Section 1.3 discusses a set of device and system applications of high speed short pulses generated by semiconductor lasers. Section 1.4 gives the outline of the rest of the thesis. The references to this chapter are listed in order of appearance in section 1.5.

1.1. - Quantum Well Lasers

This section is not intended to fully cover such a vast topic as quantum well structures and lasers, which can be treated at many different levels of complexity. Therefore, only a short overview of the most important aspects of semiconductor quantum sized structures relevant to quantum well lasers will be mentioned here. Useful review papers on quantum well structures and devices were published by L. Esaki [1] and H. Okamoto [2]. Relevant text books on these subjects are found in references 3 to 6, and the most comprehensive and up-dated publication on the field is the book on quantum well lasers edited by P. S. Zory Jr. [7].

A quantum well structure consists of one or more very thin layers of a relatively narrow bandgap semiconductor interleaved with layers of a wider bandgap semiconductor. For example, GaAs for the narrow and AlGaAs for the wider bandgap semiconductor. If these layers are thinner than the electron mean free path, the system enters into a quantum regime, in a manner analogous to the well-known quantum mechanical problem of the "particle in a box". The carriers (electrons and holes) are confined to the narrow bandgap "well" by larger bandgap "barrier" layers. For infinitely high barriers the magnitude of the wavefunction of the carriers must approach zero at the barrier wall because the probability of finding the particle within the wall is very small. The set of wavefunctions which satisfies these boundary conditions corresponds to only certain states for the carrier. The carrier motion is thus quantized, with discrete allowed energies corresponding to the different wavefunctions.

Due to the quantization of the wavefunctions in one direction (z direction, the growth direction of the epitaxial layer) in the well layer, the energy dependence of the density-of-states for electrons and holes changes to a staircase form. Figure 1.1 shows a quantum well energy bandgap structure with the quantized energy levels and the corresponding density-of-states $\rho(E)$ for quantum well and bulk materials. In bulk crystals, where the layers thickness is larger than the carrier mean free path, the density-of-states is always parabolic and it is equal to zero at the minimum energy (i. e. at the band edge). In contrast, the staircase form of $\rho(E)$ in quantum well structures has a finite non-zero value of density-of-states even at the minimum energy. Furthermore, the form of the staircase can be tailored by changing the layers' thickness of the structure, which changes the energy of the confined states.

For most practical purposes, quantum size effects are negligible for layers thicker than 20 nm. Therefore, the realisation of quantum well structures followed the advancement of crystal growth technology by molecular beam epitaxy (MBE) and metal-organic chemical vapour deposition (MOCVD), since the liquid phase epitaxy (LPE) technology usually used for bulk material growth could not grow such thin layers.

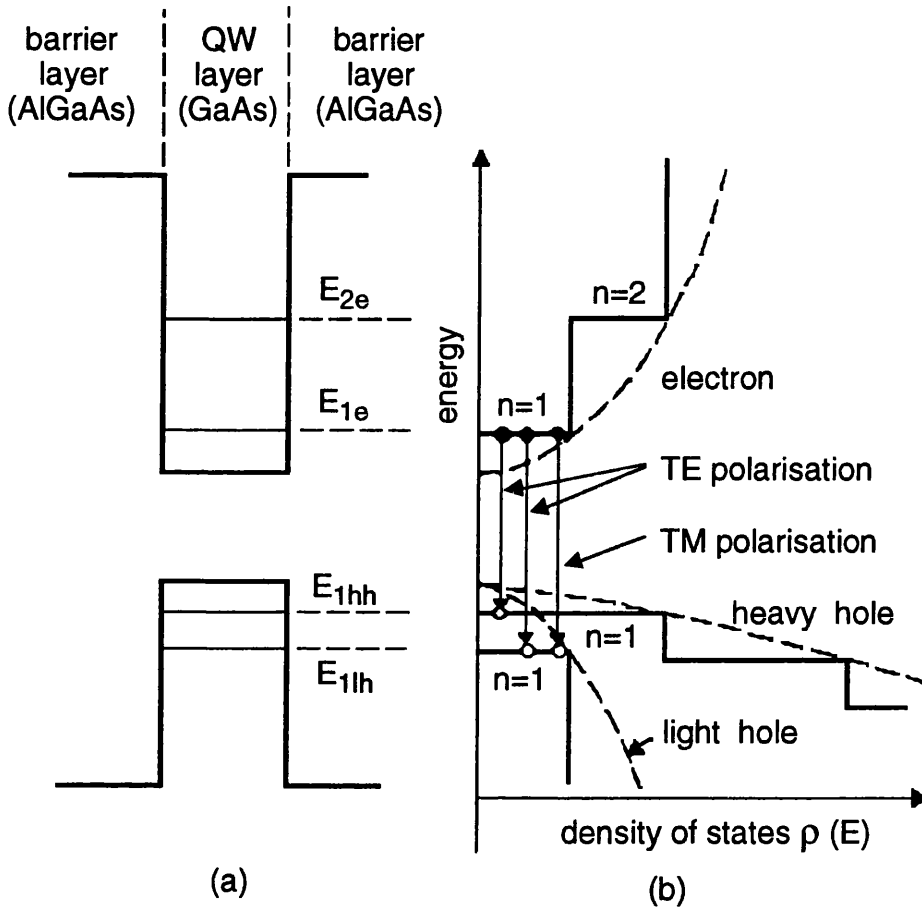


Figure 1.1: (a) Band structure for conduction and valence band with the quantum energy levels in a quantum well. E_{1e} and E_{2e} are $n=1$ and $n=2$ electron levels, and E_{1hh} and E_{1lh} are $n=1$ heavy-hole and $n=1$ light-hole levels, respectively. (b) Density of states as a function of energy for a QW structure (solid line) and for a bulk crystal (broken line) [2].

Another remarkable feature of quantum well structures is the observation of room-temperature excitons. From three dimensional (bulk) semiconductor physics it is known that the absorption spectrum is not simply determined by the creation of a free electron and a free hole. The carriers are correlated in their motion in a way that can be described as the simple Coulomb attraction of the electron and the hole. They orbit around each other as in a hydrogen atom, with the hole acting as the proton. As in the case of the hydrogen atom, this attraction leads to bound levels, the lowest of which is one effective Rydberg below the continuum level and in which the electron and the hole are bound to each other within an effective Bohr radius. Normally, excitons have such a short lifetime that their effects can only be observed at cryogenic temperatures. In quantum wells, however, the confinement of carrier motion in wells whose thickness is smaller than the excitonic Bohr diameter (28 nm in GaAs) leads to an increase of the

coulombic binding force, and consequently excitonic states become stable at room temperature [2, 5, 6]. Excitons are not important for laser action since they are screened by the high level of carrier injection in the laser material. However, excitons play a crucial role in absorption based devices such as modulators and saturable absorbers, through the quantum confined Stark effect and nonlinear effects of saturation and recovery, as will be further discussed in the subsequent chapters.

A quantum well (QW) laser diode is a double heterostructure (DH) laser whose active layer is so thin that quantum size effects are present. The use of a very thin active layer has several consequences to the laser operation [5, 6]. Firstly, the photon generation occurs through carrier transitions between confined states in the conduction band and valence band. Therefore, lasing will occur at energies determined mainly by the bandgap of the material and the confining energies of the QW states.

Due to the staircase density-of-states of quantum wells, the bottom of the conduction band and top of valence band have a finite density-of-states, whereas in DH the density-of-states is zero at minimum energy. It implies that in DH lasers the gain has to build up from carriers filling up the low density of states levels before it reaches high gain (high density-of-state) and the carriers at energies below that high gain level are useless. In QW lasers carriers contribute to gain at its peak. This contributes to a lower transparency current density and to higher differential gain (gain per injected carrier) of QW lasers. However, the price paid is that gain will saturate at a given value when the electron and hole states of a given quantized energy level are fully inverted, whereas the gain in DH hardly saturates due to the filling of an ever increasing density of states. Nevertheless, the problem of low gain saturation can be overcome by the use of several wells, rather than only one, separated by barriers, which is known as a multiple quantum well (MQW) structure. Quite obviously, MQW lasers have larger transparency current densities than single quantum well (SQW) lasers, but they offer higher differential gain and higher gain saturation. Therefore MQW lasers are more suitable for high loss cavities.

In semiconductors, narrow bandgap materials have larger refractive index, therefore a DH provides both optical and carrier confinement around the guiding/active layer. The thin active layer improves carrier confinement by concentrating the carriers in a smaller volume and population inversion is more easily reached, but, on the other hand, it reduces optical confinement of the lasing mode to the active region since the layer is too thin to work as a guiding layer for the optical mode. To overcome this problem an extra guiding layer is introduced in the structure, in the so called separate confinement heterostructure (SCH), or graded-index-SCH (GRIN-SCH) [6]. In chapter 3 a SCH-MQW laser structure is described in details and the expressions for lasing efficiency and threshold current density are given.

In summary, the advantages of QW lasers over the conventional DH lasers are shortly listed below [2, 5, 6].

- *Lower threshold current density.* It is normally lower by a factor of 3. As described above, this is due to the staircase density of states of QW lasers, which leads to a lower transparency current, higher differential gain and narrower bandwidth of the optical gain as compared with DH lasers.

- *Threshold current density less temperature sensitive.* QW lasers have larger temperature coefficient T_0 than DH lasers. GaAs QW lasers typically have T_0 in the range of 170 to 250 K.

- *Polarisation dependent optical gain, which makes the laser oscillate in the TE mode.* In QW structures, a TE polarised optical wave whose electric vector lies in the plane of the QW layers can couple with both the electron heavy-hole transition and the electron light-hole transition. The TM polarised optical wave whose electric vector is perpendicular to the plane of QW layer, on the other hand, can only couple with the latter transition (see figure 1.1). Since the density of states of the heavy-hole state is approximately 3 times larger than the light-hole one, the gain and consequently the laser emission from QW lasers is highly TE polarised. In bulk material the heavy and light hole states are degenerate, therefore the DH laser gain is less polarisation selective.

- *Higher direct modulation frequency.* It may exceed 30 GHz, which is higher by a factor of 3 as compared with DH lasers. This higher modulation speed comes from the higher differential gain of QW lasers, and specially with MQW lasers, as discussed before.

- *Higher stability in oscillation wavelength.* A QW laser has a narrower optical gain spectrum width due to the stair density of states than DH lasers, so that they oscillate more easily in a single longitudinal mode (single mode emission).

- *Reduced chirping.* Chirp is a temporal sweep of the lasing wavelength across the laser pulse, resulting from change of the refractive index due to modulation of the carrier density. This effect is reduced by a factor of 3 in QW lasers as compared with DH lasers due to the higher differential gain of QW lasers.

- *Higher reliability.* Reliability problems in semiconductor lasers come from catastrophic failure due to facet degradation and damage induced by high optical field and recombination at the facet, and gradual degradation due to dark line defects. The thin active material compared with the thick optical cavity in QW lasers reduces the effects that cause catastrophic failure and gradual degradation, improving the device reliability.

- *Easier monolithic integration.* Quantum well structures are more suitable for applications in optoelectronic integrated circuits (OEIC) than bulk semiconductors. Due to their steeper absorption edge, QWs can form lower loss passive waveguides for

integration of a laser and an optical modulator for example, making use of the electric field effect on the excitons which improves the modulation characteristics. Monolithic integration of QW lasers with photodetectors, amplifiers, modulators, switches and transistors has been realised [5, 8]. The monolithic integration of laser and saturable absorber to form a mode-locked laser will be discussed in the subsequent chapters. Also, QW structures can be intermixed by compositional disordering, which changes their bandgap and refractive index. This technique can be very useful for the realisation of very low loss passive waveguide for OEIC, monolithic extended cavity lasers, low loss optical modulators and the fabrication of quantum wire and quantum dot lasers from QW material [2, 9, 10].

The reason for most of those characteristics is essentially the staircase density of states of quantum well structures, which is the most important feature of these structures.

1.2 - Short Pulse Generation in Semiconductor Lasers

Generation of short optical pulses, in the picosecond to femtosecond range, from semiconductor lasers can be achieved basically by three techniques, namely gain-switching, Q-switching and mode-locking [4, 11-14]. The basic principle of these techniques is to switch or modulate the gain or losses of the laser. The wide gain bandwidth of semiconductor lasers, estimated to be around 15 nm (~THz), would in principle allow the generation of 50 fs pulses at 870 nm.

Gain-switched lasers employ a DC current and a short electrical pulse current sources to pump the laser. The DC current can bias the laser just below or just above lasing threshold, whereas the large amplitude short electrical pulses (of the order of tens to hundreds of picoseconds) switch the gain on and off by modulating the carrier density in the cavity. This large carrier density modulation raises the gain well above lasing threshold, leading to high intensity laser emission, which in its turn, depletes the carrier density below lasing threshold, switching the laser off until the gain recovers and is raised again. Typically, this process can generate pulses of around 10 ps width (a few round trips) at around a few gigahertz repetition rate maximum, although pulses as short as 7 ps at 100 MHz repetition rate have been achieved [15]. Pulse width and repetition rate are ultimately determined by the carrier-photon interaction in the laser and are limited by the relaxation oscillation phenomenon [12]. The relaxation oscillation frequency is given by [4]

$$f_R = \frac{1}{2\pi} \sqrt{\frac{A p_0}{\tau_p}} \quad (1.1)$$

where A is the differential optical gain, p_0 is the photon density and τ_p is the photon lifetime in the laser cavity, given by [4]

$$\tau_p = \frac{1}{v_g \left(\alpha - \frac{1}{L} \ln \sqrt{R_1 R_2} \right)} \quad (1.2)$$

where v_g is the group velocity of light, α is the loss of the cavity, L is the cavity length and R_1 and R_2 are the mirror reflectivities. The relaxation oscillation frequency also limits the speed of direct signal modulation on diode lasers [16]. Higher relaxation oscillation frequency of the laser allows shorter pulse generation at higher repetition rate. From the equations above, one can see that the maximum speed of the laser can be tailored by proper device design like cavity configuration (reducing photon lifetime by using short cavities and anti-reflection coatings), semiconductor material design (increasing the differential gain by using MQW structures for example), and optimisation of the pumping level (to increase the photon density) [12]. Also, reduction of parasitic capacitance and series resistance, which filters the high speed electrical signal, as well as the reduction of carrier transport time across the confinement heterostructure improves the laser speed [12, 16].

The pulse energy of a gain-switched laser is of the order of 4 pJ, giving about 0.3 W peak power for 13 ps pulse width [14]. The laser emits in a broad optical spectrum since many longitudinal modes of the cavity are excited as consequence of the dynamic overshooting of carrier concentration. During the emission of such high power optical pulse the wavelength of each longitudinal mode is shifted (chirp) due to the large variation of carrier concentration and the spectral line of the mode is broadened. It means that gain-switched pulses are highly chirped, i.e. far from being transform-limited pulses [12, 17]. The chirp increases as the optical pulse width decreases and it can be minimised by electrical pulse width optimisation [17].

Q-switching, on the other hand, works by modulation of the loss of the laser cavity. While the laser population inversion is building up, the switch is held off (in high loss state), ensuring a low Q of the cavity and there is no laser emission. As the carrier density in the laser reaches its peak, the cavity is rapidly switched on (low loss state), to high Q condition, and the stored energy is emitted in form of an intense optical pulse [12]. Q-switched lasers usually have two sections, a gain and a loss modulation section. If the loss modulation is provided by external electrical modulation it is called active Q-switching [12, 14]. If the loss modulation is caused by saturable absorption it is called passive or self-Q-switching [12, 18]. The loss modulator or saturable absorber region can be accomplished by reverse biasing a short segment in a split contact laser, for example. The reverse bias red-shifts the semiconductor band edge, introducing loss. In the case of active Q-switching a short electrical pulse is applied to the section, forward biasing it and opening a short time window of low loss in the cavity for the optical pulse being emitted. 15 ps pulses at 1 GHz repetition rate, with 4 pJ pulse energy were obtained with this scheme [14]. In the case of passive Q-switching, the

saturation of the absorber opens the cavity for short pulse emission. The dynamics of saturable absorption for pulse shortening will be described in detail in chapter 2. Generation of pulses as short as 2 ps at 18 GHz repetition rate, with peak power above 10 W (50 pJ pulse energy) have been achieved with passive Q-switched lasers [19].

Due to the nature of their operation, which involves high carrier density modulation and high power pulse generation, Q-switched lasers have similar speed limitations as gain-switched lasers. Pulse width and repetition rate also depend on device geometry (cavity length, gain section to absorber section length ratio), gain current and absorber reverse bias [12, 18, 19]. Therefore, these parameters can be used to tune the pulse width and repetition rate of the laser in a similar way as described for gain-switched lasers. Moreover, Q-switched pulses are also very chirped, which can be highly undesirable for some applications. However, pulse compression techniques can be used to shorten these chirped pulses and obtain short transform limited pulses from them [12].

The mode-locking technique is also based on gain or loss modulation in the cavity, but differently from the previous cases, here this modulation is small and its period must be equal to (or multiples of) the round trip time of the cavity [11-14]. It does not shut the cavity completely to allow the build up of a high gain and the emission of a high energy pulse. In mode-locked lasers the modulation is just enough to synchronise the emission or lock the phases of the several longitudinal modes oscillating in the laser cavity. Constructive and destructive interference of these highly coherent longitudinal modes leads to pulse formation in the cavity. If an external electrical signal provides gain modulation, the laser is actively mode-locked and this can be achieved by applying a fast electrical signal superimposed to the DC bias level of the gain section of the laser. Passively mode-locked lasers can be accomplished by incorporating a saturable absorber in the laser cavity, leading to internal loss modulation of the cavity. Hybrid mode-locking, which is a combination of active and passive scheme, can also be implemented.

Since the repetition rate of mode-locked pulses depends on cavity length (round trip of the cavity), external cavity configurations lead to low repetition rates, typically in the megahertz range, and the short length of monolithic cavities, typically of the order of 500 μm , gives repetition rates of the order of tens to hundreds of gigahertz. Monolithic passive mode-locked lasers can generate subpicosecond pulses at hundreds and even thousands of gigahertz because the pulse-shaping mechanisms are determined by the difference in transient saturation and recovery time constants between the gain and absorber. Therefore, in contrast to gain-switched and Q-switched lasers, it is possible to generate short optical pulses with a repetition rate beyond the relaxation oscillation frequency of the laser [20]. Pulses as short as 0.61 ps at 350 GHz repetition rate have been achieved with a monolithic passive mode-locked laser [20].

Mode-locked pulses are usually low energy, ranging from 0.02 pJ to 1 pJ, giving peak powers within the tens to hundreds of milliwatts range [14]. Furthermore, due to the relatively low carrier density modulation in the laser and the low peak power emitted, the pulses generated by mode-locked lasers are close to the Fourier transform limit, i. e. they have low levels of frequency chirp, if any. A detailed description of the mode-locking technique is given in chapter 2.

In summary, gain-switched and Q-switched lasers generate high energy pulses, at a tuneable repetition rate in the range of hundreds of megahertz up to a few tens of gigahertz. Pulse widths are of the order of 10 ps, however they are highly chirped. Mode-locked lasers generate low energy pulses (it can be about 100 times lower than in Q-switched lasers), at a fixed repetition rate given by the cavity length of the laser (it can be about 100 times higher than the Q-switched ones). Pulse widths in the range of subpicosecond up to tens of picosecond can be achieved, and they are high quality, nearly transform limited. Therefore, the present state of development of short pulse generation in semiconductor lasers indicates that gain and Q-switched lasers are more suitable for high pulse energy and relatively low speed applications, whereas mode-locked semiconductor lasers are ideal for low pulse energy, high pulse quality, high speed applications.

1.3 - Applications

The availability of a small, compact, robust, efficient, low power consuming and low cost source of short optical pulses from semiconductor and specially quantum well lasers opens a wide range of applications for these devices, which can be divided into three main categories, namely telecommunications, optical computing, and optoelectronic measurements.

Telecommunication is the most important area of application of semiconductor lasers in general. Short optical pulses from diode lasers transmit high quality voice, video and data through optical fibres. However, the demand for broad-band optical networks, in the multi-gigabit up to terabit capacity, is increasing rapidly. For example the network traffic in the USA in the year 2025 is expected to be of 4 Tb/s [21]. The achievement of such high capacity requires the efficient use of both time-division multiplexing (TDM) and wavelength-division multiplexing (WDM) [21], for example with the implementation of a TDM system within each channel of a WDM system [22]. Therefore, the realisation of these networks requires flexible use of time, wavelength and space switching [23, 24]. High speed short pulse generation for the high bit-rate TDM systems could be provided by a mode-locked quantum well laser for example, at repetition rates around 100 GHz [21, 22] with solitonic optical fibre transmission [25, 26]. Besides signal generation, other functionality required in these systems include

modu/demodulation, multi/demultiplexing [26, 27], amplification (semiconductor or EDFA), and clock signal extraction (see chapter 5) and distribution [28] for signal retiming and regeneration [22-24]. To operate at such high speed (100 GHz) these optical signal processings must be performed by nonlinear all-optical (photonic) and optoelectronic integrated circuits [5, 8, 22-24].

Another aspect of high speed short pulse generation from semiconductor lasers that concerns telecommunications is the possibility of performing opto-electrical-microwave interfacing. In simple terms, gain-switching, active Q-switching and active mode-locking transform microwave electrical signals (driving signals) into microwave optical signals (train of optical pulses at laser output). On the other hand, passive schemes use saturable absorbers inside the waveguide, which works as photodetectors, generating an electrical signal synchronised with the optical oscillation of the laser cavity. Therefore, passive Q-switching and passive mode-locking are opto to electrical microwave signal transducers [29]. These capabilities can be used in microwave optoelectronic systems to perform generation, transmission (optical fibres), processing, synchronisation and detection of microwave modulated optical signals [5, 30, 31].

Optical computing applications comprise high speed optical signal generation and processing for the realisation of optical clocks [28], optical logic gates [32], optical interconnections and optical data storage. Due to their high frequency (repetition rate) stability, mode-locked lasers can be used as optical clock generators in an optical computing system.

In optoelectronic measurement applications short optical pulses are used to test, measure or characterise systems. For example, they can be used to obtain the impulse response of optical materials and components, as in pump and probe experiments [14]. Short electrical pulses for electronic circuits testing can be generated by electrooptic sampling [33]. Laser ranging, optical time domain reflectometry and sensing can use short optical pulses from semiconductor lasers to measure distances with high accuracy for high precision manufacturing and for guiding and automatic collision avoidance systems, as well as to monitor the environment in pollution control systems for example.

1.4 - Outline of the Thesis

This thesis is organised as follows: The next chapter, chapter 2, brings a detailed review of the mode-locking technique for short pulse generation, with special emphasis on passive mode-locking of semiconductor lasers, which is the main subject of this work. Chapter 3 is dedicated to the techniques used for the fabrication of mode-locked semiconductor lasers. Detailed descriptions of wafer and waveguide structures, wafer characterisation techniques and mode-locked laser fabrication process are given.

Chapter 4 describes the techniques used for characterisation of the fabricated devices in the mode-locked laser test set-up, including power supplies for laser biasing and the time domain and frequency domain measurements. Chapter 5 shows the experimental results obtained from the fabricated mode-locked lasers. It presents original work on five different configurations of mode-locked lasers, leading to different operating characteristics for different applications. Therefore, this is the most important chapter of the thesis. Chapter 6 summarises the conclusions from each chapter.

Each chapter is organised in sections and some of them in subsections. They all have their own conclusion section, as well as a last section for their own list of references, which are organised in order of appearance.

This thesis has three appendixes at the end. Appendix 1 shows the general equations for the linear correlator used in chapter 4. Appendix 2 gives a list of publications and conference contributions that have arisen from this work, and an alphabetically ordered list of references of the entire thesis. And appendix 3 shows photocopies of the three journal publications produced from this work.

1.5 - References to Chapter 1

- [1] - L. Esaki, "A bird's-eye view on the evolution of semiconductor superlattices and quantum wells", *IEEE J. Quantum Electron.*, vol. 22, p. 1611-1624, Sep. 1986
- [2] - H. Okamoto, "Semiconductor quantum well structure for optoelectronics - Recent advances and future prospects", *Jap. J. Appl. Phys.*, vol. 26, p. 315-330, Mar. 1987
- [3] - W. T. Tsang, "Quantum Confinement Heterostructure Semiconductor Lasers", *Semiconductors and Semimetals*, vol. 24, Editor Raymond Dingle, Academic Press, 1987, Chapter 7.
- [4] - A. Yariv, *Quantum Electronics*, 3rd edition, Wiley, 1989
- [5] - R. G. Hunsperger, *Integrated Optics: Theory and Technology*, Third Edition, Optical Sciences Series, Springer-Verlag, 1991
- [6] - C. Weisbuch and B. Vinter, *Quantum semiconductor structures: fundamentals and applications*, Academic Press, 1991.
- [7] - P. S. Zory, Jr. (Editor), *Quantum Well Lasers*, Quantum Electronics: Principles and Applications Series, Academic Press, 1993.
- [8] - M. Degenais, R. F. Leheny and J. Crow (Editors), *Integrated Optoelectronics*, Quantum Electronics: Principles and Applications Series, Academic Press, 1995.
- [9] - R. M. De La Rue and J. H. Marsh, "Integration technologies for III-V semiconductor optoelectronics based on quantum well waveguides", in *Integrated Optics and Optoelectronics*, K. -K. Wong and M. Razeghi, Eds. Los Angeles, CA:SPIE (Int. Soc. Opt. Eng.), pp. 259-288, Jan. 1993.

- [10] - I. Gontijo, T. Krauss, J. H. Marsh, and R. M. De La Rue, "Postgrowth control of GaAs/AlGaAs quantum well shapes by impurity-free vacancy diffusion", *IEEE J. Quantum Electron.*, vol. 30, pp. 1189-1195, May 1994
- [11] - A. E. Siegman, *Lasers*, Oxford University Press, 1986.
- [12] - P. P. Vasil'ev, "Ultrashort pulse generation in diode lasers", *Optical and Quantum Electron.*, vol. 24, pp. 801-824, 1992.
- [13] - P. P. Vasil'ev, *Ultrafast Diode Lasers: Fundamentals and Applications*, Artech House Publishers, 1995.
- [14] - D. J. Derickson, R. J. Helkey, A. Mar, J. R. Karin, J. G. Wasserbauer and J. E. Bowers, "Short pulse generation using multisegment mode-locked semiconductor lasers", *IEEE J. Quantum Electron.*, vol. 28, pp. 2186-2202, Oct. 1992.
- [15] - H. F. Liu, M. Fukazawa, Y. Kawai and T. Kamiya, "Gain-switched picosecond pulse (<10 ps) generation from 1.3 μm InGaAsP laser diodes", *IEEE J. Quantum Electron.*, vol. 25, pp. 1417-1425, June 1989.
- [16] - R. Nagarajan, D. Tauber and J. E. Bowers, "High speed semiconductor lasers", *Intern. J. High Speed Electron. and Systems*, vol. 5, no. 1, pp. 1-44, 1994
- [17] - M. Osinski and M. J. Adams, "Picosecond pulse analysis of gain-switched 1.55 μm InGaAsP lasers", *IEEE J. Quantum Electron.*, vol. 21, pp. 1929-1936, Dec. 1985.
- [18] - D. A. Barrow, J. H. Marsh, E. L. Portnoi, "Q-switching pulses at 16 GHz from two-section semiconductor lasers", in *CLEO/Europe*, Amsterdam, The Netherlands, Aug. 1994, paper CTuE4, pp. 75.
- [19] - P. P. Vasil'ev, "Picosecond injection laser: A new technique for ultrafast Q-switching", *IEEE J. Quantum Electron.*, vol. 12, pp. 2386-2391, Dec. 1988.
- [20] - Y. K. Chen and C. W. Ming, "Monolithic colliding-pulse mode-locked quantum-well lasers", *IEEE J. Quantum Electron.*, vol. 28, pp. 2177-2185, Oct. 1992
- [21] - For a recent overview see *IEE Colloquium on Towards Terabit Transmission*, Savoy Place, London, 19th May 1995, Digest No: 1995/110
- [22] - C. Baack, and G. Walf, "Photonics in future telecommunications", *Proc. of the IEEE*, vol. 81, pp. 1624-1631, Nov. 1993
- [23] - M. J. Adams, P. E. Barnsley, J. D. Burton, D. A. O. Davies, P. J. Fiddymment, M. A. Fisher, D. A. H. Mace, P. S. Mudhar, M. J. Robertson, J. Singh and H. J. Wickes, "Novel components for optical switching", *BT Technol. J.*, vol. 11, no. 2, April 1993
- [24] - S. Shimada, K. Nakagawa, M. Saruwatari and T. Matsumoto, "Very-high-speed optical signal processing", *Proc. of the IEEE*, vol. 81, pp. 1633-1646, Nov. 1993.
- [25] - A. Hasegawa, *Optical Solitons in Fibres*, Second Edition, New York, Springer-Verlag, 1990.

- [26] - K. Iwatsuki, K. Suzuki, S. Nishi, and M. Saruwatari, "80 Gb/s optical soliton transmission over 80 km with time/polarization division multiplexing", *IEEE Photon. Technol. Lett.*, vol. 5, pp. 245-248, 1993
- [27] - P. A. Andrekson, N. O. Olsson, J. R. Simpson, T. Tanbun-Ek, R. A. Logan, and M. Haner, "16Gbit/s all optical demultiplexing using four-wave mixing", *Electron. Lett.*, vol. 27, pp. 922-924, May 1991
- [28] - P. J. Delfyett, D. H. Hartman, and S. Zuber Ahmad, "Optical clock distribution using a mode-locked semiconductor laser diode system", *IEEE J. Lightwave Technol.*, vol. 9, pp. 1646-1649, 1991
- [29] - D. J. Derickson, R. J. Helkey, A. Mar, J. G. Wasserbauer, Y. G. Wey, and J. E. Bowers, "Microwave and millimeter wave signal generation using mode-locked semiconductor lasers with intra-waveguide saturable absorbers", *IEEE Intern. Microwave Theory and Technol. Symposium*, Albuquerque, USA, 1992, paper V-2, pp. 753-756
- [30] - E. L. Portnoi, V. B. Gorfinkel, D. A. Barrow, I. G. Thayne, E. A. Avrutin, J. H. Marsh, "Optoelectronic microwave-range frequency mixing in semiconductor lasers", *IEEE J. Selected Topics in Quantum Electron.*, vol. 1, no. 2, Special issue on semiconductor lasers, June 1995.
- [31] - A. J. Seeds, "Microwave optoelectronics", *Optical and Quantum Electron.*, vol. 25, pp. 219-229, 1993
- [32] - M. N. Islam, C. E. Socolich, and D. A. B. Miller, "Low-energy ultrashort fiber soliton logic gates", *Opt. Lett.*, vol. 15, pp. 909-911, Aug. 1990
- [33] - J. A. Valdmanis and B. Mourou, "Subpicosecond electrooptic sampling: principles and applications", *IEEE J. Quantum Electron.*, vol. 22, pp. 69-78, Jan. 1986.

Chapter 2: Review of Mode-Locked Semiconductor Lasers

This Chapter is intended to review the more important aspects of mode-locking, specially concerning mode-locking of semiconductor lasers. Section 2.1 gives an overview of mode-locking, with a simple description of the general concept of mode-locking. Section 2.2 reviews the different methods that can be used to achieve mode-locking effect, as well as the different configurations of mode-locked semiconductor lasers. Section 2.3 is dedicated to the method that is used in this work, which is the passive mode-locking, and it will be described in details. In Section 2.4 the configuration which is mostly employed for the semiconductor lasers in this work will be reviewed, namely the colliding pulse mode-locking configuration. Section 2.5 gives a short overview of the causes of instability in mode-locked semiconductor lasers and the stabilisation techniques. Section 2.6 brings the conclusions and the new directions of the field of semiconductor mode-locked lasers. The references to this chapter are listed in appearance order in section 2.7.

2.1. - Simple Description of Mode-Locking

In general terms, mode-locking is a technique of short pulse generation from lasers, and it has been employed in gas, dye, solid state and semiconductor lasers. In simple terms mode-locking consists of "forcing" the phases of the longitudinal modes of a laser cavity to maintain their relative values [1-3]. Figure 2.1 illustrates the effect of the superposition of three modes which are exactly in phase at $t = 0$ and $t = T$. When the modes are in phase they interfere constructively, increasing the total field in the cavity, whereas when out of phase they interfere destructively, resulting in a decreased total field in the cavity. The overall result of this phase-locking of the longitudinal modes of a laser is that, in the time domain, it produces a pulsed intensity, with a period equal to T , as shown in figure 2.1 [1].

Although a rigorous analysis of mode-locking must go through the solution of Maxwell's equation for the electric field in the laser cavity [1-5], the simplified analysis that follows, described by Yariv [2], shows some of the general properties of mode-locked lasers. Using the complex notation one can write the total optical electric field in the cavity as [2]

$$E(t) = \sum_n E_n \cdot \exp\{i[(\omega_0 + n\omega)t + \phi_n]\} \quad (2.1)$$

Where n is the longitudinal mode number, ω_0 is an arbitrary central frequency, ω is the frequency space between longitudinal modes and ϕ_n is the phase of the n th mode. Using

this expression one can say that the mode locking technique is to induce the phase of the modes ϕ_n to maintain their relative values.

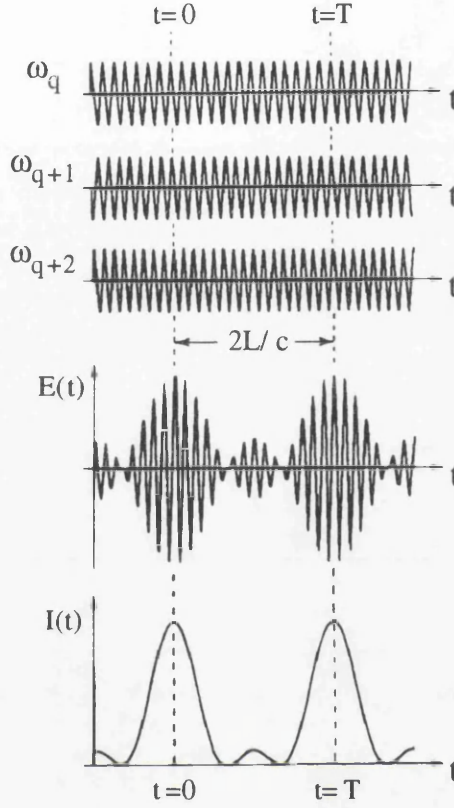


Figure 2.1: Illustration of mode-locking effect on total field and intensity for three modes of frequencies ω_q , ω_{q+1} and ω_{q+2} , which are in phase at $t = 0$ and $t = T$ [1].

One of the forms of mode-locking results when the phases are equal to zero. To simplify the analysis of this case, it is assumed that there are N oscillating modes with equal amplitudes. So taking $E_n = E$ and $\phi_n = 0$ in equation 2.1 it gives

$$E(t) = E \cdot \sum_{-(N-1)/2}^{(N-1)/2} \exp\{i(\omega_0 + n\omega)t\} \quad (2.2)$$

$$E(t) = E \cdot \exp\{i\omega_0 t\} \cdot \frac{\sin(N\omega t / 2)}{\sin(\omega t / 2)} \quad (2.3)$$

The average laser power $P(t)$ then is given by

$$P(t) \propto |E(t)|^2 = P_0 \frac{\sin^2(N\omega t / 2)}{\sin^2(\omega t / 2)} \quad (2.4)$$

Figure 2.2 shows a plot of equation 2.4 for the output power of a mode-locked laser with 3 and 5 modes of equal amplitude locked. It was calculated using Mathematica® enhanced version 2.0 software package.

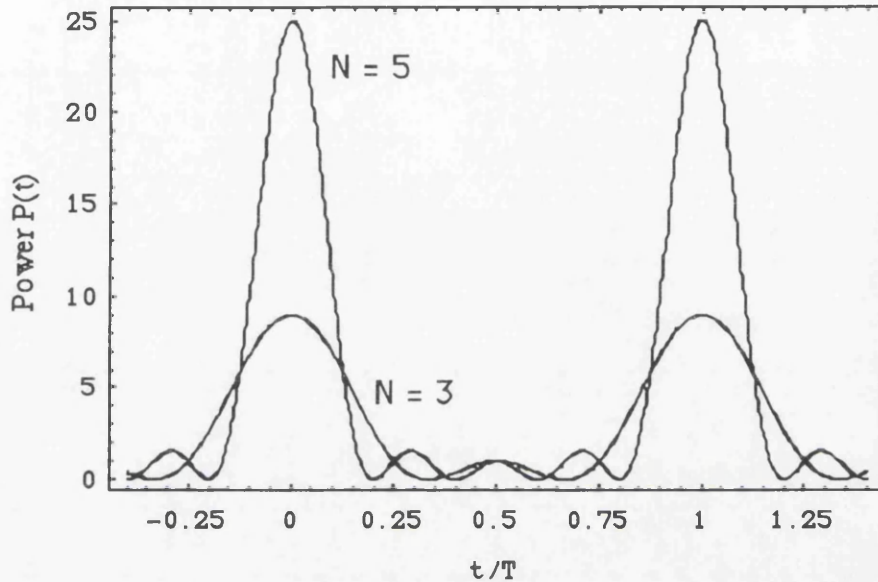


Figure 2.2: Theoretical plot of equation 2.4 for a mode-locked laser with N modes locked, with P_o equal to 1. The time scale is normalised in round-trips T .

From equation 2.4 and figure 2.2 some properties of $P(t)$ can be observed:

- The optical power is emitted in a form of a train of pulses with a period $T=2\pi/\omega = 2L/c$, which is the round trip time of the cavity.

- The peak power $P(sT)$ (for $s = 1, 2, 3, \dots$), is equal to N times the average power and to N^2 times the amplitude of a single mode, where N is the number of modes locked together.

- The individual pulse width, defined here as the time from the peak to the first zero is $\Gamma_o = T/N$.

- The number of oscillating modes can be estimated as $N \cong \Delta\omega/\omega$, that is the ratio of the transition lineshape width to the frequency spacing ω between modes. Using this relation together with $T = 2\pi/\omega$ and $\Gamma_o = T/N$ we obtain $\Gamma_o \cong 2\pi/\Delta\omega = 1/\Delta\nu$. It means that mode-locked pulses are ideally Fourier transform limited.

From these properties one can observe that for the case of semiconductor lasers, the usual short cavity length of monolithic devices ($\sim 500 \mu\text{m}$) allows the generation of a train of pulses at a very high repetition rate ($\sim 100 \text{ GHz}$). Moreover, due to the wide gain-bandwidth of semiconductor lasers ($\sim \text{THz}$), down to femtosecond optical pulses can be generated, in principle [5-7]. The small size, low power requirements and monolithic integration facilities of semiconductor devices allow a wide possibility of

applications for mode-locked lasers. It ranges from high speed telecommunication and optical computing systems to short pulse sources for optoelectronics and nonlinear optical measurements [6, 7].

2.2 - Methods and Configurations of Mode-Locking in Semiconductor Lasers

The mode-locking effect is achieved by modulating the losses or the gain of the laser at a frequency equal to the intermode frequency spacing or a multiple of it [1-3]. In other words, it can be accomplished by a small gain or loss modulation of the modes at a period equal to the round trip time of the laser cavity. There are three techniques that can be used to induce the mode-locking effect in semiconductor lasers. They are the active, passive and hybrid mode-locking. A laser can be actively mode-locked by applying a repetitive electrical pulse stream with a period equal to the laser round trip time superimposed on a DC bias. The electrical pulses must be narrow to create a very short time window of net gain in the device [6, 8-11]. Different to the active, the passive mode-locking technique uses a saturable absorber inside the laser cavity to obtain loss modulation and therefore mode-locking effect. No external electrical modulation signal is required [6, 7]. Passive mode-locking will be discussed in detail in section 2.3. Hybrid mode-locking is basically a combination of active and passive mode-locking techniques [6, 12].

These techniques can be used in external extended cavity or monolithic configurations [6-12]. Figure 2.3 shows some of the more common configurations of mode-locked semiconductor lasers. An external cavity mode-locked laser usually contains a focusing lens and a mirror in the external cavity, which is coupled to the internal laser cavity through a anti-reflection coated facet. The saturable absorber section may also be in the external cavity, in an external cavity external absorber configuration (figure 2.3-a) [13]; or integrated in the semiconductor laser, in an external cavity integrated absorber configuration (figure 2.3-b) [14]. Instead of a mirror the external cavity configuration may have a diffraction grating, which can provide optical feedback to the laser, as well as wavelength tuneability [15]. However, the mechanical instabilities of an external cavity and imperfect anti-reflection coating, which may cause multiple pulse formation, are the main drawback of the external cavity configuration in comparison to the monolithic one. This multiple pulse formation can be suppressed by a saturable absorber, which filters the secondary pulses [16]. Monolithic lasers are more compact, robust and suitable for applications in optoelectronic integrated circuits. Moreover, passive mode-locking in a monolithic cavity is the most suitable configuration for ultra-high speed (above 100 GHz) short pulse (around 1 ps) generation.

The operation of mode-locked lasers depends also on the position of the saturable absorber section in the cavity. Figure 2.3-d shows a laser which has the absorber section placed in the middle of the laser cavity in a configuration known as colliding pulse mode-locking (CPM). CPM lasers have distinct features and they will be discussed in detail in section 2.4.

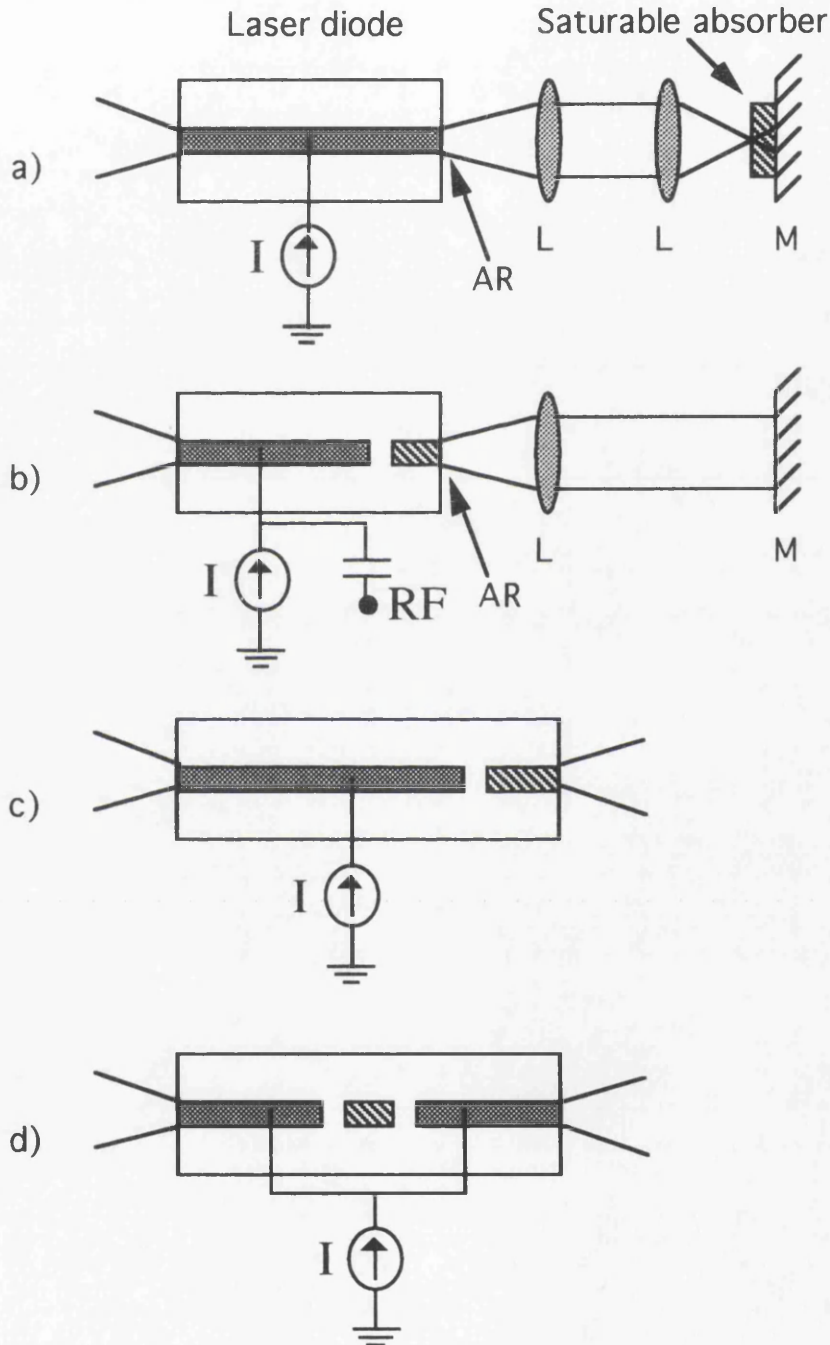


Figure 2.3: Some configurations of mode-locked semiconductor laser: a) passive in external cavity external absorber, b) hybrid in external cavity integrated absorber, c) passive monolithic integrated, and d) passive monolithic CPM. Dark areas indicate gain sections of the laser diode and hatched areas indicate saturable absorber sections. L is lens, M is mirror and AR is anti-reflection coating.

Mode-locked lasers in monolithic cavities can also incorporate an embedded grating, in a distributed Bragg-reflector (DBR) configuration, which provides spectral filtering and bandwidth limitation [11, 17]. Other configurations for mode-locked lasers include ring cavity lasers (see section 5.3 of Chapter 5) and vertical-cavity surface-emitting lasers (VCEL) [18].

2.3 - Passive Mode-locking

2.3.1 - Pulse shortening effect

In semiconductors the saturable absorber works as a slow saturable absorber, which means that its recovery time is longer than the mode-locked pulse duration [1, 19]. Therefore, for this type of passive mode-locking, the gain and absorption saturation and recovery times are mainly responsible for the pulse shortening effect. Figure 2.4 shows the dynamics of the time dependent gain and absorption loss in a passive mode-locked laser system with a slow saturable absorber [19].

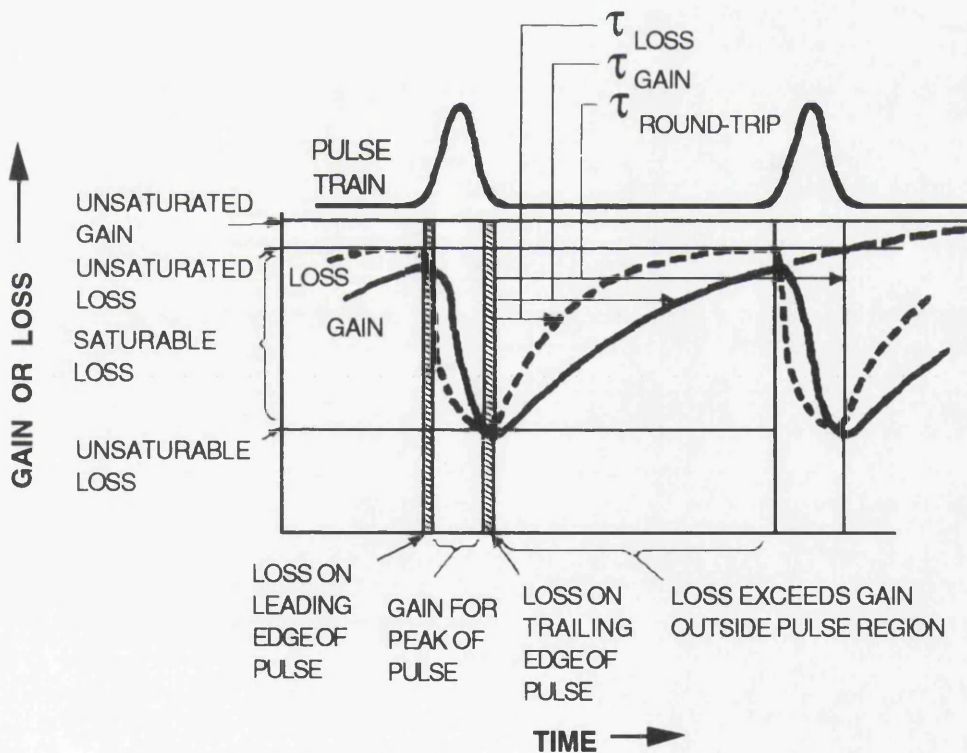


Figure 2.4: Gain and loss dynamics for ideal mode locking with a slow saturable absorber [19].

The dynamics of passive mode-locking pulse build up and shortening can be described as follows [1, 19]: In a very early stage the laser reaches a first threshold at which the laser gain first equals the total losses due to the unsaturated absorber, cavity output coupling and all other cavity losses. After that, the laser cavity will be amplifying the

weak noise that comes from the spontaneous emission. At some point the laser reaches a second threshold, beyond which some single preferred noise spike becomes powerful enough to start saturating the absorber on succeeding round trips. Therefore this pulse will experience a higher net gain than the others in the cavity. It will grow more rapidly and make the cavity even lossier for lower intensity peaks due to gain saturation. Before the arrival of this pulse in the absorber the loss is then larger than the gain. Therefore the leading edge of the pulse experiences loss. As the intensity of the pulse increases, however, the loss should saturate faster than the gain, so that the central part of the pulse will be amplified. When the gain becomes saturated below the unsaturable loss (facet reflectivity, waveguide loss, etc.), the trailing edge of the pulse will experience loss. If the recovery time of the loss is faster than that of the gain, then the loss will remain higher than the gain everywhere except near the peak of the pulse. On a round trip in the resonator, the combined action of gain and loss saturation and recovery at appropriate times is to shorten the pulse by amplifying the centre and attenuating its leading and trailing edges, as shown in figure 2.4 [19]. The final generated pulse width, in the steady state (after several round trips), will depend on the balance between this pulse shortening effect and the pulse broadening effect which will be described in section 2.3.4.

2.3.2 - Conditions for mode-locking

The two underlined requirements in the above section represent the conditions for mode-locking that a saturable absorber must satisfy [6, 7, 19]. The first one implies that the saturation energy of the gain must be larger than the saturation energy of the absorber section. The saturation energy of the gain (g) or absorber (a) is given by:

$$E_{sat_{g,a}} = \frac{h\nu A_{g,a}}{\partial[g,a]/\partial N_{g,a}} \quad (2.5)$$

where h is the Planck's constant, ν is the optical frequency, $A_{g,a}$ is cross sectional area of the laser beam in the gain or absorber section, and $\partial[g,a]/\partial N_{g,a}$ is the differential gain or absorption with respect to carrier density N . Therefore the first condition can be written as:

$$\frac{h\nu A_g}{\partial g/\partial N_g} > \frac{h\nu A_a}{\partial a/\partial N_a} \quad (2.6)$$

The second condition is that the recovery time of the saturable absorber must be shorter than the recovery time of the gain, i. e.

$$\tau_a < \tau_g \quad (2.7)$$

2.3.3 - Techniques for producing saturable absorption in semiconductors

The first condition for mode-locking, given by equation 2.6, is satisfied in a semiconductor due to the sublinear dependence of the differential gain on the carrier density [6, 7], as illustrated in figure 2.5. The larger differential gain at the absorbing region (lower carrier density) compared with the smaller differential gain at the gain region (higher carrier density) guarantees that the first condition is achieved. The reduction in differential gain with increased carrier density is particularly large in quantum well lasers due to the step-like density of states function of quantum wells [6]. The mode cross sectional area A can be used to reduce the saturation energy of saturable absorbers, specially in an external cavity external absorber configuration as shown in figure 2.3-a where the laser beam can be easily tight focused in the saturable absorber. In monolithic cavities it can be more difficult since the optical mode is already tightly confined in the waveguide, although a non-conventional non-uniform waveguide could be constructed for this purpose.

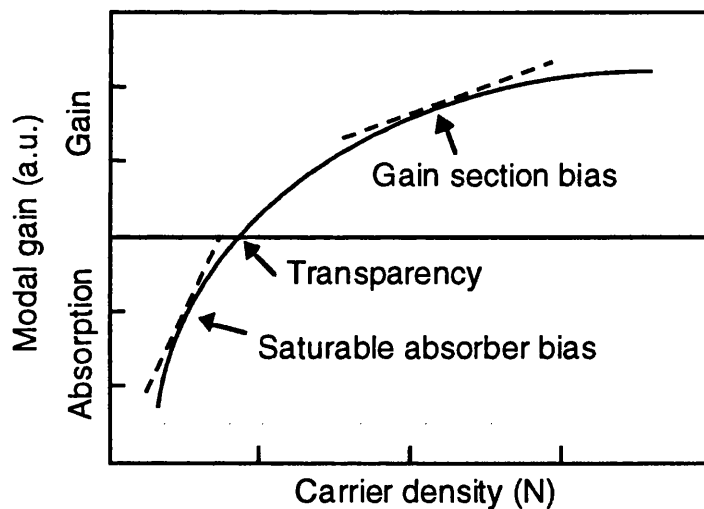


Figure 2.5: Saturation characteristics of the modal gain (gain or absorption) in semiconductors as a function of carrier density. The differential gain is represented by dashed lines.

The second condition for mode-locking, given by equation 2.7, is not automatically satisfied in semiconductors. The spontaneous emission recombination time, typically 1 ns, is too long for effective absorption recovery. Several techniques have been used to decrease the absorption recovery time of semiconductor saturable absorbers and they will be described here.

A - Aging: By aging the laser to the point of severe degradation one can introduce dark line defects. These defects act as source of non-radiative recombination, which have fast recovery time [20]. This technique has produced 0.58 ps pulsewidth

[21]. However the concentration of the defects increases rapidly and results in accelerated degradation and failure of the lasers.

B - Tight focusing: As mentioned before, this technique can be used in external absorbers, where the laser beam can be tightly focused. In this scheme the recovery time of the absorber can have a large contribution of lateral diffusion of carriers out of the interaction region, reducing the overall recovery time [13, 19]. Although this technique has produced 1.6 ps pulses [13], it is limited in speed and is not convenient for monolithic configurations.

C - Proton bombardment and ion implantation: These techniques use proton bombardment [19, 22] or heavy ion implantation [23-25] to damage the semiconductor material near one laser facet, creating fast recombination centres. Pump and probe measurements of the recovery time of proton bombarded absorbers showed that, depending on the proton dose, up to 10 ps recovery time can be achieved [19]. 0.65 ps pulses at 1 GHz repetition rate have been produced with this technique [22]. Nitrogen and oxygen ion implantation have produced 5 ps pulses at 40 GHz repetition rate [24], and up to 200 GHz repetition rates [25]. However, although effective, these techniques produce instabilities in the laser operation due to the process of auto-annealing of the bombarded regions and the long term reliability of the devices is questionable.

D - Non-uniform injection in split contacts: This technique uses a short section formed by splitting the contact of the laser as a saturable absorber, which is reverse biased [14, 26-28]. The reverse bias introduces a controllable amount of absorption in the section as it will be described later. When an intense pulse reaches the absorber section it is saturated by mostly band filling. The electric field produced by the applied reverse bias then sweeps out the generated carriers from the absorber region, returning it to the unsaturated state. Since this technique does not rely on any damage of the material it is inherently more reliable [6, 14]. Pump and probe measurements of the absorption recovery time of such type of saturable absorbers showed that the absorption recovers in approximately 10 ps [6, 16]. This technique is employed in most of the recent work involving semiconductor integrated saturable absorbers and it is also used in the experimental results presented in Chapter 5.

Semiconductor quantum well materials offer extra features to saturable absorbers. Firstly, as it was mentioned before, the sublinear dependence of the modal gain with carrier density in quantum well is more favourable to satisfy the first condition of mode-locking (equation 2.6 and figure 2.5). Also, the introduction of absorption by reverse biasing the semiconductor material is more efficient in quantum wells than in bulk material due the electric field dependent bandgap shifting effect known as the quantum confined Stark effect [29-31]. An electric field applied perpendicular to the quantum well layers causes a tilt of the band structure, as illustrated in figure 2.6. The electron and hole wavefunctions tend to move to opposite

sides of the well but the walls prevent them from going too far. Absorption occurs below the band edge due to the evanescent tails of the wavefunctions in the conduction and valence band into the forbidden gap [29]. The equivalent mechanism in 3D (bulk material), the Franz-Keldysh effect, is a less efficient optical modulator because the wavefunctions are free to smear out to opposite sides of conduction and valence band, leading to diminished spatial overlap [29, 30]. Moreover, excitons are preserved in reverse biased quantum well structures. Although the saturation of the absorber is mostly due to band filling [29-31], there might be a contribution of excitonic saturation in the quantum wells, which would lead to a fast recovery component of the saturable absorber [32]. Section 5.2 of Chapter 5 discusses the issue of the fast components of saturable absorption in bulk and quantum well materials and their contribution to the operation of ultra-high-speed mode-locked lasers (at repetition rates above 200 GHz).

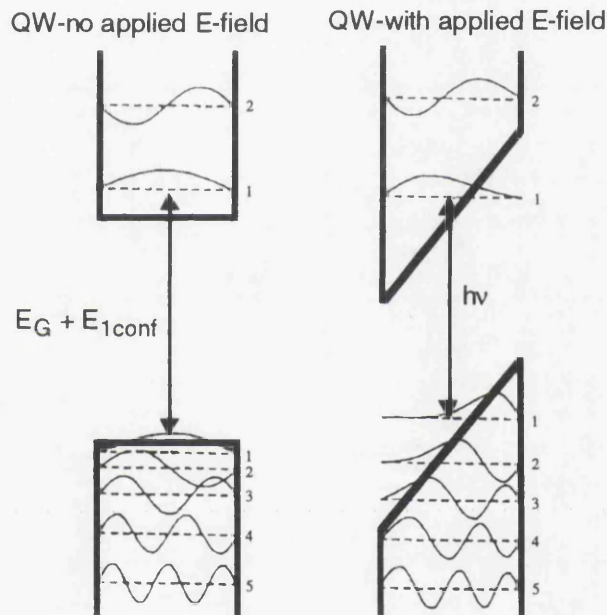


Figure 2.6: Schematics of the effect of an electric field applied transversally to a quantum well (quantum confined Stark effect) [29].

2.3.4 - Pulse broadening effect

In the steady state, the pulse shortening effect discussed in section 2.3.1 is balanced by a pulse broadening effect due to the combined effect of group velocity dispersion and self-phase modulation [6, 33-36]. Figure 2.7 shows the effect of self-phase modulation (SPM) in mode-locked semiconductor lasers due to the Kerr effect, gain and absorption saturation [36]. The Kerr effect introduces an intensity dependent contribution to the refractive index as follows [37]

$$n = n_o + n_2 I(t) \tag{2.8}$$

where n_0 is the linear (intensity independent) refractive index, n_2 is the nonlinear refractive index and I is the instantaneous intensity of the pulse. Therefore, in the Kerr effect SPM the index of refraction change is proportional to the instantaneous intensity of the pulse. The changes in the index of refraction cause modulation of the phase of the optical pulse (ϕ), as well as of its instantaneous frequency (ω_i), which is defined as follows [1, 37].

$$\omega_i = -\frac{d\phi(t)}{dt} = -\frac{2\pi L}{\lambda} \cdot \frac{dn}{dt} \tag{2.9}$$

where L is the optical cavity length, λ is wavelength and n is the index of refraction. It can be seen from equation 2.9 that bandwidth broadening due to SPM is inversely proportional to the pulsewidth, i.e. shorter pulses produce more changes in the refractive index per unit of time, generating more instantaneous frequencies.

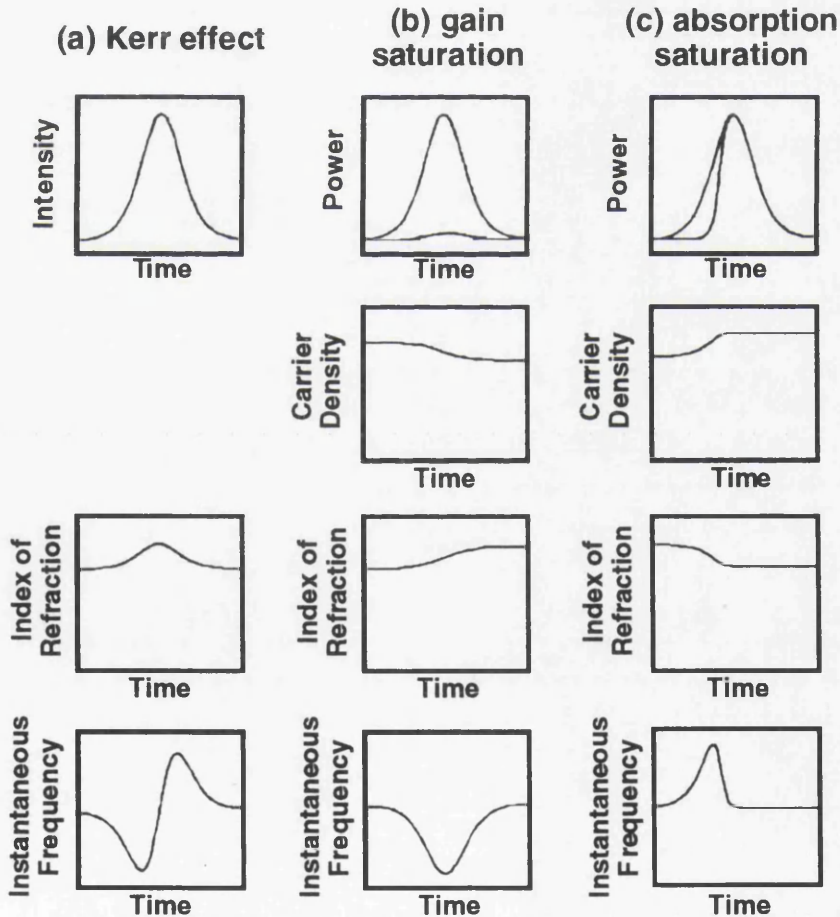


Figure 2.7: Self-phase modulation effects in mode-locked semiconductor lasers due to (a) Kerr effect, (b) gain saturation and (c) absorption saturation [36].

The Kerr effect SPM induces a linear chirp across the central part of the pulse. However the dominant SPM effect in a passively mode-locked semiconductor laser

comes from gain and absorption saturation. When the optical pulse is intense enough to saturate the gain of the amplifier section, it produces a depletion of carrier density in that region, which in turn increases the index of refraction. Changes in the index of refraction are coupled to changes in gain or absorption through the linewidth enhancement factor (α) [38, 39], given by [38]

$$\alpha = -\frac{d[\text{Re}\{\chi(N)\}]/dN}{d[\text{Im}\{\chi(N)\}]/dN} \quad (2.10)$$

where χ is the linear susceptibility and N is carrier density. Typical values of α range from 0.5 to 8 in semiconductor lasers [38].

As illustrated in figure 2.7 and equations 2.9 and 2.10, the self-phase modulation in the saturable gain and absorber medium of the laser cause nonlinear chirp and excess optical bandwidth, beyond the Fourier transform limit, to short optical pulses, but it does not broaden the pulse by itself. Pulsewidth broadening is caused by the group velocity dispersion in the laser cavity, which can be enhanced by the spectral broadening caused by SPM [35, 40]. GVD causes temporal broadening of the pulse since each wavelength component of the pulse travels at a different velocity in the cavity. The GVD parameter is defined as [37]

$$\beta_2 = -\frac{1}{v_g^2} \frac{dv_g}{d\omega} \equiv \frac{\lambda^3}{2\pi c^2} \frac{d^2n}{d\lambda^2} \quad (2.11)$$

where v_g is the group velocity and c is the speed of light in vacuum. GVD in semiconductor lasers is caused basically by chromatic dispersion and gain dispersion [35]. Chromatic dispersion comes from the frequency (or wavelength) dependence of the refractive index of the material [37]. Gain dispersion is due to the finite gain bandwidth of semiconductor lasers. Optical pulses shorter than a few picoseconds have a wide enough spectrum so that different spectral components experience different gain. Because of the interrelationship between gain and refractive index, given by the linewidth enhancement factor (equation 2.10), this gain dispersion enhances the group velocity dispersion [35], according to equation 2.11.

Therefore, the pulse broadening due to GVD can be enhanced by the spectral broadening due to SPM [35, 40], and the overall pulse broadening effect due to GVD and SPM increases as the pulsewidth is reduced due to the pulse shortening effect described earlier. These effects ultimately balance each other and limit the width and overall quality of pulses from mode-locked lasers. A possible way to diminish the pulse broadening effect, specially for high power extended cavity lasers, is the insertion of a

bandwidth limiting element like a grating in the external cavity [9] or an integrated Bragg-reflector in a monolithic cavity [11]. This combination of pulsewidth and spectral broadening effects is less pronounced in short monolithic cavity lasers because of the typical low peak power generated by these devices.

2.4 - Colliding Pulse Mode Locking

The colliding pulse configuration of mode-locked lasers consists of positioning the saturable absorber section exactly in the middle of the laser cavity. This geometrical factor induces the formation of two counter-propagating pulses which collide in the absorber section. It is due to the fact that two pulses colliding in the absorber saturate the absorber more easily than only one, whereas they experience less gain saturation when in the two gain sections. Therefore, this is a less lossy solution for the laser operation and this colliding pulse effect makes the laser satisfy the conditions of mode-locking (section 2.3) more easily than a non-colliding pulse configuration [6, 40, 41]. Figure 2.8-a shows the schematic diagram of a colliding pulse mode-locked (CPM) laser.

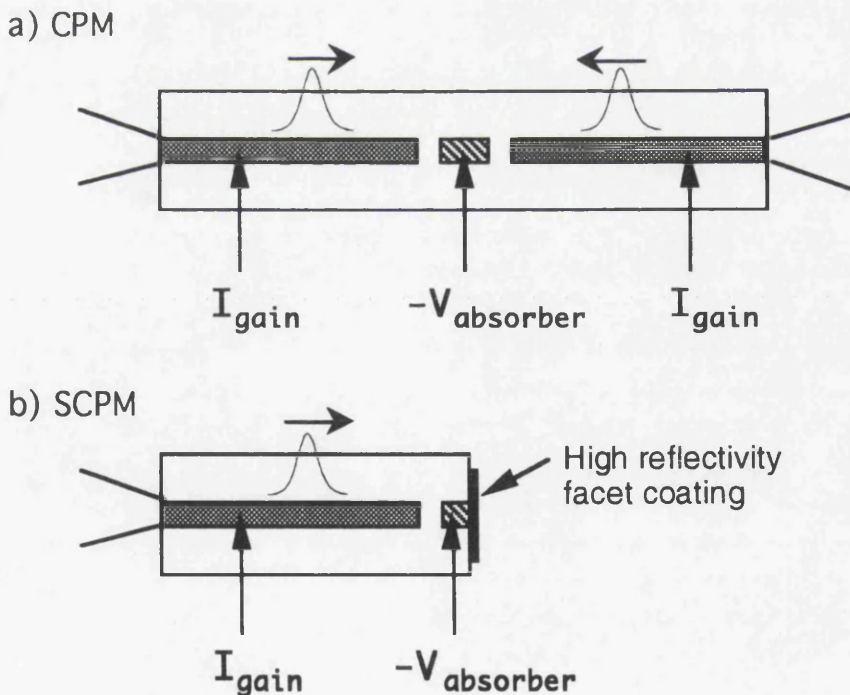


Figure 2.8: Schematic top view diagram of: a) the colliding pulse mode-locked (CPM), and b) the self-colliding pulse mode-locked (SCPM) laser configuration.

Because of the two pulses circulating in the cavity the repetition rate of a CPM laser is doubled. Also the separation between longitudinal modes is twice the value of a non-colliding pulse mode-locked laser of the same cavity length. The repetition rate (f)

and the longitudinal mode separation ($\Delta\lambda$) of CPM and ordinary (non-CPM) lasers are given by:

$$f_{CPM} = \frac{c}{L \cdot n} \quad (2.12)$$

$$f_{ord} = \frac{c}{2L \cdot n} \quad (2.13)$$

$$\Delta\lambda_{CPM} = \frac{\lambda^2}{L \cdot n} = \frac{\lambda^2 \cdot f_{CPM}}{c} \quad (2.14)$$

$$\Delta\lambda_{ord} = \frac{\lambda^2}{2L \cdot n} = \frac{\lambda^2 \cdot f_{ord}}{c} \quad (2.15)$$

where c is the velocity of light in vacuum, n is the index of refraction, λ is lasing wavelength and L is cavity length. This doubling of the pulse repetition rate and longitudinal mode separation can be understood as if the presence of the two pulses in the cavity introduces an even symmetry in the cavity, which changes the resonance conditions of the cavity. Effectively, due to this even symmetry, the cavity behaves as if its length is half of its real value. This effect is useful to detect mode-locking operation of the laser, since the intermode spacing can easily be measured from the optical spectrum of a laser of typical cavity length, around $500 \mu\text{m}$ (see Chapter 5).

Figure 2.8-b shows the schematic diagram of a self-colliding pulse mode-locked (SCPM) laser. In the SCPM laser configuration the saturable absorber is placed at one end of the cavity, near the facet, which is coated to have a high reflectivity, ideally 100%. This causes the single mode-locked pulse in the cavity to collide with itself at the saturable absorber section, benefiting from the same colliding pulse effects described before for the CPM configuration. From the mode-locking point of view these two configurations are equivalent. However, the SCPM has the advantage of needing a shorter cavity to achieve the same pulse repetition rate, which is important for the fabrication of low repetition rate lasers. Also it does not have the requirement of symmetry on the position of the saturable absorber in the cavity as in the CPM configuration. Moreover, due to the high reflectivity facet and the smaller gain section the lasing threshold is lower and the lasing efficiency is higher. On the other hand, the facet coating is an extra elaborated fabrication step, and a non-perfect (not 100% reflectivity) coating leads to a diminished colliding pulse effect [6, 40].

The colliding pulse effect described before, which reduces the requirement on the saturation energy of the absorber, improving pulse shortening, is sometimes called incoherent colliding pulse effect since it does not take into account the coherent effects

of the collision of the pulses, which lead to the formation of a transient grating in the absorber [6, 40]. The pulse overlap creates a transient standing wave pattern in the optical field and consequently a transient grating of carriers in the absorber. This coherent colliding pulse effect increases the optical intensity at the peaks of the standing wave pattern and reduces the total volume of absorber material to be saturated since the saturation is not required at the valleys of the grating [6, 40, 41]. Therefore, it further reduces the necessary pulse energy to saturate the absorber. It can also improve the recovery of the absorber since, after the passage of the pulse, the carrier grating can diffuse from the saturated grating peaks to the unsaturated valleys. The colliding pulse effect allows a passively mode-locked laser to operate at a lower pulse energy for maximum pulse shortening effect, reducing the pulse broadening effect due to self-phase modulation and group velocity dispersion [6].

The CPM configuration was first implemented in dye lasers [42] where the coherent colliding pulse effect proved to improve synchronisation, stability and the generation of short pulses. It allowed the removal of dispersive intracavity elements, such as prisms or diffraction gratings, used to limit the oscillating bandwidth and yet producing shorter transform limited pulses [42-45].

In semiconductors, CPM lasers have been realised in external extended cavity [46, 47], as well as in monolithic cavities using either passive [41, 48, 49] or active techniques [41, 50]. These monolithic CPM lasers, realised by Chen et al, have shown to generate short pulses, ranging from 0.65 ps to 3 ps, at repetition rates between 40 GHz and 350 GHz [41]. CPM quantum well lasers have also been theoretically investigated [51].

2.5 - Mode-Locking Stabilisation

Most mode-locked laser applications require the generation of an ideally stable train of pulses, with low timing jitter and low frequency and energy fluctuations. However, semiconductor mode-locked lasers have been shown to produce these kinds of instabilities, due to phase noise caused by the relatively large index of refraction variation induced by carrier fluctuation in the semiconductor material [6, 52, 53]. Among the different methods of mode-locking, passive mode-locked lasers have shown to produce larger timing jitter levels due to the fact that they are free running oscillators, with no electrical synchronisation signal, and with a relatively low Q cavity [6, 53].

It is also desirable to synchronise and even frequency tune the train of pulses produced by the mode-locked laser to other optoelectronic devices. This task can be particularly difficult in monolithic short cavity passively mode-locked lasers due to the lack of a synchronisation signal and their high repetition rate. However, the saturable

absorber of a passive mode-locked laser also acts as a photodetector, generating an electrical train of pulses, as an electrical oscillator in phase with the optical oscillator (the laser). This microwave signal [54] can be used in an external electrical or optoelectronic feedback circuitry to stabilise and synchronise the mode-locked laser oscillation [40, 55, 56]. These feedback stabilisation techniques have produced a reduction of 40 dB in the phase noise and a reduction of nearly 10 dB in the level of timing jitter in a passively mode-locked laser [55].

2.6 - Conclusions

This chapter has reviewed the principles and the physics involved in the mode-locking process, with particular emphasis on passively mode-locked semiconductor lasers. The different methods, configurations and design considerations to achieve mode-locking in semiconductors have been discussed, specially for the passive colliding pulse configuration, which is the subject of the investigation described in Chapter 5. Also, some aspects of timing stabilisation of these mode-locked lasers have been looked at.

In summary, mode-locked semiconductor lasers are capable of generating down to subpicosecond pulses at repetition rates ranging from hundreds of megahertz to hundreds of gigahertz or more. The main advantage of semiconductor mode-locked lasers over other types of mode-locked lasers is their manufacturability. Monolithic devices can be mass produced, leading to the realisation of a low cost, small size, small weight, robust, low power consumption and long life time sources of short pulses, which can be monolithically integrated with other optoelectronic devices. The major limitation of semiconductor mode-locked lasers is their low pulse energy (about 10 pJ), and this is one of the emerging subjects of research in the field. A promising way of solving this problem is the use of semiconductor amplifiers in flared waveguides, in either discrete or integrated configuration. The use of flared amplifiers to obtain high powers from mode-locked lasers is addressed in section 5.4 of Chapter 5.

Another recent theme of investigation in semiconductor mode-locked lasers is the pursuit of ultra-high-speed operation, i.e. the generation of short pulses at ultra-high repetition rates, reaching the terahertz range. This can be accomplished by inducing the laser to operate at harmonics of its repetition rate. These lasers can have an important role on future broadband (\sim THz) time-division-multiplexed (TDM) communication systems. Section 5.2 of Chapter 5 is concerned with the ultra-high-speed mode-locking operation of semiconductor lasers, as well as the physical processes involved in this fast operation.

For near future application of semiconductor mode-locked lasers in communication systems, the repetition rate of the lasers must be in the range of 10 GHz

to 40 GHz. These repetition rates can only be achieved with cavity length longer than 1 mm. Achieving good CW mode-locking lasing with such long cavities in a monolithic device is presently the topic of several research teams. One possibility is the use of a quantum well intermixing technique to passivate part of the laser cavity [57, 58], producing an integrated extended cavity. Also the use of a ring cavity, which has a higher Q factor than linear Fabry-Perot cavities, allows CW mode-locked operation of long semiconductor lasers. Moreover, ring cavities are more attractive for applications of mode-locked lasers in optoelectronic integrated circuits. These matters, concerning mode-locked ring lasers, are addressed in section 5.3 of Chapter 5.

The realisation of more complex integrated devices based on mode-locked lasers to execute several different functions is also one of the current areas of research and development. A monolithic multisection mode-locked laser device could provide optical and microwave emission, with wavelength and repetition rate tuneability, timing stabilisation, power amplification, as well as light detection for monitoring and synchronisation, all in one chip [40, 54]. Likewise, the use of mode-locked lasers to perform signal processing, as in a clock recovery device for all optical signal regeneration, which is further discussed in section 5.5 of Chapter 5. The above listed current topics, among many others not mentioned, highlight the importance of research and development on semiconductor mode-locked laser physics and technology.

2.7 - References to Chapter 2

- [1] - A. E. Siegman, *Lasers*, Oxford University Press, 1986.
- [2] - A. Yariv, *Quantum Electronics*, 3rd edition, Wiley, 1989, Chapter 20.
- [3] - G. H. C. New, "The generation of ultrashort laser pulses", *Reports on Progress in Phys.*, vol. 46, pp. 877-971, 1983
- [4] - H. A. Haus, "Theory of mode locking with a fast saturable absorber", *J. Appl. Phys.*, vol. 46, pp. 3049-3058, July 1975, and H. A. Haus, "Theory of mode locking with a slow saturable absorber", *IEEE J. Quantum Electron.*, vol. 11, pp. 736-746, Sep. 1975
- [5] - K. Y. Lau, "Narrow-band modulation of semiconductor lasers at millimeter wave frequencies (>100 GHz) by mode locking", *IEEE J. Quantum Electron.*, vol. 26, pp. 250-261, Feb. 1990
- [6] - D. J. Derickson, R. J. Helkey, A. Mar, J. R. Karin, J. G. Wasserbauer and J. E. Bowers, "Short pulse generation using multisegment mode-locked semiconductor lasers", *IEEE J. Quantum Electron.*, vol. 28, pp. 2186-2202, Oct. 1992.
- [7] - P. P. Vasil'ev, "Ultrashort pulse generation in diode lasers", *Optical and Quantum Electron.*, vol. 24, pp. 801-824, 1992.
- [8] - P.-T. Ho, L. A. Glasser, E. P. Ippen and H. A. Haus, "Picosecond pulse generation with a CW GaAlAs laser diode", *Appl. Phys. Lett.*, vol. 33, pp. 241-242, Aug. 1978
- [9] - J. Kuhl, M. Serenyi and E. O. Göbel, "Bandwidth-limited picosecond pulse generation in an actively mode-locked GaAs laser with intracavity chirp compensation", *Optics Lett.*, vol. 12, pp. 334-336, May 1987
- [10] - R. S. Tucker, U. Koren, G. Raybon, C. A. Burrus, B. I. Miller, T. L. Koch and G. Eisenstein, "40 GHz active mode-locking in a 1.5 μm monolithic extended-cavity laser", *Electron. Lett.*, vol. 25, pp. 621-622, May 1989
- [11] - P. B. Hansen, G. Raybon, U. Koren, B. I. Miller, M. G. Young, M. Chien, C. A. Burrus, and R. C. Alferness, "5.5-mm long InGaAsP monolithic extended-cavity laser with a integrated bragg-reflector for active mode-locking", *IEEE Photon. Technol. Lett.*, vol. 4, pp. 215-217, Mar. 1992.
- [12] - A. G. Waber, M. Schell, G. Fischbeck and D. Bimberg, "Generation of single femtosecond pulses by hybrid mode locking of a semiconductor laser", *IEEE J. Quantum Electron.*, vol. 28, pp. 2220-2229, Oct. 1992.
- [13] - Y. Silberberg, P. W. Smith, D. J. Eilenberger, D. A. B. Miller, A. C. Gossard and W. Wiegmann, "Passive mode locking of a semiconductor diode laser", *Optics Lett.*, vol. 9, pp. 507-509, Nov. 1984
- [14] - C. Harder, J. S. Smith, K. Y. Lau and A. Yariv, "Passive mode-locking of buried heterostructure lasers with nonuniform current injection", *Appl. Phys. Lett.*, vol. 42, pp. 772-774, May 1983

- [15] - T. Schrans, S. Sanders and A. Yariv, "Broad-band wavelength tunable picosecond pulses from CW passively mode-locked two-section multiple quantum-well lasers", *IEEE Photon. Technol. Lett.*, vol. 4, pp. 323-326, Apr. 1992
- [16] - D. J. Derickson, R. J. Helkey, A. Mar, J. R. Karin, J. E. Bowers and R. L. Thornton, "Suppression of multiple pulse formation in external-cavity mode-locked semiconductor lasers using intrawaveguide saturable absorbers", *IEEE Photon. Technol. Lett.*, vol. 4, pp. 333-335, Apr. 1992
- [17] - S. Arahira, Y. Matsui, T. Kunii, S. Oshiba and Y. Ogawa, "Optical short pulse generation at high repetition rate over 80 GHz from a monolithic passively modelocked DBR laser diode", *Electron. Lett.*, vol. 29, pp. 1013-1015, May 1993
- [18] - W. Jiang, M. Shimizu, R. P. Mirin, T. E. Reynolds and J. E. Bowers, "Femtosecond periodic gain vertical-cavity lasers", *IEEE Photon. Technol. Lett.*, vol. 5, pp. 23-25, Jan. 1993
- [19] - P. W. Smith, Y. Silberberg and D. A. B. Miller, "Mode locking of semiconductor diode lasers using saturable excitonic nonlinearities", *J. Opt. Soc. Am. B*, vol. 2, pp. 1228-1236, July 1985
- [20] - E. P. Ippen, D. J. Eilenberger and R. W. Dixon, *Picosecond Phenomena II*, edited by R. Hochstrasser, W. Kaiser, and C. V. Shank, pp. 21-25, Springer, New York, 1980
- [21] - H. Yokoyama, H. Ito, and H. Inaba, "Generation of subpicosecond coherent optical pulses by passive mode locking of an AlGaAs diode laser", *Appl. Phys. Lett.*, vol. 40, pp. 105-107, Jan. 1982
- [22] - J. P. Van der Ziel, W. T. Tsang, R. A. Logan, R. M. Mikulyak and W. M. Augustyniak, "Subpicosecond pulses from passively mode-locked GaAs buried optical guide semiconductor lasers", *Appl. Phys. Lett.*, vol. 39, pp. 525-527, Oct. 1981
- [23] - E. L. Portnoi and A. V. Chelnokov, "Characteristics of heterostructure lasers with a saturable absorber fabricated by deep ion implantation", *Sov. Tech. Phys. Lett.*, vol. 15, pp. 432-433, 1989
- [24] - J. H. Zarrabi, E. L. Portnoi and A. V. Chelnokov, "Passive mode locking of a multistriple single quantum well GaAs laser diode with an intracavity saturable absorber", *Appl. Phys. Lett.*, vol. 59, pp. 1526-1528, Sep. 1991
- [25] - E. L. Portnoi and A. V. Chelnokov, "Passive mode-locking in a short cavity diode laser", in *12th IEEE International Semiconductor Laser Conference*, Davos, Switzerland, 1990, pp. 140-141.
- [26] - P. P. Vasil'ev and A. B. Sergeev, "Generation of bandwidth-limited 2 ps pulses with 100 GHz repetition rate from multisegment injection laser", *Electron. Lett.*, vol. 25, pp. 1049-1050, Aug. 1989
- [27] - S. Sanders, L. Eng, J. Paslaski and A. Yariv, "108 GHz passive mode locking of a multiple quantum well semiconductor laser with an intracavity absorber", *Appl. Phys. Lett.*, vol. 56, pp. 310-311, Jan. 1990

- [28] - S. Sanders, L. Eng, and A. Yariv, "Passive mode-locking of monolithic InGaAs/AlGaAs double quantum well lasers at 42 GHz repetition rate", *Electron. Lett.*, vol. 26, pp. 1087-1089, July 1990
- [29] - C. Weisbuch and B. Vinter, *Quantum semiconductor structures: fundamentals and applications*, Academic Press, 1991.
- [30] - S. Schmitt-Rink, D. S. Chemla and D. A. B. Miller "Linear and nonlinear optical properties of semiconductor quantum wells" *Advances in Physics*, vol. 38, no. 2, pp. 89-188, 1989.
- [31] - D. S. Chemla, D. A. B. Miller and P. W. Smith, "Nonlinear optical properties of multiple quantum well structures for optical signal processing", *Semiconductors and Semimetals*, vol. 24, Editor Raymond Dingle, Academic Press, 1987, Chapter 5.
- [32] - H. A. Haus and Y. Silberberg, "Theory of mode locking of a laser diode with a multiple-quantum-well structure", *J. Opt. Soc. Am. B*, vol. 2, pp. 1237-1243, July 1985.
- [33] - O. E. Martinez, R. L. Fork and J. P. Gordon, "Theory of passively mode-locked lasers including self-phase modulation and group-velocity dispersion", *Optics Lett.*, vol. 9, pp. 156-158, May 1984
- [34] - G. P. Agrawal and N. A. Olsson, "Self-phase modulation and spectral broadening of optical pulses in semiconductor laser amplifiers", *IEEE J. Quantum Electron.*, vol. 25, pp. 2297-2306, Nov. 1989.
- [35] - G. P. Agrawal, "Effect of gain dispersion on ultrashort pulse amplification in semiconductor laser amplifiers", *IEEE J. Quantum Electron.*, vol. 27, pp. 1843-1849, June 1991
- [36] - D. J. Derickson, R. J. Helkey, A. Mar, J. G. Wasserbauer, W. B. Jiang and J. E. Bowers, "Modelocked semiconductor lasers: short pulse, small package!", *Optics & Photonics News*, vol. 3, no. 5, pp. 14-20, May 1992
- [37] - G. P. Agrawal, *Nonlinear Fiber Optics*, Quantum Electronics: Principles and Applications Series, Academic Press, 1989.
- [38] - M. Osinski and J. Buus, "Linewidth broadening factor in semiconductor lasers - an overview", *IEEE J. Quantum Electron.*, vol. 23, pp. 9-29, Jan. 1987
- [39] - L. Olofsson and T. G. Brown, "On the linewidth enhancement factor in semiconductor lasers", *Appl. Phys. Lett.*, vol. 57, pp. 2773-2775, Dec. 1990
- [40] - R. Helkey and J. Bowers, "Mode locked semiconductor lasers", *Semiconductor Lasers: Past, Present and Future*, Edited by G. P. Agrawal, American Institute of Physics Press, 1993.
- [41] - Y. K. Chen and C. W. Ming, "Monolithic colliding-pulse mode-locked quantum-well lasers", *IEEE J. Quantum Electron.*, vol. 28, pp. 2177-2185, Oct. 1992
- [42] - R. L. Fork, B. I. Greene and C. V. Shank, "Generation of optical pulses shorter than 0.1 psec by colliding pulse mode locking", *Appl. Phys. Lett.*, vol. 38, pp. 671-672, May 1981

- [43] - D. Kühlke, W. Rudolph and B. Wilhelmi, "Influence of transient absorber gratings on the pulse parameters of passively mode-locked cw dye lasers", *Appl. Phys. Lett.*, vol. 42, pp. 325-327, Feb. 1983
- [44] - R. L. Fork, C. V. Shank, R. Yen and C. A. Hirlimann, "Femtosecond optical pulses", *IEEE J. Quantum Electron.*, vol. 19, pp. 500-505, Apr. 1983
- [45] - M. S. Stix and E. P. Ippen, "Pulse shaping in passively mode-locked ring dye lasers", *IEEE J. Quantum Electron.*, vol. 19, pp. 520-525, Apr. 1983
- [46] - P. P. Vasil'ev, V. N. Morozov, Y. M. Popov and A. B. Sergeev, "Subpicosecond pulse generation by a tandem-type AlGaAs DH laser with colliding pulse mode locking", *IEEE J. Quantum Electron.*, vol. 22, pp. 149-151, Jan. 1986
- [47] - C. F. Lin and C. L. Tang, "Colliding pulse mode locking of a semiconductor laser in an external ring cavity", *Appl. Phys. Lett.*, vol. 62, pp. 1053-1055, Mar. 1993
- [48] - Y. K. Chen, M. C. Wu, T. Tanbun-Ek, R. A. Logan and M. A. Chin, "Subpicosecond monolithic colliding-pulse mode-locked multiple quantum well lasers", *Appl. Phys. Lett.*, vol. 58, pp. 1253-1255, Mar. 1991.
- [49] - Y. K. Chen, M. C. Wu, T. Tanbun-Ek, R. A. Logan and M. A. Chin, "Multicolor single-wavelength sources generated by a monolithic colliding pulse mode-locked quantum well laser", *IEEE Photon. Technol. Lett.*, vol. 3, pp. 971-973, Nov. 1991
- [50] - M. C. Wu, Y. K. Chen, T. Tanbun-Ek, R. A. Logan, M. A. Chin and G. Raybon, "Transform-limited 1.4 ps optical pulses from a monolithic colliding-pulse mode-locked quantum well laser", *Appl. Phys. Lett.*, vol. 57, pp. 759-761, Aug. 1990.
- [51] - L. M. Zhang and J. E. Carroll, "Dynamic response of colliding-pulse mode-locked quantum-well lasers", *IEEE J. Quantum Electron.*, vol. 31, pp. 240-243, Feb. 1995
- [52] - S. Sanders, T. Schrans, A. Yariv, J. Paslaski, J. E. Ungar and H. A. Zarem, "Timing jitter and pulse energy fluctuations in a passively mode-locked two-sections quantum-well laser coupled to an external cavity", *Appl. Phys. Lett.*, vol. 59, pp. 1275-1277, Sep. 1991
- [53] - D. J. Derickson, P. A. Morton, J. E. Bowers and R. L. Thornton, "Comparison of timing jitter in external and monolithic cavity mode-locked semiconductor lasers", *Appl. Phys. Lett.*, vol. 59, pp. 3372-3374, Dec. 1991
- [54] - D. J. Derickson, R. J. Helkey, A. Mar, J. G. Wasserbauer, Y. G. Wey, and J. E. Bowers, "Microwave and millimeter wave signal generation using mode-locked semiconductor lasers with intra-waveguide saturable absorbers", in *IEEE International Microwave Theory and Technology Symposium*, Albuquerque, USA, 1992, paper V-2, pp. 753-756
- [55] - R. J. Helkey, D. J. Derickson, A. Mar, J. G. Wasserbauer, J. E. Bowers and R. L. Thornton, "Repetition frequency stabilisation of passively mode-locked semiconductor lasers", *Electron. Lett.*, vol. 28, pp. 1920-1922, Sep. 1992

[56] - J. B. Georges, L. Buckman, D. Vassilovski, J. Park, M.-H. Kiang, O. Solgaard and K. L. Lau, "Stable picosecond pulse generation at 46 GHz by modelocking of a semiconductor laser operating in an optoelectronic phaselocked loop", *Electron. Lett.*, vol. 30, pp. 69-71, Jan. 1994

[57] - R. M. De La Rue and J. H. Marsh, "Integration technologies for III-V semiconductor optoelectronics based on quantum well waveguides", in *Integrated Optics and Optoelectronics*, K. -K. Wong and M. Razeghi, Eds. Los Angeles, CA:SPIE (Int. Soc. Opt. Eng.), pp. 259-288, Jan. 1993.

[58] - I. Gontijo, T. Krauss, J. H. Marsh, and R. M. De La Rue, "Postgrowth control of GaAs/AlGaAs quantum well shapes by impurity-free vacancy diffusion", *IEEE J. Quantum Electron.*, vol. 30, pp. 1189-1195, May 1994

Chapter 3: Device Fabrication

The monolithic colliding pulse mode-locked (CPM) laser configuration consists of a laser which has a saturable absorber section integrated in the middle of the cavity. Figure 3.1 shows a schematic diagram of a CPM laser, where one can see the saturable absorber section in between the gain sections of the laser. This particular geometry induces the laser to generate short pulses at a repetition rate that is dependent on the cavity length. In other words the laser is mode-locked. The peculiarity of this device, which is having different sections monolithically integrated, demands specific fabrication procedures in order to construct the device, as well as to obtain the desired performance from it. For example the dimension, position and isolation of each section from each other determine the characteristics and operation conditions of the device. This chapter covers the fabrication of monolithic CPM semiconductor lasers, from the description of the wafer used, up to mounting the device for tests.

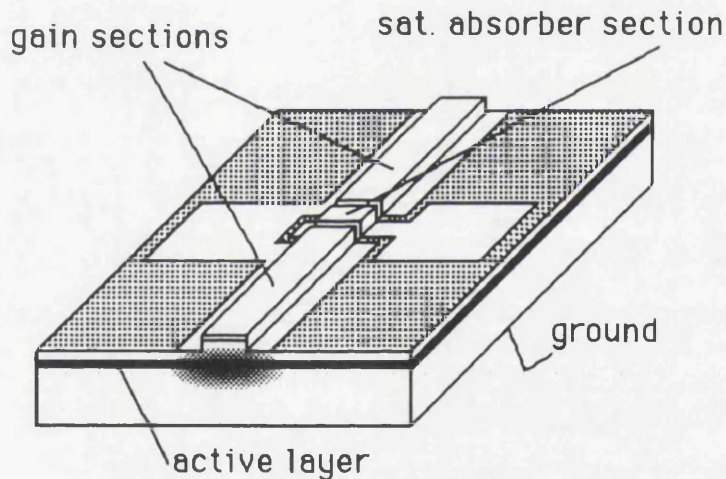


Figure 3.1: Schematic diagram of the colliding pulse mode-locked (CPM) laser configuration. Gradient indicates laser output at the waveguide.

Section 3.1 describes the semiconductor material structure as well as the procedure to characterise it as a laser, where parameters such as efficiencies, losses and current densities are obtained. Section 3.2 is concerned with the waveguide structure used in the mode-locked lasers, whereas in section 3.3 every process of fabrication of the lasers is described in details. Section 3.4 emphasises and further discusses some crucial steps of the fabrication procedure. It also brings the analysis of preliminary tests performed on the devices and the conclusion of the chapter. The references to this chapter are listed in section 3.5.

3.1 - Material Structure and Characterisation

The lasers are fabricated using a wafer which includes an active layer of GaAs/AlGaAs 4 quantum wells, grown by atmospheric pressure metal organic vapour phase epitaxy (APMOVPE) in Sheffield University. The semiconductor material structure consists of a 0.2 μm thick, heavily p-doped with zinc ($2 \times 10^{19} \text{ cm}^{-3}$), GaAs cap layer. It is followed by 1 μm p-type carbon doped ($2.2 \times 10^{17} \text{ cm}^{-3}$) $\text{Al}_{0.43}\text{Ga}_{0.57}\text{As}$ upper cladding layer. The quantum well structure consists of four 10 nm GaAs wells spaced by three 10 nm $\text{Al}_{0.20}\text{Ga}_{0.80}\text{As}$ barriers and they are surrounded by two 0.1 μm $\text{Al}_{0.20}\text{Ga}_{0.80}\text{As}$ layers in a separate confinement structure. These guiding layers are undoped. The lower cladding layer is formed by $\text{Al}_{0.43}\text{Ga}_{0.57}\text{As}$ silicon n-doped ($1.4 \times 10^{17} \text{ cm}^{-3}$) layer 1.7 μm thick. A Hitachi GaAs substrate and a 1 μm thick GaAs buffer layer, both n-doped with silicon ($1.5 \times 10^{18} \text{ cm}^{-3}$), are used. This material structure is shown in figure 3.2.

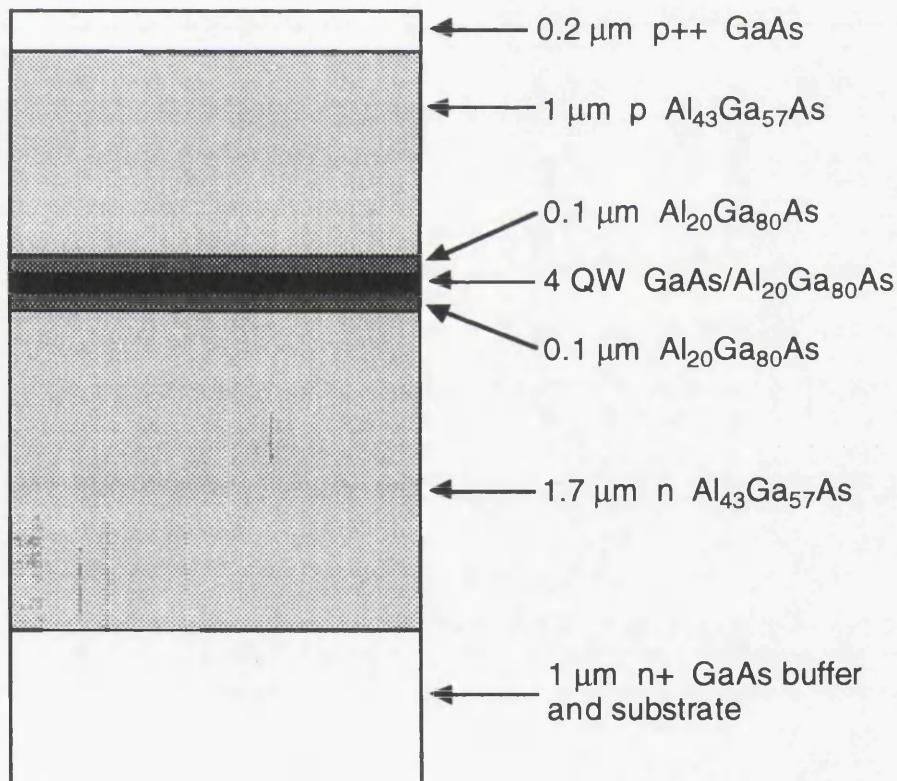


Figure 3.2: Cross-section of the gallium arsenide/aluminium gallium arsenide semiconductor material, with thickness and composition of each layer.

The characterisation of the wafer as a laser material is performed by fabricating a simple wide oxide stripe gain guided laser and obtaining the internal losses, quantum efficiency, threshold current density, transparency current density and differential gain from it [1]. This structure is suitable for the characterisation purposes since the 75 μm wide stripe used allows the neglect of the current spreading effect in the upper cladding

layer of the material. The current spreading makes the effective current injection area larger than the actual area of the stripe structure, which introduces an error to the calculation of the current densities [1, 2]. Besides, the gain guiding structure is free from extra losses (mainly scattering) that could be introduced by an index guided structure like rib or ridge waveguides, for example. Therefore the characteristics measured here are concerned to the quality of the semiconductor material only. It is useful to have an idea of the quality of the material prior to the fabrication of more complex structures and devices.

Lasers are cleaved into 3 different lengths, which are 400 μm , 600 μm and 1000 μm . Light versus current ($L \times I$) curves for 5 lasers of each length are measured and threshold currents, slope efficiencies and external quantum efficiencies near threshold are obtained. Table 3.1 list the average results for each laser cavity length.

L (μm)	400	600	1000
I_{th} (mA)	175	240	330
J_{th} (A/cm^2)	583	533	440
η_{slope} (W/A)	0.85	0.76	0.69
η_{ext} (%)	60	53	48

Table 3.1: Average values of threshold current I_{th} , threshold current density J_{th} , slope efficiency of both facets η_{slope} and external quantum efficiency of both facets η_{ext} for each cavity length L .

The measured slope efficiency is defined as the ratio between the output power of the laser and the injected current in the laser and it is sometimes called incremental efficiency [1]. A conversion factor of 0.7 (for 870 nm wavelength) is used to obtain the external quantum efficiency, which is defined as the ratio between the number of photons ejected from the laser and the number of carriers injected in the laser [3]. Plotting $1/\eta_{\text{ext}}$ as a function of the cavity length, as shown in figure 3.3, and using the expression for the external quantum efficiency [1, 3]

$$\frac{1}{\eta_{\text{ext}}} = \frac{1}{\eta_{\text{int}}} \cdot \left(\frac{\alpha \cdot L}{\ln\left(\frac{1}{R}\right)} + 1 \right) \quad (3.1)$$

where α is the total internal loss (including scattering and free carriers absorption losses), R is the facet reflectivity (0.31) and η_{int} is the internal quantum efficiency; one can obtain the α and η_{int} , which are $\alpha = 5.5 \text{ cm}^{-1}$ and $\eta_{\text{int}} = 69 \%$. Typical values found in the literature indicate that a good laser should have losses lower than 10 cm^{-1}

and internal efficiency around 90 %. Therefore these results indicate that the material has low losses and reasonably good efficiency.

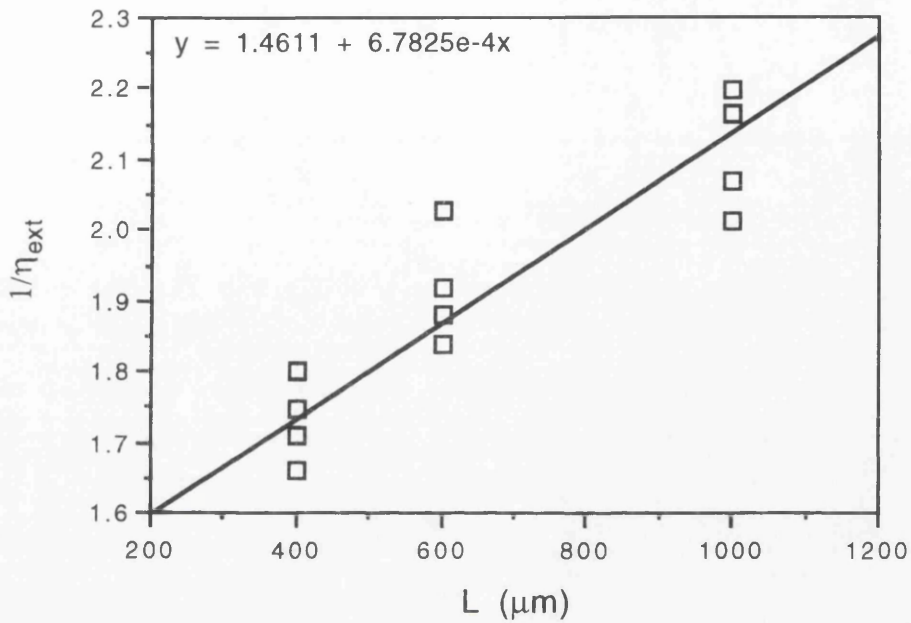


Figure 3.3: Reciprocal of external quantum efficiency η_{ext} plotted versus the length of the laser cavity L (empty squares). Linear fitting (line) and fitting equation are also shown.

Further characterisation can be performed by plotting the average values of the threshold current density shown in table 3.1 versus the reciprocal of the cavity length, as shown in figure 3.4; and using the equation for J_{th} [4]

$$J_{th} = \frac{J_o}{\eta_{int}} + \frac{\alpha}{\Gamma \eta_{int} A} + \frac{1}{\Gamma \eta_{int} A} \cdot \left(\frac{1}{2L}\right) \cdot \ln\left(\frac{1}{R_1 R_2}\right) \quad (3.2)$$

where J_o is the transparency current density and represents the injected current needed to provide population inversion up to the point where the material is transparent, with no absorption nor gain. A is the differential gain and represents the rate of gain increase with injected current (dg/dJ). Γ is the optical confinement factor. It represents the overlap of the optically guided mode with the quantum wells [4], and it is given by an approximate expression [5]

$$\Gamma = 0.3N(L_z / L_o) \quad (3.3)$$

where N is the number of quantum wells, L_z is the width of the well in angstroms and L_o is 1000 Å. For the material structure used and described above $N = 4$ and $L_z =$

100 Å, which gives $\Gamma = 0.12$. Using figure 3.4 and equation 3.2, with the values of α and η_{int} obtained from equation 3.1 and figure 3.3, the values of J_0 and A can be obtained, which are $J_0 = 220 \text{ A/cm}^2$ and $A = 1.48 \text{ cm/A}$.

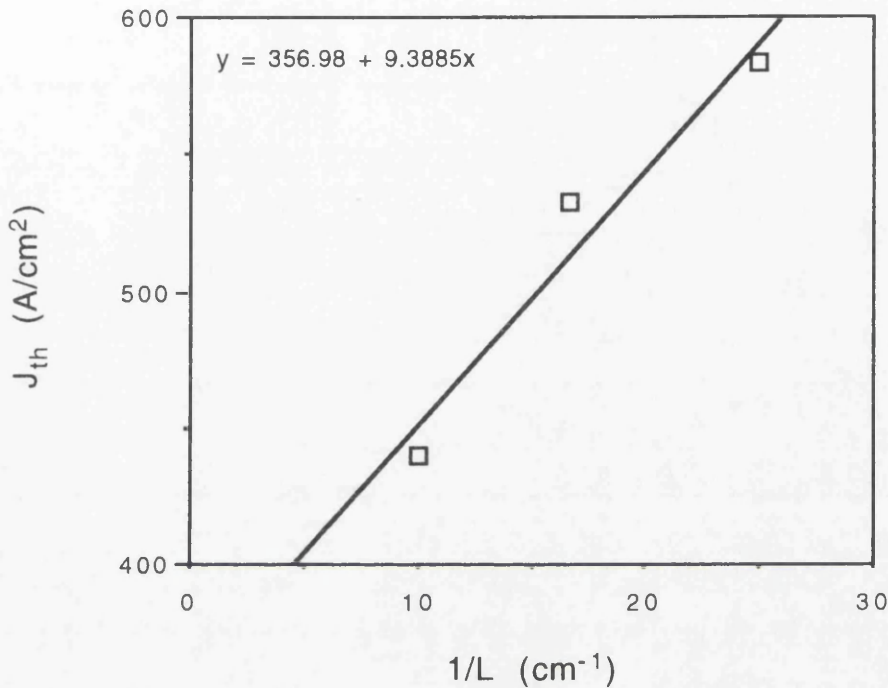


Figure 3.4: Threshold current density J_{th} plotted versus reciprocal of cavity length L (empty squares). Linear fitting (line) and fitting equation are also shown.

3.2 - Waveguide Structure

The semiconductor material structure described above provides optical confinement in the vertical direction (perpendicular to the layers) due to its different aluminium composition in each layer. The refractive index of $\text{Al}_x\text{Ga}_{1-x}\text{As}$ based materials decreases as the amount of aluminium (x) increases [1, 6]. But in order to obtain low threshold lasers optical confinement in the horizontal direction (parallel to the layers) must also be granted. 3-D index guiding in semiconductor lasers is usually accomplished by fabricating strip-loaded or buried channel waveguides [1, 7]. The former seems to be the best compromise in terms of cost, complexity and performance. Figure 3.5 shows the cross-section of the strip-loaded (or rib) waveguide fabricated. The stripe width is $3 \mu\text{m}$ and its height is $0.6 \mu\text{m}$. The layers of the material structure and the fundamental mode of propagation are also shown. The contours shown represent 10 % (outer) and 30 % (inner) of the peak field value for the fundamental TE mode of propagation at 870 nm wavelength. They were obtained from numerical calculations performed with Fwave III software [8] for this waveguide structure. The refractive indices used for each layer in the calculations are 3.62 for GaAs, 3.48 for

$\text{Al}_{0.20}\text{Ga}_{0.80}\text{As}$ and 3.34 for $\text{Al}_{0.43}\text{Ga}_{0.57}\text{As}$ [1, 6]. The fabrication proceedings used in order to construct this waveguide will be discussed in detail in the following section.

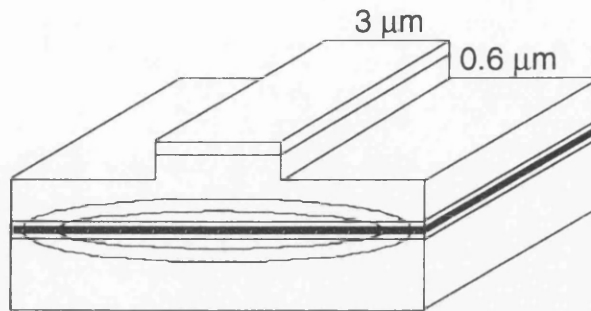


Figure 3.5: Perspective view of the cross-section of the rib waveguide laser. Contours of the fundamental mode of propagation and layers of semiconductor material structure are also shown. The dark line represents the 4 quantum well layers.

3.3 - Fabrication Technique

The technique employed to fabricate the monolithic mode-locked semiconductor lasers is described here, step by step, starting from the scribing of the semiconductor wafer up to the point where the laser is ready for tests. The general technology and processes for semiconductor device fabrication can be found in reference 6. The fabrication procedure is:

1) Sample cleaving: cleavage of a 11 x 11 mm sample from the semiconductor wafer using the wafer scribe. The cleavage must follow the crystal orientation of the semiconductor material.

2) Sample cleaning: by immersion in the organic solvents: trichloroethane ($\text{C}_2\text{H}_3\text{Cl}_3$), methanol (CH_3OH) and acetone ($\text{C}_3\text{H}_6\text{O}$), in this order, in ultrasonic bath for 5 minutes for each solvent. It is followed by R. O. (reverse osmosis) water rinsing and nitrogen blow drying.

3) Resist spinning: using photoresist S1400-17 spun at 4000 rpm for 30 seconds. This is a positive photoresist and its final thickness is approximately 0.5 μm .

4) Resist baking: place sample with resist in the oven at 90°C for 30 minutes.

5) Photolithography: for waveguide definition using the contact printer. The use of contact printer and thinner resist seem to give better results than the more usual mask aligner and thicker resist (S1400-31, 1.8 μm thick), in terms of pattern definition. The waveguide mask consists of 19 stripes, each one being 3 μm wide and 10 mm long, separated from each other by 600 μm , which forms a 10 by 10 mm mask. The alignment of the waveguide stripes parallel to the cleaved edge of the sample is very important and critical. It will guarantee laser facets perpendicular to the laser waveguide at the laser cleaving stage. The use of a mask aligner instead of a contact printer should

make this alignment much easier without serious disadvantage in terms of pattern definition. Exposure time and developing are as standard.

6) Hard mask deposition: evaporation of 20 nm of nichrome (NiCr), which is an alloy of nickel (90%) and chromium (10%), to serve as a metal hard mask for the dry etching process (with SiCl_4) that will form the waveguide. The use of a metal mask for dry etching the semiconductor presents some advantages to the use of more standard SiO_2 layer as a hard mask. Firstly it saves time and it is a simpler process, since the silica technique involves SiO_2 deposition and dry etching (with C_2F_6) to form the mask, which is a more delicate and time demanding process than metal evaporation and lift-off. More importantly, the final result of etching with a metal mask has been shown to be consistently better than with silica mask. It gives better verticality and less roughness to the waveguide walls, and it makes measurements of etch depth more accurate. This is because there is some erosion of the silicon dioxide mask when the sample is under SiCl_4 dry etching.

7) Lift-off: by immersing the sample in acetone for a few minutes. Rinse sample in R. O. water afterwards. A thicker resist is usually applied for lift-off, but in this case the thin metal layer can be easily lifted-off with the thin resist.

8) Dry etching: reactive ion etching (RIE) using silicon tetrachloride (SiCl_4) is performed in order to form the waveguide. Differently from the chemical wet etching, the dry etching is an anisotropic process and it removes the semiconductor material from the non-masked region by physical-chemical reactions with a plasma formed with the etchant gas (SiCl_4 in this case) [9]. The final etch depth is 0.6 μm and the typical etch rate is 150 nm/min. At this stage the waveguide, as shown in figure 3.5, is fabricated.

9) Removal of metal mask: by wet etching the NiCr mask with hydrochloric acid (HCl) diluted in water (HCl - 4, H_2O - 1). The etch rate is 10 nm/min approximately, but 50% over-etching is performed in order to guarantee the complete removal of the metal from the top of the waveguide. Therefore the etch time is 3 minutes. The etch rate of nichrome etchant on GaAs is only 5 nm/min, which is too low to actually damage the GaAs cap layer of the material for the etching time used.

10) Sample cleaning: as in step 2.

11) Silica deposition: SiO_2 deposition by plasma enhanced chemical vapour deposition (PECVD) [10]. Layer thickness is 200 nm. This silicon dioxide layer will serve as a current injection blocking layer.

12) Sample cleaning: as in step 2.

13) Resist spinning: using photoresist S1400-17 spun at 4000 rpm for 30 seconds, as in step 3.

14) Resist baking: place sample with resist in the oven at 90°C for 30 minutes, as in step 4.

15) Photolithography: to open a current injection window on top of the waveguide using the mask aligner. The thinner resist used makes the mask alignment easier than with thicker ones, since the mask can come closer to the sample before touching the resist layer. The dark field ferric oxide mask consists of a set of 7 μm wide stripes, fitting the waveguide mask described in step 5. 50% overexposure and 20% over-development is used to ensure the removal of the resist. The quality of the transferred pattern is not a critical issue here since the resist will serve as a mask for a wet etching process.

16) Post-baking: place sample with resist in the oven at 120°C for 60 minutes. The post-baking is required to harden the resist before etching.

17) Wet etching: wet chemical etching with buffered hydrofluoric acid (HF) is used to remove the silicon dioxide layer from the top of the waveguide, opening a current injection window on it. The etch rate is approximately 10 nm/s, but 100% over-etching is used to ensure the total removal of the silica. The etching time is 40 seconds. HF does not etch GaAs.

18) Sample cleaning: as in step 2.

19) Resist spinning: using photoresist S1400-31 spun at 4000 rpm for 30 seconds. This is a positive photoresist and its final thickness is approximately 1.8 μm .

20) Resist baking with chlorobenzene: place sample with resist in the oven at 90°C for 15 minutes. Then immerse the sample in chlorobenzene ($\text{C}_6\text{H}_5\text{Cl}$) for 15 minutes and finally bake it again at 90°C for 15 minutes. The use of thicker resist and chlorobenzene facilitate the lift-off of thick layers of metal.

21) Photolithography: to define the metallised sections of the laser. The dark field ferric oxide mask will define the layout of the top metallisation of the laser, delimiting its different sections. The gain and saturable absorber sections are separated by a gap of 10 μm . The contact pads to the different sections and laser cleavage marks are also included in this mask. Exposure time and developing are as standard.

22) Deoxidising etch: with HCl and water (HCl - 4, H_2O - 1) for 30 seconds, to remove any spurious oxide layer that may have been formed on the semiconductor and silica surface prior to the metallic deposition. It improves considerably the adhesion of the metal to the silica layer as well as the electrical properties of the contact. A poor adhesion of the metal to the silica layer underneath it makes gold wire bonding to the contact pads very difficult. This etching is performed just before loading the sample in the vacuum chamber of the evaporator.

23) Top metallisation: deposition of p-type metallic contact by evaporation. An ohmic contact is formed with the deposition of NiCr/Au (20 nm of nichrome and 200 nm of gold). The use of an ohmic contact is an important issue for semiconductor mode-locked lasers since, in the saturable absorber section, carriers are to be removed by reverse biasing the section. In order to achieve good adhesion of the metal to the

silica layer a double de-gas procedure is performed prior to the evaporation. The de-gas process consists of starting the evaporation up to melting the metals to remove impurities from the evaporating boat or crucible and to release any spurious gases from the melted metal, which could contaminate the sample. The first de-gas is done before loading the sample in the chamber, at low vacuum. The second is performed with the sample already loaded, at high vacuum. Typical chamber vacuum for evaporation is 3×10^{-6} mbar. In order to have uniform metal deposition on the walls of the waveguide, the evaporation is performed with the sample tilted by about +45 degrees to one side and -45 degrees to the other side of the waveguide.

24) Lift-off: by immersing the sample in acetone. Rinse sample in R. O. water afterwards. At this point the pattern on top of the sample is completed, with the contacts for gain and absorber sections, contact pads for wire bonding and cleaving marks for more accurate cleaving of individual lasers.

25) Dry etching: to improve the electrical isolation between sections. The electrical isolation between gain and absorber sections is an important issue on the design and fabrication of semiconductor mode-locked lasers, as it will be further discussed in section 3.4. The isolation can be improved by removing the highly doped GaAs cap layer from the gap region between the sections using the selective dry etching technique, which stops on the AlGaAs layer. The metallic contacts and the silica layer on the sample work as the mask for the etching of the gap region only. Two selective etchants were tried. One of them uses the gas Freon-12 (CCL_2F_2 , dichlorodifluoromethane) [11]. This technique has the disadvantage of affecting the SiO_2 layer and of using a non-environmentally-friendly gas. The other uses SiCl_4 at low power [12] and it is the preferred technique. By measuring the resistance between gain and absorber sections when no bias is applied, a DC electrical isolation of $1 \text{ k}\Omega$ is found before etching and $1.5 \text{ k}\Omega$ is obtained after the selective dry etching. These measurements were made with a Hewlett Packard 4145A semiconductor parameter analyser.

26) Resist spinning: using the resist S1400-31 to protect the top of the sample, with waveguide and metallic contacts, prior to the thinning process.

27) Sample cleavage: the $11 \times 11 \text{ mm}$ sample is divided into four $5.5 \times 5.5 \text{ mm}$ samples by cleavage in the scribe. It makes the succeeding thinning process safer and more uniform.

28) Substrate thinning: mechanical polishing of the substrate to thin the samples, reducing the series resistance of the lasers and improving the heat sinking. The initial sample thickness is approximately $450 \mu\text{m}$. The final thickness, after thinning, is approximately $200 \mu\text{m}$.

29) Sample cleaning: by immersion in the organic solvents: trichloroethane for 10 minutes, methanol for 5 minutes, trichloroethane for 5 minutes, methanol for 5

minutes and acetone for 5 minutes, in this order. This process is done in a refluxing condenser with boiling solvents. It is followed by R. O. water rinsing and nitrogen blow drying. Cleaning in the ultrasonic bath is not advisable for metallised and thinned samples since it deteriorates the metal adhesion and it may also break the samples. The longer and repeated immersion in trichloroethane is to ensure the removal of wax used in the previous thinning process to fix the samples.

30) Substrate wet etching: using sulphuric acid (H_2SO_4) diluted in hydrogen peroxide (H_2O_2) and water ($\text{H}_2\text{SO}_4 - 1$, $\text{H}_2\text{O}_2 - 8$, $\text{H}_2\text{O} - 1$), for 2 minutes. The etch rate is $30 \mu\text{m}/\text{min}$. The samples are fixed on a glass slide with wax for easy handling during etch and to protect the top of the sample from the etchant.

31) Sample cleaning: as in step 29.

32) Deoxidising etch: with ammonia diluted in water ($\text{NH}_3 - 1$, $\text{H}_2\text{O} - 2$) for 2 minutes. The samples are fixed on a glass slide with resist for easy handling during etch and subsequent metal evaporation, and to protect the top from the etchant.

33) Base metallisation: deposition of n-type metallic contact by evaporation. An ohmic contact is formed with the deposition of Au/Ge/Au/Ni/Au (14 nm of gold, 14 nm of germanium, 14 nm of gold, 11 nm of nickel and 200 nm of gold). De-gas procedures are used, as in step 23. The figure 3.6 shows the cross-section of the sample at the waveguide at this stage of fabrication.

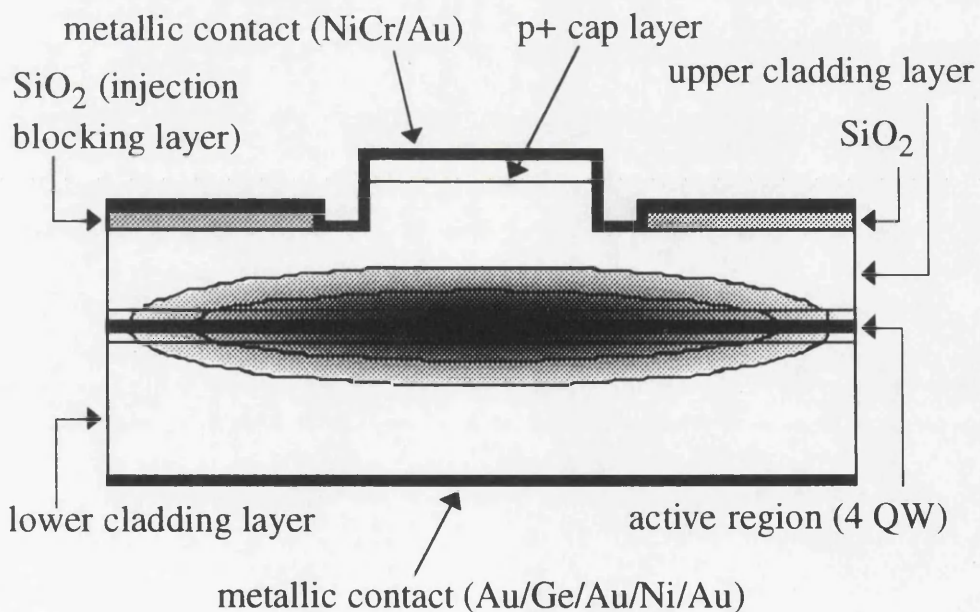


Figure 3.6: Cross-section of the laser at the waveguide. The layers of material structure and the dielectric and metallic layers deposited during the fabrication process are shown. The fundamental TE mode of propagation, with contours of 10% (outer) and 30% (inner) of the peak value of the field at 870 nm, are also shown. The contours were calculated with Fwave III software, as discussed in Section 3.3.

34) Sample cleaning: as step 29.

35) Laser cleavage: using the wafer scribe. Accurate cleavage is a very important issue for the fabrication of mode-locked lasers since the cavity length determines the repetition rate. For colliding pulse mode-locked (CPM) lasers the cleavage requirements are even more demanding because the position of the saturable absorber section in the cavity is critical for its operation. In order to achieve this accuracy, cleavage marks were introduced by photolithography (see step 21) alongside the laser waveguide for individual laser cleavage. The cleavage marks consist of a series of squares ($100 \text{ by } 100 \text{ }\mu\text{m}$) $100 \text{ }\mu\text{m}$ distant from each other, which are arranged along both sides of the waveguide, as shown in figure 3.7. It allows cleavage of cavity lengths in steps of $200 \text{ }\mu\text{m}$. Smaller squares would allow cleavage in smaller steps. The lasers are to be cleaved individually, therefore the sawing of the side facet of the lasers is performed first, by scribing the sample. The cleavage of the end facet of each laser is accomplished by aligning the scribe with one of the edges of the square marks. The device is wide enough ($600 \text{ }\mu\text{m}$) for the scribe to mark the edge of the laser for cleaving without damaging the waveguide at the facet.

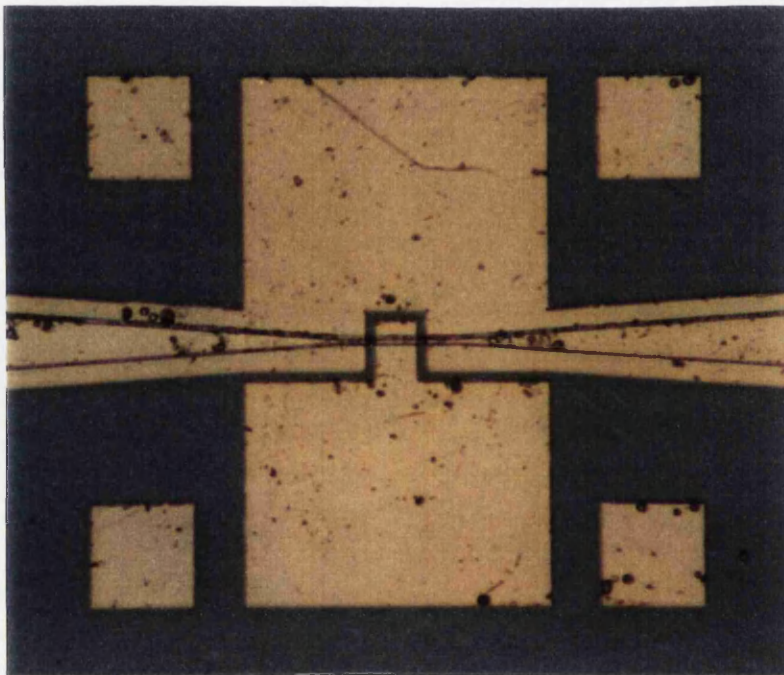


Figure 3.7: Optical microscope photograph of the pattern on top of a sample, where one can see the waveguide (in bow-tie shape), the metallic contact for gain and absorber sections, the contact pads and the cleavage marks ($100 \times 100 \text{ }\mu\text{m}$ squares).

36) Laser soldering: by indium soldering. For CW operation the laser has to be mounted on a base that provides proper heat sinking. The base used is a copper block coated with gold. The laser is soldered to the base with indium. The softness of the indium solder absorbs the strain caused by the different thermal expansion coefficient

between the semiconductor and the metal base. The soldering is accomplished by heating the base to melt the indium solder. A liquid flux (made by RS Co.), which is soluble in trichloroethane, is used to avoid oxidation of the solder. The soldering procedure is: 1) remove the remains of the solder used for previous devices by scraping the surface of the base; 2) apply the liquid flux on the soldering place; 3) heat the base to 180°C; 4) place the indium solder ball at soldering spot, imbedded in flux; 5) place the laser, p-side up, just beside the solder; 6) move the laser towards the solder, turning it to ensure uniform distribution of the solder underneath it and position the laser at the edge of the base; 7) remove the base from the heater and leave it to cool down; 8) clean the base removing the flux by immersing it in trichloroethane for 5 minutes and methanol for 5 minutes (no ultrasonic cleaning nor refluxing condenser are necessary). If the base is heated before the flux is applied to the remaining solder left from previous device, it will oxidise and the soldering spot cannot be re-utilised.

37) Wire bonding: gold wire (25 μm thick) bonding is made from the contact pads on the laser to the pads on the laser mounting, from which the electrical connections to the power supplies will be made. The ultrasonic bonding is performed with a Kulicke & Soffa 4123 wedge bonder. After wire bonding the laser is ready for tests.

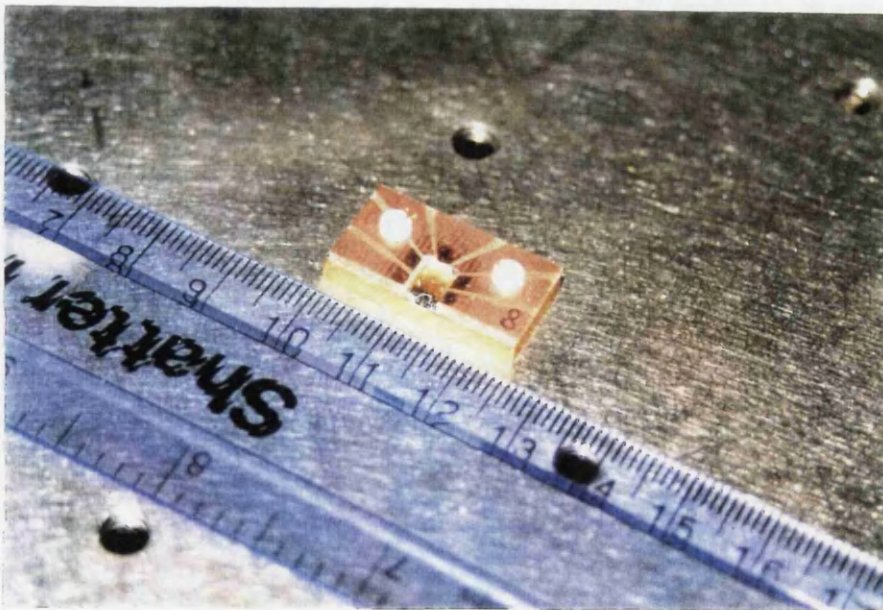


Figure 3.8: Photograph of the multisection mounting used for the mode-locked lasers.

3.4 - Discussions and Conclusions

Some aspects of the design and fabrication of monolithic semiconductor mode-locked lasers are peculiar to this type of device and they will be further discussed here.

The electrical isolation between gain and absorber sections is an important issue on the design and fabrication of mode-locked lasers. Poor isolation allows current to

leak from the gain to the absorber section, decreasing the efficiency of the reverse bias on the absorber. It also drains current from the gain section in the vicinity of the absorber section, making the latter effectively wider. A relatively short and efficient absorber section is important for its saturation and recovery characteristics. As described in step 25 of section 3.3, the electrical isolation can be improved by removing the highly doped GaAs cap layer from the gap regions between sections using a selective dry etching technique, which stops on the AlGaAs layer. In order to assess the effectiveness of this technique, mode-locked lasers with several different gap widths were fabricated. Figure 3.9 shows the measured resistance between sections as a function of the gap width before and after the selective etching. It is observed that this technique gives about 50% improvement on the original isolation (without etching) for narrow gaps (up to 10 μm). Although the isolation increases as the gap width increases, the benefit of the selective etching decreases, from an initial near 50% improvement towards 25%, for very wide gaps. Better isolation can be achieved by deeper etching into the upper cladding layer, using standard (non-selective) dry etching. The resistance increases from 1.5 $\text{k}\Omega$ to 2 $\text{k}\Omega$ when 0.1 μm of cladding layer is etched from the gap region. The isolation also depends on the doping level and thickness of the upper cladding layer and the figures presented here are for our particular material structure. Other authors have successfully used the removal of the cap layer as a method to improve the isolation between sections, obtaining similar resistances to those achieved here [13-16].

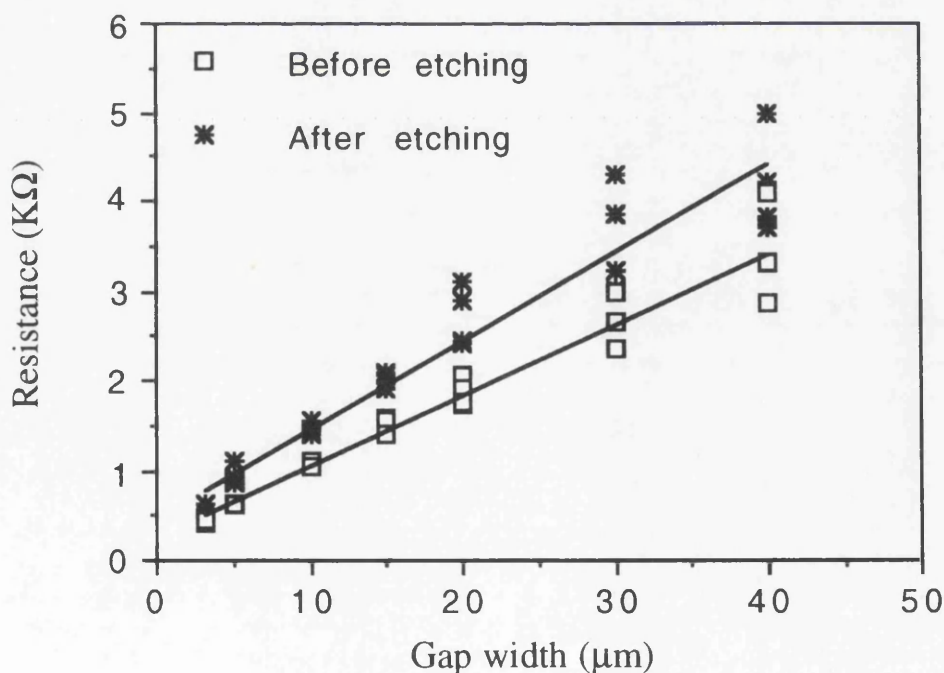


Figure 3.9: Electrical isolation between gain and absorber sections as a function of the width of the gap between sections, before and after the selective etching. The lines are the linear fit to the measured resistance (squares and stars).

In order to achieve the best performance of the metallic contacts for wire bonding, several proceedings were taken, including the use of a deoxidising etching before contact evaporation, the use of a de-gas procedure before evaporation, the use of NiCr/Au p-type contact and the use of cleaning processes other than ultrasonic, as described in section 3.3. Another important process that affects the contacts is the thermal annealing. It was found that the usual temperatures used for annealing the contacts (above 250°C) deteriorate the adhesion of the metal to the silica layer underneath it. The annealed contact peels off when wire bonding is tried. Therefore non-annealed lasers were experimented. Electrical tests were performed with the parameter analyser, which show that the non-annealed lasers have a typical dynamic resistance of 20 Ω and a reverse breakdown voltage of 15 V. Figure 3.10 shows the $I \times V$ curve of a mounted non-annealed laser. Although a lower resistance can be achieved with other contact recipes and annealing, the one used with no annealing seems to be the best compromise in terms of the electrical and mechanical properties of the contact. Future studies of new metallic contact recipes and other wire bonding processes should lead to improvements in the dynamic resistance and contact adhesion, with benefits to the overall laser operation, such as lower threshold current and higher efficiency.

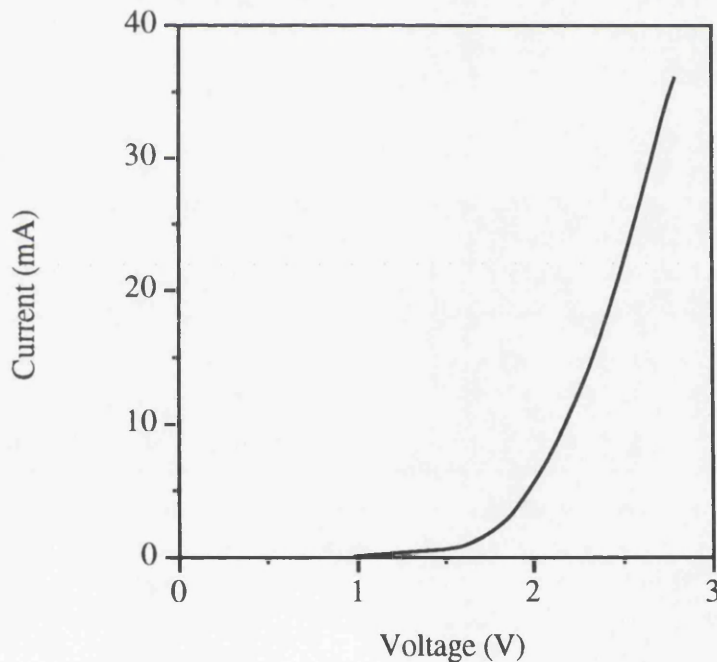


Figure 3.10: Current versus voltage ($I \times V$) curve of a mounted and non-annealed mode-locked laser. The dynamic resistance is 20 Ω at 30 mA (around threshold current).

Accurate cleavage of the end facets of Fabry-Perot cavity mode-locked lasers is crucial for their operation, as discussed in step 35 of section 3.3. The cleavage mark

technique introduced represents a significant improvement on quality and accuracy of cleavage in relation to the usual and more standard way of doing it, which consists of moving the sample with a micrometer and defining the cavity length from its reading. Cavity lengths are of the order of a few hundreds of microns ($500\ \mu\text{m}$ for example). Assuming an underestimated relative error on the micrometer of 2%, the inaccuracy of the cavity length would be of $10\ \mu\text{m}$. Besides, backlash and reading errors are likely to contribute to a larger inaccuracy of cavity length measurements. The cleavage mark technique overcomes these problems and its limitations lie mainly in accurate alignment of the scriber to the marks. It is performed with the use of 2 optical monoculares. One points from the top of the sample, with 50 times magnification maximum, and a referenced eye piece. The other is pointed to the side of the sample, at approximately 45 degrees, with 5 times magnification. The estimated error is of 3 to $5\ \mu\text{m}$ maximum. It represents an inaccuracy of 750 MHz (1%) in the determination of the repetition rate of a $500\ \mu\text{m}$ long CPM laser. The use of a monocular with 100 times magnification should improve on it. CPM lasers require the saturable absorber section to be positioned at the centre of the cavity. But it was found that the operation of the laser is not significantly affected as long as the exact centre point of the cavity still lies within the saturable absorber region. Since the shortest saturable absorber used is $15\ \mu\text{m}$ long, the $5\ \mu\text{m}$ inaccuracy does not represent a severe limitation from this point of view. Another technique for laser cleavage was tested. It consists of making the scribing marks for cleavage by wet etching rather than with the scriber. The marks were defined by photolithography. However, the etching scribing was found to be not efficient at defining the cleavage point.

The fabrication technique developed for mode-locked lasers and described in this chapter is simpler and of lower cost than the buried heterostructure used in recent publications [15, 16] since it does not involve any regrowth process. These monolithic semiconductor chips can be mass produced, being low cost, robust, efficient and reliable devices. These are crucial features if ultrashort pulses of light are to find widespread application outwith the laboratory.

3.5 - References to Chapter 3

- [1] - G. H. B. Thompson, *Physics of Semiconductor Laser Devices*, Wiley, 1980.
- [2] - H. C. Casey Jr and M. B. Panish, *Heterostructure Lasers, B*, Academic Press, 1978, Section 7.
- [3] - A. Yariv, *Quantum Electronics*, 3rd edition, Wiley, 1989, Chapter 11.
- [4] - C. Weisbuch and B. Vinter, *Quantum Semiconductor Structures: fundamentals and applications*, Academic Press, 1991, Chapter V.
- [5] - Y. Arakawa and A. Yariv, "Theory of Gain, Modulation Response and Spectral Linewidth in AlGaAs Quantum Well Lasers", *IEEE J. of Quantum Elec.*, vol. 21, pp. 1666-1674, Oct. 1985.
- [6] - S. M. Sze, *Semiconductor Devices: Physics and Technology*, Wiley, 1985.
- [7] - D. L. Lee, *Electromagnetic Principles of Integrated Optics*, Wiley, 1986.
- [8] - M. R. S. Taylor, *Fwave III: A vector E-M wave solver*, unpublished, 1993.
- [9] - S. J. Pearton, "Dry Etching Techniques and Chemistries for III-V Semiconductors", *Mat. Res. Soc. Symp. Proc.*, vol. 216, pp. 277-290, 1991.
- [10] - P. N. Kember, "Plasma deposition of insulators for semiconductor applications", *Plasma News, Oxford Plasma Technology*, no. 4, Sept. 1992.
- [11] - N. I. Cameron, G. Hopkins, I. G. Thayne, S. P. Beaumont, C. D. W. Wilkinson, M. Holland, A. H. Kean and C. R. Stanley, "Selective reactive ion etching of GaAs/AlGaAs metal-semiconductor field effect transistors", *J. Vac. Sci. Tech. B*, vol. 9, no. 6, pp. 3538-3541, 1991.
- [12] - S. K. Murad, S. P. Beaumont and C. D. W. Wilkinson, "Selective and nonselective RIE of GaAs/AlGaAs in SiCl₄ plasma", *Microelectronic Eng.*, vol. 23, pp. 357-360, 1994.
- [13] - P. P. Vasil'ev, V. N. Morozov, Y. M. Popov and A. B. Sergeev, "Subpicosecond pulse generation by tandem-type AlGaAs DH laser with colliding pulse mode locking", *IEEE J. Quantum Electron.*, vol. 22, pp. 149-151, Jan. 1986.
- [14] - S. Sanders, L. Eng and A. Yariv, "Passive mode-locking of monolithic InGaAs/AlGaAs double quantum well lasers at 42 GHz repetition rate", *Electron. Lett.*, vol. 26, pp. 1087-1089, July 1990.
- [15] - Y. K. Chen, M. C. Wu, T. Tanbun-Ek, R. A. Logan and M. A. Chin, "Subpicosecond monolithic colliding-pulse mode-locked multiple quantum well lasers", *Appl. Phys. Lett.*, vol. 58, pp. 1253-1255, Mar. 1991.
- [16] - S. Arahira, S. Oshiba, Y. Matsui, T. Kunii and Y. Ogawa, "500 GHz optical short pulse generation from a monolithic passively mode-locked distributed Bragg reflector laser diode", *Appl. Phys. Lett.*, vol. 64, pp. 1917-1919, Apr. 1994.

Chapter 4: Device Characterisation Techniques

The mode-locked semiconductor lasers are characterised by obtaining the width of the generated pulses, the pulse repetition rate, the degree of coherence of laser emission and the lasing wavelength. These are achieved from frequency and time domain measurements. The characterisation of the mode-locked lasers in the frequency domain is performed by measuring the time averaged optical spectrum of the laser emission. The time domain characterisation is accomplished here with a correlation method [1]. The use of an indirect method is justified by the typical characteristics expected from monolithic mode-locked lasers. The low peak power short pulse generation (around 1 ps pulsewidth) at very high repetition rate (around 100 GHz) is beyond the present measurement capabilities of direct methods employing commercially available fast photodetectors [2] and streak cameras [3]. Also important in the characterisation of semiconductor lasers is to obtain the output optical power, the threshold current and current density, and lasing efficiency. This is carried out by measuring the output power as a function of injected current ($L \times I$ curve).

This chapter describes the techniques employed to characterise the fabricated mode-locked lasers. Section 4.1 describes the mode-locked laser test set-up. Section 4.2 is concerned with the correlator set-up for time domain measurements. The linear correlation technique employed will be discussed in detail and comparisons with other indirect methods of short pulse measurement will be made, specially with the nonlinear autocorrelation technique by second harmonic generation. Section 4.3 will introduce some equations to describe the linear correlation technique and simulations of its output will be compared to the experimental results presented in section 4.2. Section 4.4 will summarise the chapter, giving the conclusions and highlighting the limitations of the characterisation techniques employed as well as the improvements that can be introduced to them. Finally, section 4.5 gives the references to the chapter in order of appearance.

4.1 - Mode-Locked Laser Test Set-up

Figure 4.1 shows a schematic diagram of the mode-locked laser test set-up. It consists of two power supplies for laser biasing, a heatsink temperature controller, a power meter, an optical spectrum analyser, the correlation set-up and a computer to perform control and data acquisition. One of the power supplies is an ILX Lightwave LDC-3752 laser diode controller and it provides CW current to be injected in the gain sections of the laser. The other power supply is home-made and it provides CW voltage to reverse bias the absorber sections of the laser. A Beckman Tech 310 voltage meter is

used to measure the voltage between the absorber and ground contacts of the laser. The temperature of the heatsink is controlled and stabilised by a peltier and a Photon Control temperature controller. The light generated from the laser is collimated and focused into an optical fibre by two objective lenses. Movable mirrors can direct the collimated beam into an Anritsu ML9001A optical power meter or to the correlator set-up, which will be described in detail in section 4.2. The optical fibre guides the laser light into an Advantest Q8381 optical spectrum analyser, which has a narrowest spectral resolution of 0.1 nm. An Apple Macintosh SE/30 is connected to the spectrum analyser and to the correlator to perform control and data acquisition using a LabVIEW[®] 2 software package.

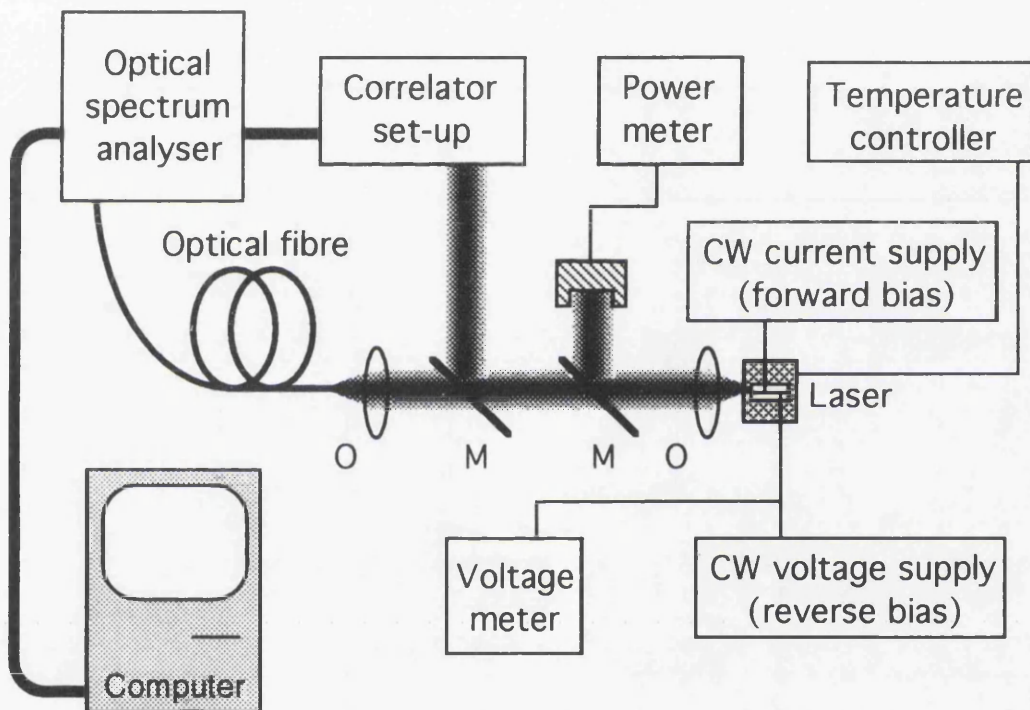


Figure 4.1: Experimental set-up for test and characterisation of mode-locked semiconductor lasers. "O" is objective and "M" is movable mirror.

4.2 - Linear Cross-Correlator

Direct detection and measurement of the generated train of pulses from monolithic passive mode-locked lasers are very difficult because of their inherent speed of operation. The required bandwidth to detect pulses of around 1 ps width at around 100 GHz repetition rate is far beyond the available bandwidth of present commercially available high-speed photodetectors and sampling oscilloscopes [2]. Besides, the nature of pulse generation in passive mode-locked lasers, which does not employ nor generate any electrical triggering signal, provides no low-speed signal to synchronise a sampling oscilloscope. Today's development of state-of-art ultra-fast photodetectors may

overcome these speed limitations and allow direct detection of such high-speed signals in the future [2].

Streak cameras have been often used to characterise extended cavity mode-locked lasers, which generate relatively long pulses, longer than 5 ps, at relatively low repetition rates, in the hundreds of megahertz range [1]. However the best temporal resolution of a typical streak camera is 2 ps [3]. This would limit the pulsewidth measurements of monolithic semiconductor mode-locked lasers, which usually generate shorter pulses. Moreover, the low peak optical power and the lack of triggering electrical signal from these lasers make both single shot and synchroscan operation of streak cameras very difficult. One possible scheme is to use the more sensitive synchroscan operation by triggering the camera with a tuneable frequency synthesiser. Synchroscan operation requires an electrical signal of up to 170 MHz repetition rate to synchronise the camera with the optical signal [3]. The synthesiser can have its frequency tuned until it matches a sub-harmonic of the repetition rate of the mode-locked laser signal. Although this technique was successfully employed in the characterisation of the CPM laser described in section 5.1 of Chapter 5, it produces a poor signal to noise ratio measurement and it is very time consuming. Therefore, considering their high cost and resolution limitations, streak cameras are not a cost-effective method for time domain measurement of monolithic semiconductor mode-locked lasers.

Indirect methods based on correlation techniques are an alternative for characterisation of repetitive train of short pulses. The most commonly used is the auto-correlation by second harmonic generation (SHG) in a nonlinear crystal [1, 4-6]. It consists of a Michelson interferometer with a movable arm in which one of the laser beams is delayed. The two beams containing the train of pulses are overlapped in a suitable nonlinear crystal to generate second harmonic light, in accordance with the phase matching conditions of the crystal. The detection of the time averaged second harmonic signal as a function of the delay between pulses gives information about pulse width. This nonlinear correlation method has proved to be able to measure femtosecond pulses and its resolution depends primarily on the accuracy of the mechanic and electronic mechanisms involved in the control and measurement of the delay in the interferometer and the detection of the SHG signal. However, the modest output powers from monolithic mode-locked laser can make SHG in the nonlinear crystal very difficult. Therefore a linear correlation method would be attractive.

A linear correlation technique has been recently developed by Choi and Taylor for the characterisation of pulses from mode-locked semiconductor lasers [7]. This linear correlator uses a Michelson interferometer to scan a pulse through itself and its neighbours in a train of pulses, obtaining pulse width, repetition rate and coherence length of the laser. This technique detects the mixing signal between light from each

arm of the interferometer at a low speed photodetector and it does not employ second harmonic generation. It has shown to be able to measure a pulsewidth of 260 fs from a mode-locked semiconductor laser [7]. The low cost and low optical power requirement of this technique makes it very attractive for characterisation of monolithic semiconductor mode-locked lasers. It was employed in the characterisation of the mode-locked lasers described in section 5.2 of Chapter 5. The linear correlator set-up used in the measurements is shown in figure 4.2 and it is similar to the one proposed by Choi and Taylor in reference 7.

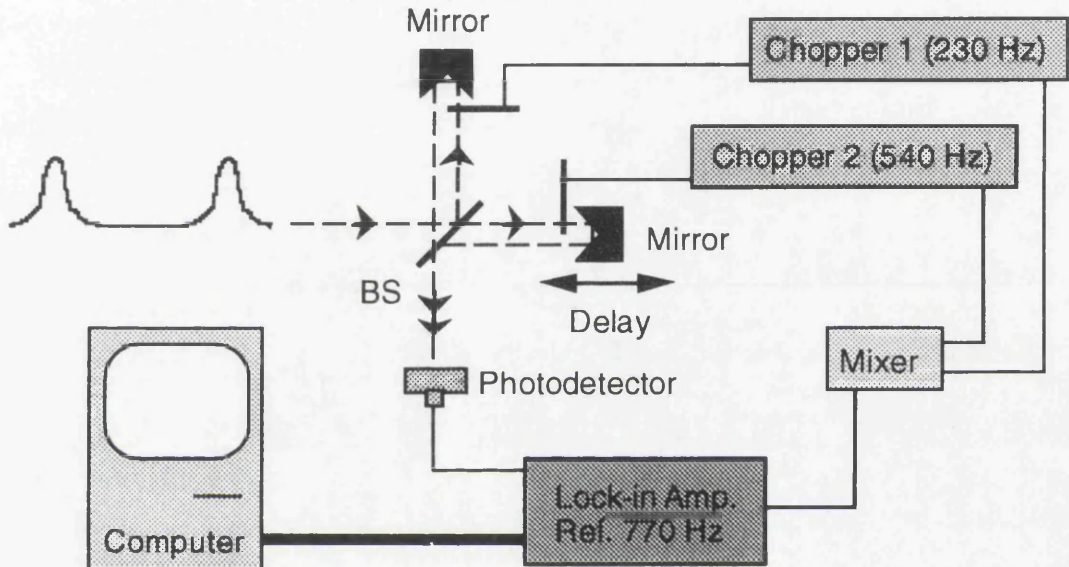


Figure 4.2: Linear cross-correlator set-up. "BS" is beam splitter.

The Michelson interferometer comprises two corner cube mirrors and a 50% reflectivity beam splitter. The use of this type of reflector facilitates the alignment of the interferometer and prevents coupling of the back reflected light from the interferometer into the laser. One of the retro-reflectors is mounted on an inch-worm driven by a Burleigh 7000 Controller. This system is capable of moving in steps of 4 nm, measurable in steps of 50 nm, with a full span of 7 mm. This interferometer was built by N. M. Bett as part of his M.Sc. work at Glasgow University [8]. Each arm of the interferometer has a Scitec Instruments optical chopper, which operate at different frequencies, 230 and 540 Hz. The reference signals from the two choppers are mixed in a home-made electronic mixing circuit. It generates a reference signal at the sum of the chopper ones, at 770 Hz, to synchronise the EG&G 5210 lock-in amplifier. The optical signal from the interferometer is detected by a low-cost low-speed broad-area silicon photodiode. The mixing technique employing the lock-in amplifier and the two choppers removes the dc level generated by the direct detection of light from each individual arm of the interferometer. Therefore only the pulse overlapping signal is

obtained from the lock-in [7]. The computer performs data acquisition from the lock-in amplifier, as described in section 4.1.

Figure 4.3 shows a set of cross-correlation and optical spectrum measurements of a semiconductor laser for different regimes of operation, including spontaneous emission, single mode laser operation, multimode (free-running, non-mode-locked) and mode-locked operation. This will illustrate the different kinds of information that can be obtained from the linear correlation measurements and will help on the interpretation and understanding of the results. The semiconductor laser used here is a multiple colliding pulse mode-locked (MCPM) laser, which is described in detail in section 5.2 of Chapter 5. The total cavity length is 600 μm and the saturable absorber section is 30 μm long. The laser operates on CW regime and, when every section is forward biased, the threshold current is 30 mA.

Figures 4.3-a and b show the cross-correlation and optical spectrum of the spontaneous emission of the laser when it is operating below threshold, at 25 mA. The laser emits in a very broad spectral range, with no observable longitudinal modes. The only feature observed in the correlation trace is a short double-sided exponential peak at zero delay. The fast exponential decay with delay from the zero point of the interferometer indicates that the emission is highly incoherent, as expected from spontaneous emission [1]. The typical fringes produced in interferograms are not resolved here.

When every section of the laser is forward biased and it operates at currents not far beyond threshold, the laser emits in a single longitudinal mode. It is shown in figures 4.3-c and d for 60 mA pumping current. The side mode suppression is of about 25 dB (not measurable from the figure 4.3-d). The correlation trace is flat in the observed range of 45 ps. No decay can be noticed, indicating the laser has a long coherence length [1].

Multimode (free-running, non-locked) operation occurs for currents very close to threshold and also for high currents, above the single mode operation region. Figures 4.3-e and f show the correlation and optical spectrum for multimode operation when 35 mA is applied to the laser. Figure 4.3-e shows peaks at the fundamental repetition rate of the cavity (60 GHz), which correspond to 0.15 nm spacing between modes in figure 4.3-f. These peaks arise from beating of the several longitudinal modes observed in the spectrum. This mode beating effect means that, in the time domain, the laser produces a sequence of spikes in the form of a pulse train [1, 9]. Therefore, there is here an apparent ambiguity between multimode and mode-locked operation. The ambiguity is removed by analysing the coherence properties of the laser. The difference between mode-locking and multimode behaviour is that, with a mode-locked laser, the modes add together coherently and that there is a strong phase relationship between pulses in the pulse stream [1, 9]. In an ideal mode-locked case, where the phases of the modes are

exactly the same, the coherence length of the laser would be infinite. A laser is considered to be mode-locked if its coherence time is much longer than the round-trip-time of the cavity, or photon lifetime - for a typical Fabry-Perot semiconductor laser those two times are of the same order of magnitude. If the coherence time of the laser emission is short compared to the round-trip time, the spikes produced within each round-trip in the laser will have a small degree of repetitiveness, which implies that a regular train of pulses will not be formed. This represents the multimode operation [1, 9]. If the coherence time is much longer than the round-trip time of the laser the sequence of spikes will be shaped to a regular train of pulses in a long time averaged scale. This represents the non-ideal mode-locked operation that occurs in most cases, where not every mode is locked and the phase of the modes locked are not exactly the same as in the ideal case, due to group velocity dispersion for example. One can observe in figure 4.3-e a pronounced exponential decay on the amplitude of the peaks, indicating that the laser has a short coherence time, of about 20 ps, which is very close to the round trip time (16.4 ps). This means that there is no constant phase relationship between modes and the sequence of spikes produced by them is formed and shaped in a rather chaotic and noisy fashion, not having the high regularity in shape and amplitude typical of mode-locked pulses.

The kind of ambiguity discussed above also exists in the non-linear correlation methods [1, 4]. In the autocorrelation by second harmonic generation technique, peaks also appear for multimode operation and the ambiguity is solved by observing the contrast ratio (peak to background), which is 3:1 for ideal mode-locking and 3:2 for multimode operation. In most cases the laser is considered to be mode-locked if the contrast ratio is close to the one for ideal mode-locking [1, 4].

Figures 4.3-g and h show the case of mode-locking operation of the MCPM laser at its first harmonic of the repetition rate, at 60 GHz. In contrast to the case of multimode operation discussed before, the coherence time of the laser observed in the correlation of figure 4.3-g is much longer than in figure 4.3-e. The measurement of the coherence length is limited by the continuous scanning range of the interferometer, which is 15 mm (50 ps) in our setup. But a non-continuous scan measurement, up to pulses 10 round-trips apart (150 ps), showed no noticeable change in pattern. This long coherence time compared to the round trip time (16.4 ps) and the photon lifetime (about 5 ps) is the indication of mode-locking operation from the linear correlation measurement.

The linear correlation technique has the disadvantage, compared to the second harmonic generation autocorrelation technique, that it is not sensitive to the effect of frequency chirp on pulsewidth [1, 7]. Therefore pulsewidth information is limited to the minimum pulsewidth possible assuming unchirped pulses, that is assuming bandwidth limited pulses. This assumption is reasonable for monolithic semiconductor

mode-locked lasers because there has been no evidence of significant chirping from these lasers and measurements have generally indicated transform limited pulses [7].

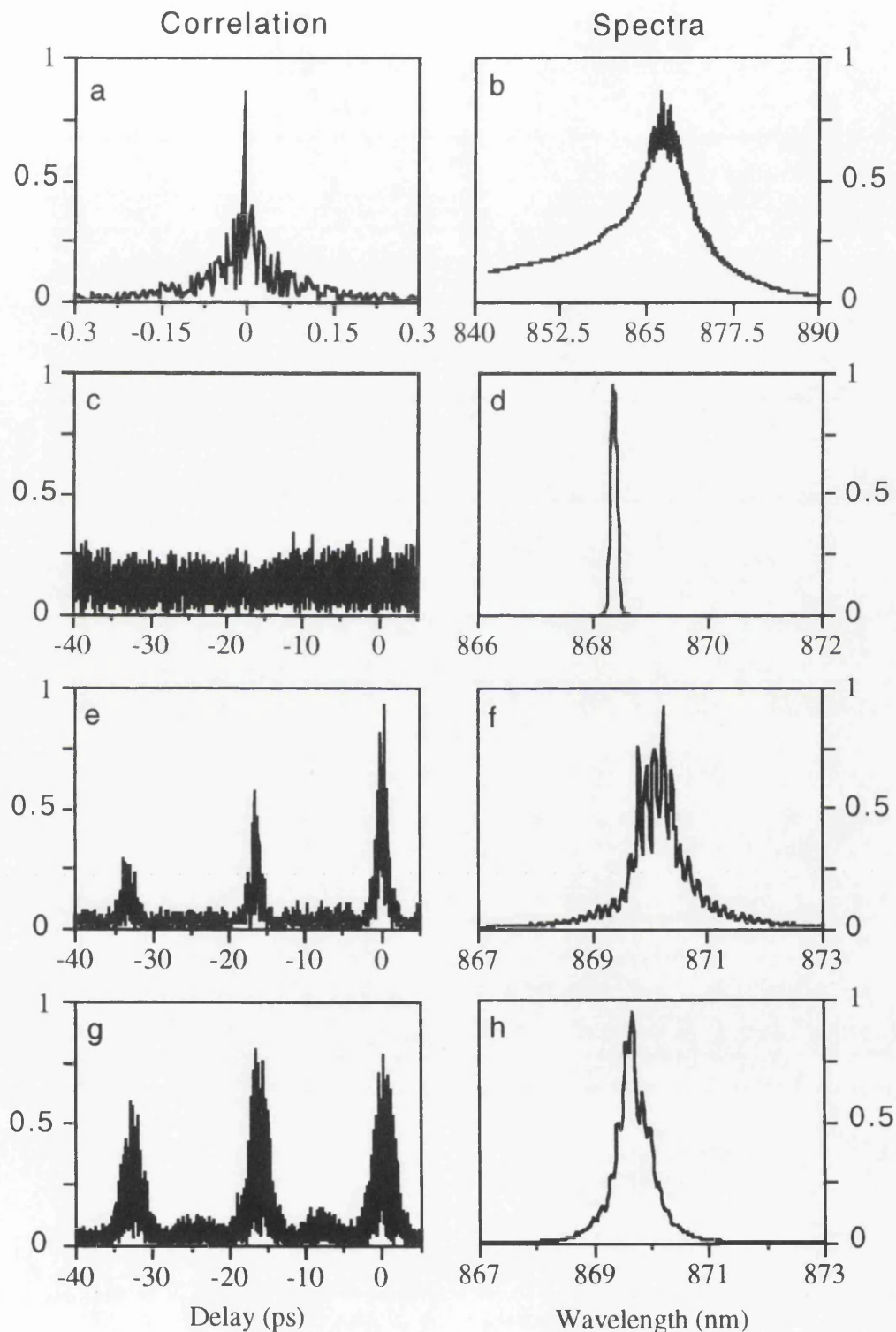


Figure 4.3: Linear correlation traces and optical spectra of a 600 μm long MCPM laser for different modes of operation: spontaneous emission (a and b); single longitudinal mode laser operation (c and d); multimode (e and f); and mode-locked laser operation (g and h). Vertical axes represent intensity in arbitrary units.

Therefore, bearing in mind the above, the average width of the correlation trace pulses in figure 4.3-g is 3 ps, obtained by measuring the width of each pulse shown. Assuming here a hyperbolic secant pulse shape the deconvolution factor of 1.54 is used to obtain the actual pulse width [4], which is 2 ps FWHM.

4.3 - Simulations of the Linear Correlator

In order to have a better understanding of the information that can be obtained from the linear correlation measurement technique, the general equations that describe the Michelson interferometer are shown here. These simple analytical equations are written following the formalism developed by Petermann in references 10 and 11, and they are described in detail in the appendix 1. The output of the interferometer for different regimes of laser operation, including single mode, multimode and mode-locking are studied. Using the Mathematica® enhanced version 2.0 software package [12], the equations for the output of the linear correlation are plotted and comparison with the experimental results presented in the previous section can be made. The goal of these simulations is not to describe the laser operation, but to analyse the response of the correlation method to the different regimes of operation of the laser, instead. It gives an insight into the characteristics and limitations of the linear correlation method for time domain characterisation of mode-locked lasers.

The complex electric field $E(t)$ of the laser output emitting into k longitudinal modes is written as:

$$E(t) = \sum_k \sqrt{P_k(t)} \cdot \exp[j\omega_k t + j\phi_k(t)] \quad (4.1)$$

where $P_k(t)$ is the light power and $\phi_k(t)$ is the phase of the k^{th} lasing mode emitting at the wavelength $\lambda_k = 2\pi c/\omega_k$. Therefore the output intensity of the laser is:

$$I(t) \propto P(t) = |E(t)|^2 \quad (4.2)$$

The total field at the output of an interferometer, where the signal is delayed in one of its arms by τ , is:

$$E_\tau(t) = A[E(t) + E(t - \tau)] \quad (4.3)$$

where A is a constant (A is 0.5 for a Michelson interferometer). Therefore the output power is:

$$P_\tau(t, \tau) = A^2 \{ |E(t)|^2 + |E(t - \tau)|^2 + 2\text{Re}[E(t) \cdot E^*(t - \tau)] \} \quad (4.4)$$

The average output power of the interferometer, which involves the first order correlation function, can then be written as follows. (For the sake of comparison with the experimental results, the equation is written in the same form as the results are measured: with the dc level removed and then applying the absolute value to it, in arbitrary units).

$$\langle P_T(t, \tau) \rangle = \left| \cos(\omega_o \tau) \cdot \sum_k P_k \cdot \cos(k\Delta\omega\tau) \cdot \text{Re}\{\langle \exp[j\Delta\phi_k(t, \tau)] \rangle\} \right| \quad (4.5)$$

where $\omega_k = \omega_o + k\Delta\omega$, $k = \pm 0, \pm 1, \pm 2, \dots$, $\Delta\phi_k(t, \tau) = \phi_k(t) - \phi_k(t-\tau)$, and it is assumed that the amplitude of each mode is not time dependent (i.e. $P_k(t) = P_k(t-\tau) = P_k$), which only implies that amplitude noise is not being taken into account.

Equation 4.5 describes the general time averaged output power from the interferometric system used in the experiments, but it does not include effects of amplitude and frequency noise. A comprehensive study of noise in interferometers can be found in references 10 and 11. The particular cases of single mode, multimode and mode-locked laser operation will be analysed.

For single mode operation $k = 0$ and equation 4.5 is reduced to

$$\langle P_T(t, \tau) \rangle = \left| \cos(\omega_o \tau) \cdot P_o \cdot \text{Re}\{\langle \exp[j\Delta\phi_o(t, \tau)] \rangle\} \right| \quad (4.6)$$

The evaluation of the mean value $\langle \exp[j\Delta\phi_k(t, \tau)] \rangle$ involves the consideration that the phase change $\Delta\phi$ with delay is introduced by a large number of independent noise events due to spontaneous emission, with a Gaussian probability density distribution, and that its variance increases proportionally to the delay, with the proportionality factor defined as the coherence time t_c [10, 11]. This evaluation is carried out in the appendix 1 and it yields:

$$\langle P_T(t, \tau) \rangle = \left| P_o \cdot \cos(\omega_o \tau) \cdot \exp(-|\tau|/t_c) \right| \quad (4.7)$$

Figure 4.4 shows a plot of the equation 4.7 as a function of the delay τ for ω_o corresponding to a wavelength of 870 nm, P_o equal to 1, and t_c equal to 100 ps. The graph is configured in the same way as in figure 4.3-c to facilitate the comparison of the theoretical with the experimental results. The dark area comes from the fast oscillation of the cosine at the angular frequency ω_o in equation 4.7. It corresponds to the fringes produced by the interferometer, which are not resolved. The coherence time t_c produces the exponential decay observed in figure 4.4. Since no decay can be noticed in figure

4.3-c the coherence time of the actual device operating single mode is much longer than 100 ps used in the simulation.

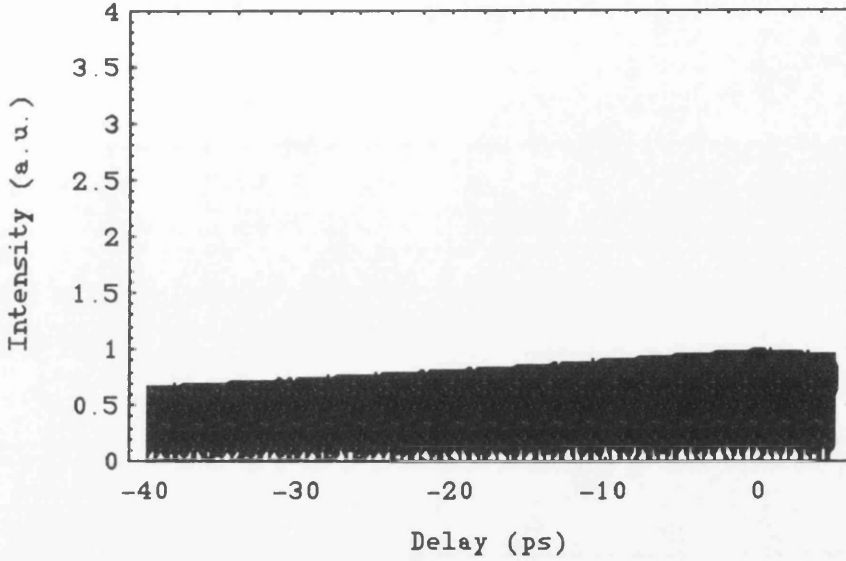


Figure 4.4: Simulation of the output of the linear correlator for single mode laser operation described in equation 4.7, with $\lambda = 870 \text{ nm}$, $P_o = 1$, and $t_c = 100 \text{ ps}$.

For the case of multimode laser operation, similar considerations regarding the phase change, as described previously and in the appendix 1, are made and it is assumed that every lasing mode has the same coherence time. Therefore equation 4.5 can be written as:

$$\langle P_T(t, \tau) \rangle = \left| \cos(\omega_o \tau) \cdot \sum_k P_k \cdot \cos(k\Delta\omega\tau) \cdot \exp(-|\tau|/t_c) \right| \quad (4.8)$$

Figure 4.5 shows the plot of equation 4.8 with parameters corresponding to the experimental results shown in figure 4.3-e. Hence, the simulation of the correlator output for multimode laser operation is obtained with $\Delta\omega$ corresponding to a longitudinal mode separation $\Delta\lambda$ equal to 0.15 nm, which represents the case of a 600 μm long laser. The lasing wavelength is 870 nm and the coherence time is 20 ps, which is close to the round-trip time (16 ps). Here the spectrum of laser emission $P(k)$ is assumed to have a hyperbolic secant profile, with 7 longitudinal modes in its FWHM. The total number of modes k considered within the profile is always four times the number of modes in its FWHM plus one. The comparison of figure 4.5 with figure 4.3-e reveals the perfect match between the simulation and experimental results for multimode laser operation.

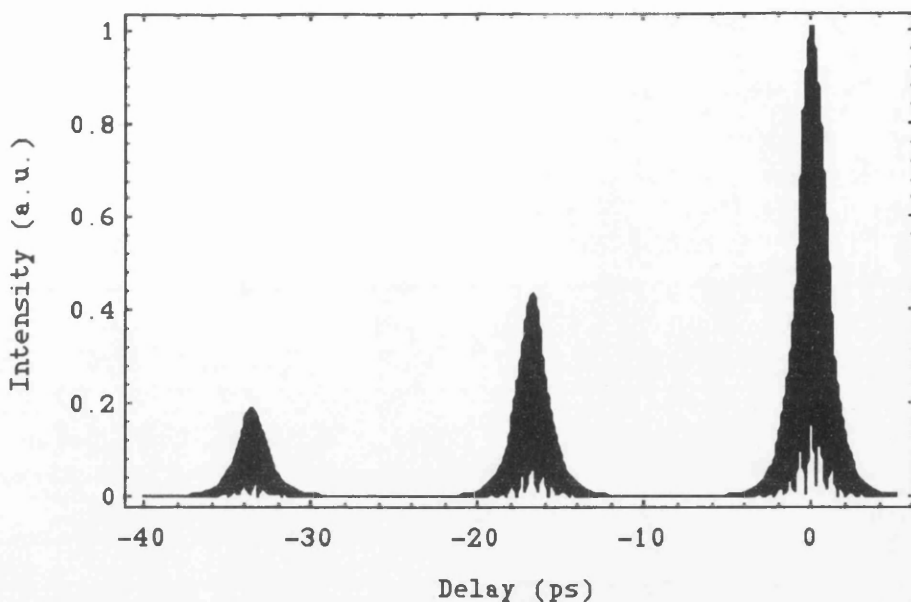


Figure 4.5: Simulation of the output of the linear correlator for multimode laser operation described in equation 4.8. $\lambda = 870 \text{ nm}$, $\Delta\lambda = 0.15 \text{ nm}$, $t_c = 20 \text{ ps}$ and with 7 modes at FWHM of the spectral profile.

In order to simulate the case of spontaneous emission from the laser, the coherence time is made very small in equation 4.8. Figure 4.6 shows the output of the interferometer for the same conditions of figure 4.5 but with 30 fs coherence time. Figure 4.6 resembles the experimental result shown in figure 4.3-a

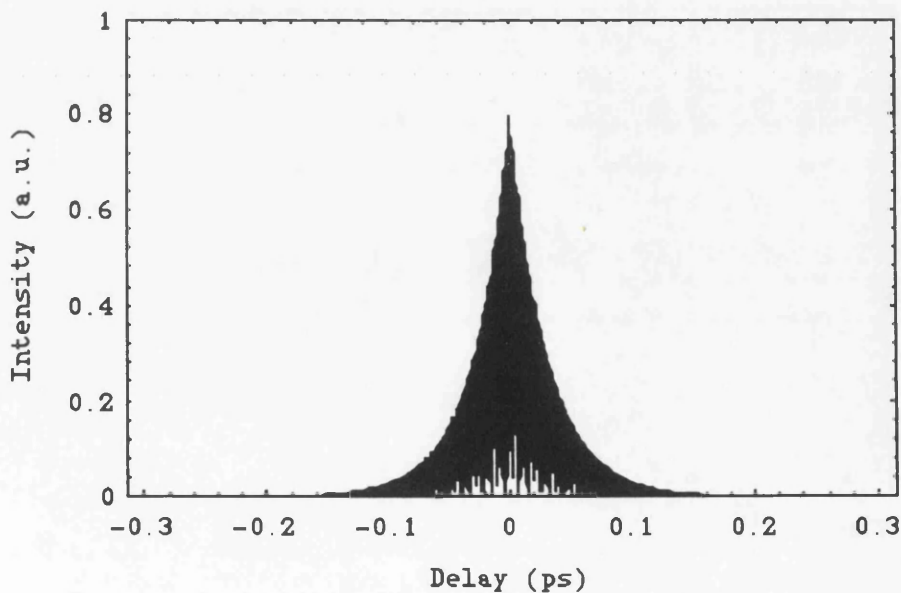


Figure 4.6: Simulation of the output of the linear correlator for spontaneous emission of the laser from equation 4.8, with $\lambda = 870 \text{ nm}$, $\Delta\lambda = 0.15 \text{ nm}$, and $t_c = 0.03 \text{ ps}$.

The case of ideal mode-locking operation, where the phases of the modes are exactly the same, can be easily represented by imposing no phase change ($\Delta\phi(t, \tau) = 0$) into equation 4.5, yielding:

$$\langle P_T(t, \tau) \rangle = \left| \cos(\omega_o \tau) \cdot \sum_k P_k \cdot \cos(k\Delta\omega\tau) \right| \quad (4.9)$$

Figure 4.7 shows the plot of equation 4.9 for conditions similar to figure 4.5, with $\lambda = 870$ nm, $\Delta\lambda = 0.15$ nm but with 5 modes at FWHM of the spectral profile. However, since in this ideal mode-locked laser case there is no phase change, the coherence time of the laser is infinite and therefore there is no decay on the amplitude of the peaks of the correlation, as shown in figure 4.7. Although this simulation uses an unrealistic ideal mode-locked laser it is comparable with the experimental correlation shown in figure 4.3-g. The difference between them should mainly be due to the non-perfect phase locking of the modes of the real mode-locked laser, noise and the spectral profile which may not be exactly a hyperbolic secant. In accordance with equation 4.9 and figure 4.7, figure 4.3-g presents a long coherence time, as discussed in section 4.2. The pulse widths measured from both figures are approximately the same, around 3 ps. It is due to the same number of modes considered in the FWHM of the spectral profile used in the simulation and observed in the optical spectrum of the laser shown in figure 4.3-h.

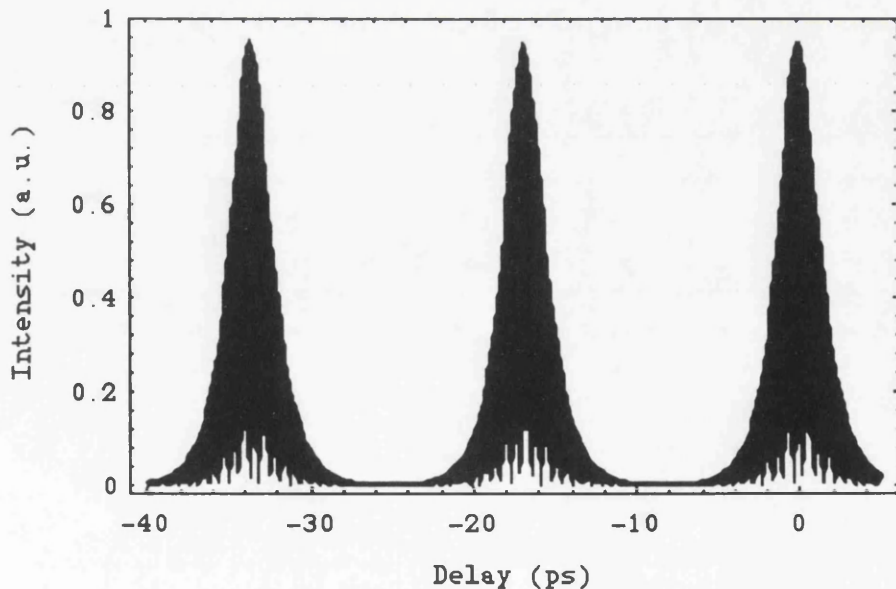


Figure 4.7: Simulation of the output of the linear correlator for an ideal mode-locked laser, obtained from equation 4.9 with $\lambda = 870$ nm, $\Delta\lambda = 0.15$ nm and 5 modes at FWHM of the spectral profile.

For the case of an ideal mode-locked laser, with no time dependent phase change, the intensity as a function of time is simple to obtain from equation 4.2 and it is shown in figure 4.8 for the same conditions as for the figure 4.7 above. The pulse shape is hyperbolic secant squared, in accordance with the shape assumed for the spectral profile. The pulsewidth obtained from figure 4.8 is 1.94 ps. It corresponds to the pulsewidth obtained from figure 4.7 taking into account the deconvolution factor of 1.54 for hyperbolic secant square pulse shape [4]. The correspondence between figures 4.7 and 4.8 and the similarities between figure 4.7 and the experimental result of figure 4.3-g indicate that figure 4.8 should be a close representation of the actual train of pulses generated by the mode-locked laser studied in figure 4.3-g.

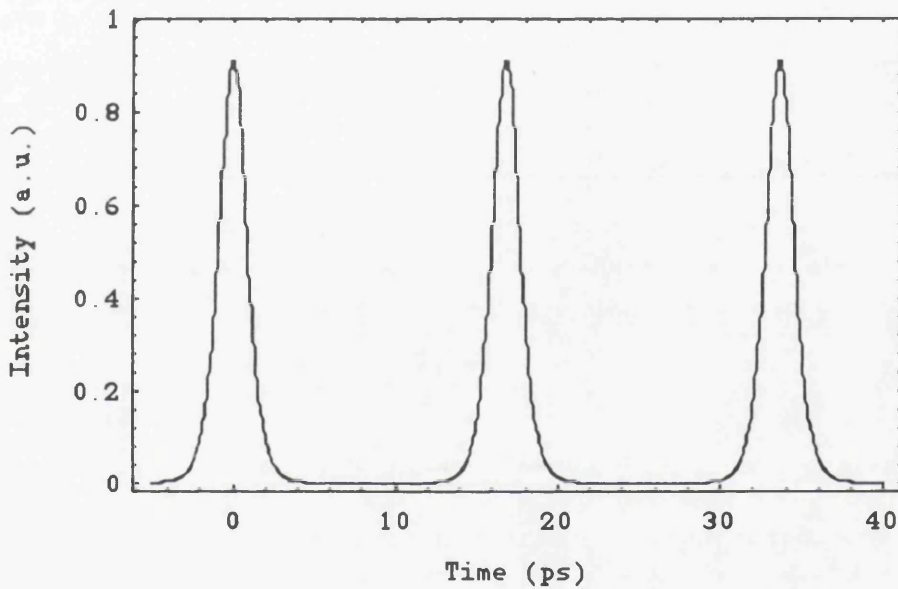


Figure 4.8: Simulation of the temporal evolution of the output of an ideal mode-locked laser at the same conditions of figure 4.7, with 600 μm cavity length ($\Delta\lambda = 0.15 \text{ nm}$), emitting at $\lambda = 870 \text{ nm}$.

So far in the simulation results for ideal mode-locked lasers, the spectral phase of the modes has been taken as zero. In order to simulate a train of chirped pulses one can write the spectral phases as:

$$\varphi_k = \beta_2 (\omega_k - \omega_0)^2 = \beta_2 (k\Delta\omega)^2 \quad (4.10)$$

where β_2 is a constant. This quadratic dependence of the phase with the frequency can be caused by group velocity dispersion, for example [13]. In this case the phase of each mode still does not change in time, therefore it still is an unrealistic mode-locking situation, as discussed before. However it illustrates some important characteristics of the linear correlation method. Figure 4.9 shows the simulation of the laser output train

of pulses for the same conditions as for figure 4.8, but with the phase as in equation 4.10, with β_2 equal to 1.4. Comparing figures 4.8 and 4.9 one can see that for the same spectral profile and width the latter shows wider pulses, i. e. the phase as given by equation 4.10 produces wider pulses, which are therefore non-Fourier-transform-limited. The phase distribution of equation 4.10 means that the different frequency components of a pulse travel at different speeds, inducing a sweep of frequencies across the pulse, which is called chirp. The pulse can maintain its width only if all spectral components travel together, or equivalently if $\beta_2 = 0$, which means that the pulse has no chirp and it is transform limited [13].

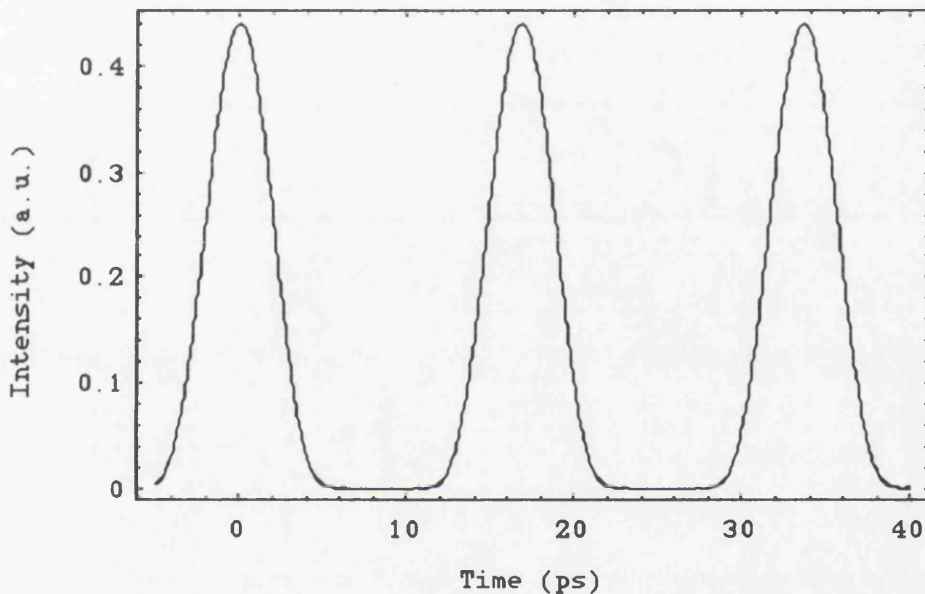


Figure 4.9: Simulation of the temporal evolution of a train of chirped pulses from the output of a mode-locked laser at the same conditions of figure 4.8, but with the phase given by equation 4.10 with $\beta_2 = 1.4$.

However the simulation of the output of the linear interferometer for these chirped pulses gives exactly the same result as for unchirped ones, shown in figure 4.7. This can be seen from the equations point of view since the phase in equation 4.10 is time independent. Hence they are cancelled in the calculations of equation 4.5 for the output of the interferometer. This illustrates the major limitation of the linear correlation method, which is its insensitivity to frequency chirp on pulses. Therefore, the pulsewidth information obtained from it is limited to the minimum pulsewidth possible, which is for unchirped pulses.

The nonlinear correlation method involving second harmonic generation does not have this limitation since it consists of a correlation of intensity, rather than field as in the linear method. The information about the time independent phase is present in the

pulse intensity profile generated by the SHG process. Therefore, the nonlinear method does give information about the actual pulsewidth from a train of repetitive pulses.

4.4 - Conclusions

This chapter is concerned with the description of the technique of measurement and characterisation of the laser emission from the fabricated mode-locked lasers. The description of the mode-locked laser test set-up, with characteristics and specifications of each equipment used, is given in section 4.1. The bulk of the chapter consists of sections 4.2 and 4.3, which are dedicated to the linear correlation technique used for time domain measurements. In section 4.2 the linear correlator set-up is described and its measurements are discussed using experimental results obtained from a semiconductor laser operating at different regimes, including below lasing threshold (spontaneous emission) and lasing at a single longitudinal mode, multimode and mode-locked. In section 4.3, the equations that describe the linear correlation method are written and from them, simulations of the output from the interferometer were obtained. The simulations are for laser operation regimes similar to the ones studied in section 4.2, therefore comparisons between experimental and simulated results were made.

Sections 4.2 and 4.3 also give the advantages and disadvantages of the linear correlation technique in relation to the more conventional and more widely used nonlinear technique employing second harmonic generation. In summary, the linear technique is simpler and of lower cost to implement. Its main advantage is that it uses low optical powers to obtain the measurements, which suits the monolithic mode-locked semiconductor lasers since they usually generate only a few tens of milliwatts peak power. These low peak powers make SHG difficult to obtain. The main disadvantage of the linear technique is its insensitivity to frequency chirp on pulses. This limits the pulsewidth measurement to the minimum pulsewidth possible, which is for unchirped, Fourier-transform-limited pulses. However this limitation is acceptable for the characterisation of monolithic mode-locked semiconductor lasers because these devices usually generate transform limited pulses [7].

The mode-locked laser test set-up described in section 4.1 could be improved by extending the computer control to every equipment in the set-up, including the power meter, temperature controller and power supplies. Along with the use of fixed beam splitters instead of movable mirrors, it would allow simultaneous measurement of optical power, spectrum and correlation trace as a function of current and reverse bias. This would perform a systematic and detailed set of measurements on the lasers. Following the same idea, the correlator set-up could be improved by computer controlling the Burleigh controller. Another possible improvement could be the extension of the total span of the inch-worm. The one used in the set-up has a total span

of 7 mm, but a 2 cm version is commercially available. The longer span would allow a more accurate measurement of the coherence length of the lasers, as well as the measurement of the repetition rate of longer cavity (lower repetition rate) lasers.

The future development of the mode-locked laser test set-up could involve the use of the standard nonlinear autocorrelation technique based on SHG in a nonlinear crystal [1, 4], or the use of a semiconductor waveguide autocorrelator. This is a novel technique, developed in Glasgow University, and is based on two-photon absorption in a semiconductor waveguide [14]. Moreover, the information from both linear and nonlinear correlation techniques can be used to reconstruct the pulse, obtaining pulse shape and chirp structure [15, 16].

4.5 - References to Chapter 4

- [1] - D. J. Bradley and G. H. C. New, "Ultrashort pulse measurements", *Proc. of IEEE*, vol. 62, pp. 313-345, Mar. 1974.
- [2] - J. E. Bowers and Y. G. Wey, "High-speed photodetectors", *Handbook of Optics*, 2nd Edition, Edited by M. Bass, E. Van Stryland, D. Williams and W. Wolfe, Optical Society of America, 1994, Chapter 17.
- [3] - Hamamatsu streak camera, technical information and specifications, 1993.
- [4] - J. P. Curtis and J. E. Carroll, "Autocorrelation systems for the measurement of picosecond pulses from injection lasers", *Int. J. Electron.*, vol. 60, pp. 87-111, 1986.
- [5] - K. L. Sala, G. A. Kenney-Wallace and G. E. Hall, "CW autocorrelation measurements of picosecond laser pulses", *IEEE J. Quantum Electron.*, vol. 16, pp. 990-996, Sept. 1980.
- [6] - W. A. Lopes, M. O. Morales, M. A. Rieffel, J. A. Giacoletti, J. T. Thorpe and L. A. Westling, "Intensity autocorrelation measurements of an AlGaAs diode laser", *Opt. Lett.*, vol. 18, pp. 820-822, May 1993.
- [7] - K. N. Choi and H. F. Taylor, "Novel cross-correlation technique for characterisation of subpicosecond pulses from mode-locked semiconductor lasers", *Appl. Phys. Lett.*, vol. 62, pp. 1875-1877, Apr. 1993.
- [8] - N. M. Bett, "An interferometric auto-correlator", M.Sc. Thesis, Glasgow University, 1990.
- [9] - H. Bachert, P. G. Eliseev, M. A. Manko, V. P. Strahov, S. Raab and Chan Min Thay, "Multimode operation and mode-locking effect in injection lasers", *IEEE J. Quantum Electron.*, vol. 11, pp. 507-510, July 1975.
- [10] - K. Petermann and E. Weidel, "Semiconductor laser noise in an interferometer system", *IEEE J. Quantum Electron.*, vol. 17, pp. 1251-1256, July 1981.
- [11] - K. Petermann, *Laser Diode Modulation and Noise*, Advances in Optoelectronics, Kluwer Academic Publishers, 1988, Chapters 7 and 8.
- [12] - S. Wolfram, *Mathematica: A System for Doing Mathematics by Computer*, Second Ed., Addison-Wesley, 1991.
- [13] - G. P. Agrawal, *Nonlinear Fiber Optics*, Quantum Electronics: Principles and Applications Series, Academic Press, 1989.
- [14] - F. R. Laughton, J. H. Marsh, D. A. Barrow and E. L. Portnoi, "The two-photon absorption semiconductor waveguide autocorrelator", *IEEE J. Quantum Electron.*, vol. 30, pp. 838-845, Mar. 1994.
- [15] - K. Naganuma, K. Mogi and H. Yamada, "General method for ultrashort light pulse chirp measurement", *IEEE J. Quantum Electron.*, vol. 25, pp. 1225-1233, June 1989.
- [16] - R. A. Salvatore, T. Schrans and A. Yariv, "Pulse characteristics of passively mode-locked diode lasers", *Optics Lett.*, vol. 20, pp. 737-739, Apr. 1995.

Chapter 5: Experimental Results

This chapter is concerned with the characterisation work carried out on colliding pulse mode-locked (CPM) lasers. The main results are organised in sections according to their emphasis and contribution to the area of short pulse generation from monolithic mode-locked lasers. Section 5.1 describes and analyses the experimental results obtained from a standard CPM laser configuration, from which some new TE-TM polarisation effect could be seen. Section 5.2 deals with an original configuration of CPM laser, which is called multiple colliding pulse mode-locked laser (MCPM). Section 5.3 is concerned with the realisation of a monolithic CPM laser in a ring shape cavity, the CPM ring laser. Section 5.4 presents the progress towards the realisation of a CPM laser using flared waveguide as an attempt to obtain higher output power from the laser, which is called bow-tie CPM laser. Section 5.5 is dedicated to the development of an all optical clock recovery device based on a CPM laser. Section 5.6 comprises a compilation of the conclusions of each section as a summary of the chapter. And finally section 5.7 gives the list of references to this chapter in order of appearance.

5.1 - GaAs/AlGaAs CPM Quantum Well Lasers

The monolithic passive colliding pulse mode-locked (CPM) semiconductor quantum well lasers have been the subject of intensive investigations recently due to their potential applicability in optoelectronically generated short pulses for optical fibre communication systems. Relevant review papers have been produced and are listed in references 1, 2 and 3. These lasers have been shown to be capable of producing transform limited, sub-picosecond pulses, down to around 640 fs at repetition rates as high as 350 GHz [4]. Briefly, the device consists of a saturable absorber integrated in the middle of a laser resonator, which makes the laser generate two counter propagating pulses that collide in the absorber section. The saturable absorber is simply a reversed biased section which provides absorption due to an electric field dependent decrease in the semiconductor band-gap, known in quantum wells as the quantum confined Stark effect. The reverse bias also decreases the absorption recovery time by sweeping out the carriers from the absorber section [1-5]. A more detailed description of basic CPM laser operation with quantum well saturable absorbers is given in Chapter 2.

All of the work so far reported in monolithic CPM lasers has been on long-haul communication wavelength devices (~1550 nm). Here the realisation of a short wavelength (~860 nm) monolithic passive CPM laser is reported [6]. A short wavelength external extended cavity CPM laser based on bulk semiconductor has been reported in reference 7. The shorter wavelength device produces photon energies above

the band-gap energies of GaAs and Si and may find applications in high-speed optical sampling and in short-haul communications as a compact, efficient source of ultrashort pulses. Results on the polarisation dependence of the CPM laser output are also presented, where both TE and TM polarisation are seen at different wavelengths. This type of operation arises from polarisation dependence of the gain and saturable absorber sections particularly prevalent in quantum well based devices.

The laser was fabricated in the four quantum well GaAs/AlGaAs material described in Chapter 3. The monolithic CPM laser is shown in figure 5.1.1. Figure 5.1.1(a) shows a diagram of the laser structure and (b) shows a scanning electron micrograph (SEM) of the laser. As described above, the device consists of the monolithic integration of a saturable absorber in the middle of a laser cavity. Details of fabrication technique are also given in Chapter 3.

Figure 5.1.2 shows the experimental set-up for CPM laser test and characterisation. It consists of a pulse generator or CW laser power supply for gain section forward biasing, whereas another power supply reverse biases the central absorber section of the laser. The laser beam is collimated and focused by objective lenses on an optical power meter or an optical fibre which leads it to an optical spectrum analyser. A computer performs the control and data acquisition. The correlation method for time domain measurement described in Chapter 4 was not available at the time of these devices were tested. Several devices of different lengths have been fabricated. They have different mode-locked repetition frequencies in the range 73-129 GHz. Figure 5.1.3 shows the optical spectrum for a cleaved 560 μm long laser which has 60 μm long saturable absorber section in the middle and is driven by 1 μs pulses at 1 kHz repetition rate (although the laser has also operated CW mode-locked). When both gain and absorber sections are equally forward biased the laser threshold current is 40 mA. The continuous line in figure 5.1.3 shows its optical spectra for a forward bias current of 60 mA. The longitudinal mode separation in this case is measured to be 64.5 GHz (0.16 nm on figure 5.1.3). When 0.3 V reverse bias is applied to the absorber section one can observe the longitudinal mode separation of laser emission doubles to 129 GHz (0.32 nm on figure 5.1.3). The change in the longitudinal mode separation indicates that the CPM effect is taking place. From previous work [1, 2, 4] it is clear that this is the standard behaviour of a semiconductor CPM laser and it indicates that 2 pulses are circulating in the cavity and colliding in the saturable absorber. The pulse repetition rate is then 129 GHz. Although this repetition rate was subsequently confirmed by synchroscan streak camera measurements (From Hadlands Photonics Ltd.) where also 2 ps resolution limited pulse width was measured, these results cannot be reproduced here.

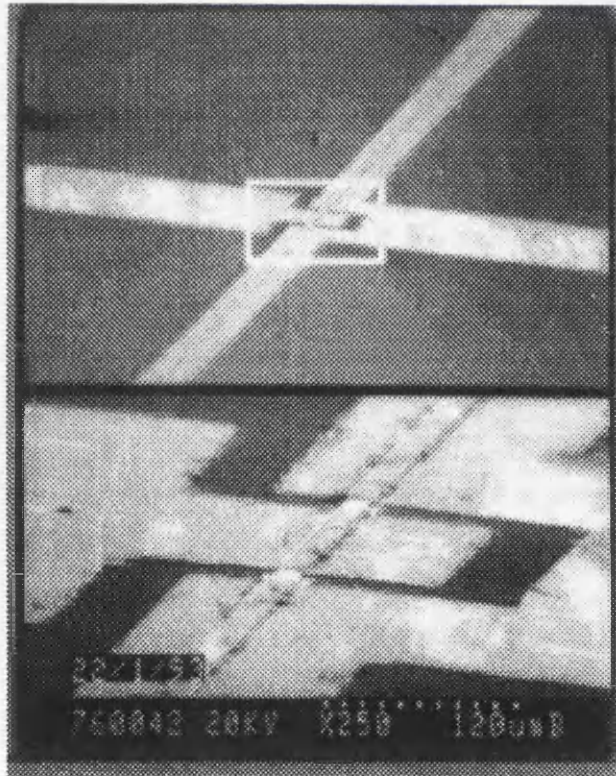
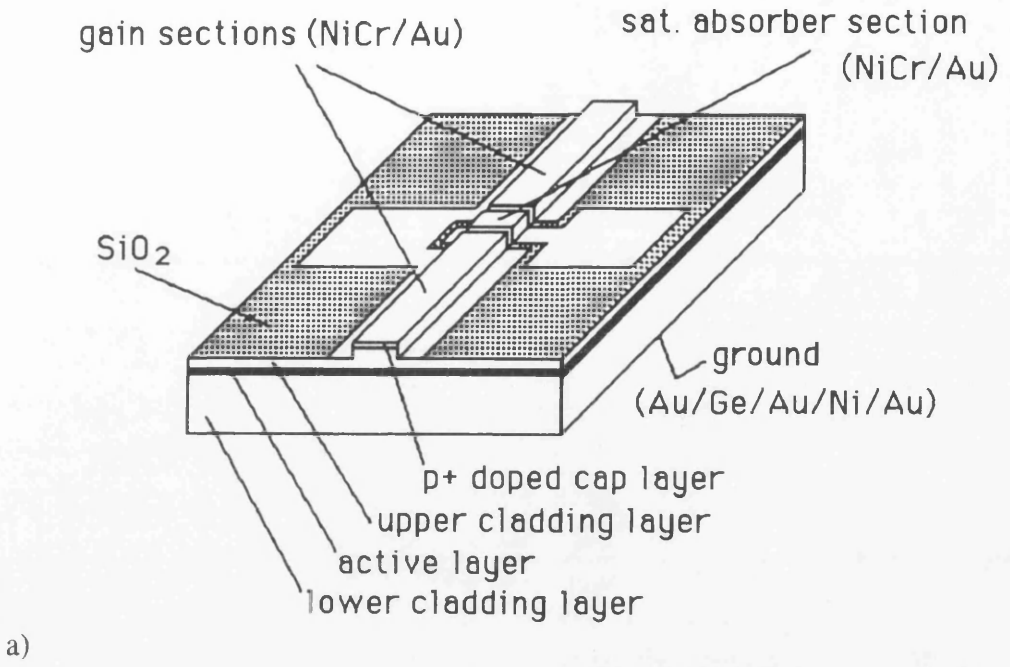


Figure 5.1.1: Colliding pulse mode-locked (CPM) laser diagram (a) and SEM (b).

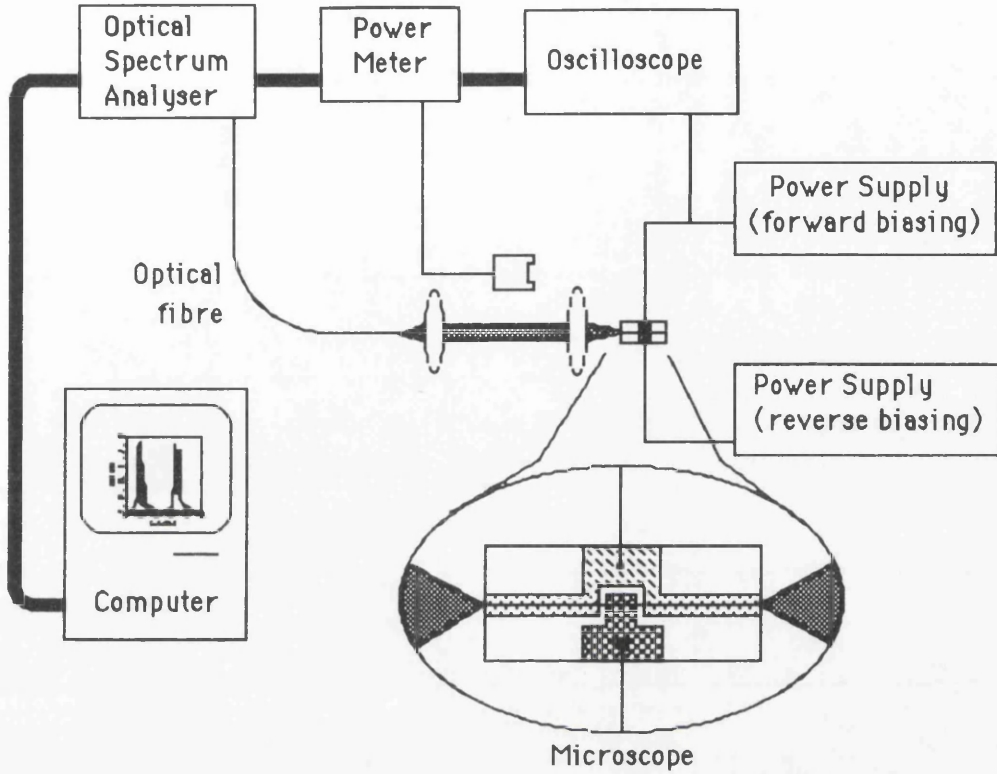


Figure 5.1.2: CPM laser test set-up.

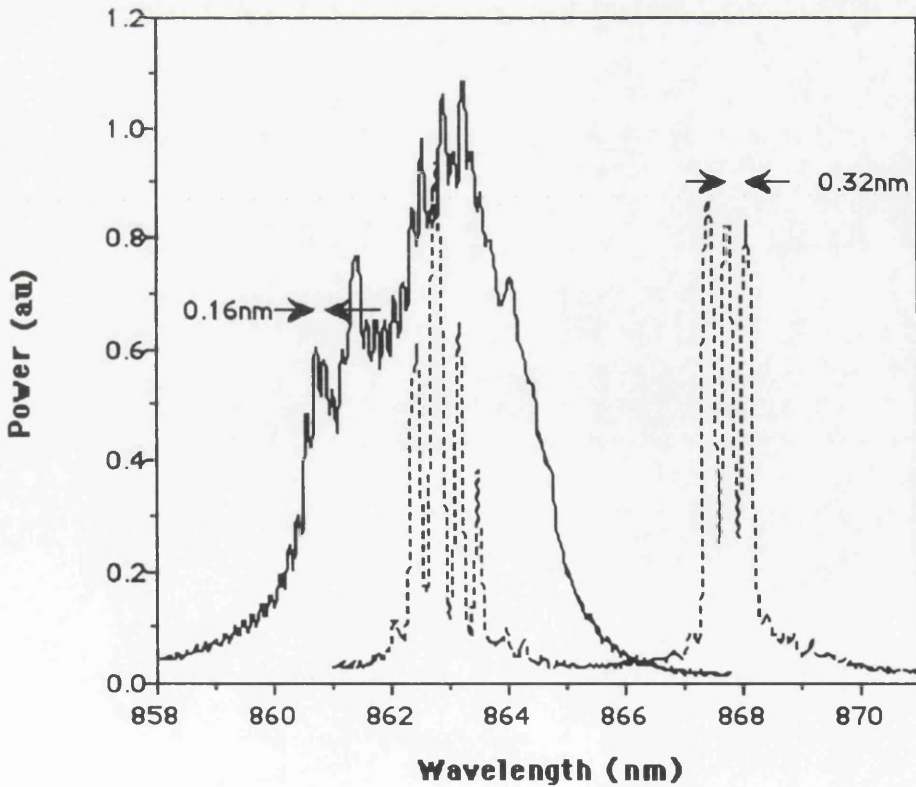


Figure 5.1.3: Optical spectrum of a 560µm long CPM laser when fully forward biased (line) and 0.3V reverse biased (dashed).

Figure 5.1.3 also shows that the CPM laser emits in two different wavelength groups separated by about 5 nm. Polarisation selective optical spectra were performed and showed that, for the fully forward biased condition, the laser emits in TE polarisation only, whereas when the absorber is reverse biased the laser emits in both TE and TM polarisation. Figure 5.1.4 shows optical spectra for TE and TM polarisation when 1.5 V reverse bias is applied. One can see that for TM only one group of peaks appears corresponding to the light hole emission, whereas for TE two groups of peaks can be seen, corresponding to light and heavy hole emissions. This effect arises from the polarisation dependence of the gain and reverse biased absorber sections which is important in quantum well lasers. Figure 5.1.5 shows the spectrum of transmitted light through a quantum well waveguide as a function of the applied reverse bias for TE and TM polarisation. To obtain those the output of a tuneable Ti:sapphire laser was coupled into a quantum well laser waveguide. The whole device was reverse biased for better contrast. The output intensity was measured using a photodiode and lock-in amplifier. In figure 5.1.5 one can see that for a given wavelength near the band edge the losses of a reverse biased quantum well waveguide are higher for TE than for TM polarisation. This illustrates that the polarisation dependence of both the gain and the saturable absorber sections can be crucial to the operation of quantum well CPM lasers.

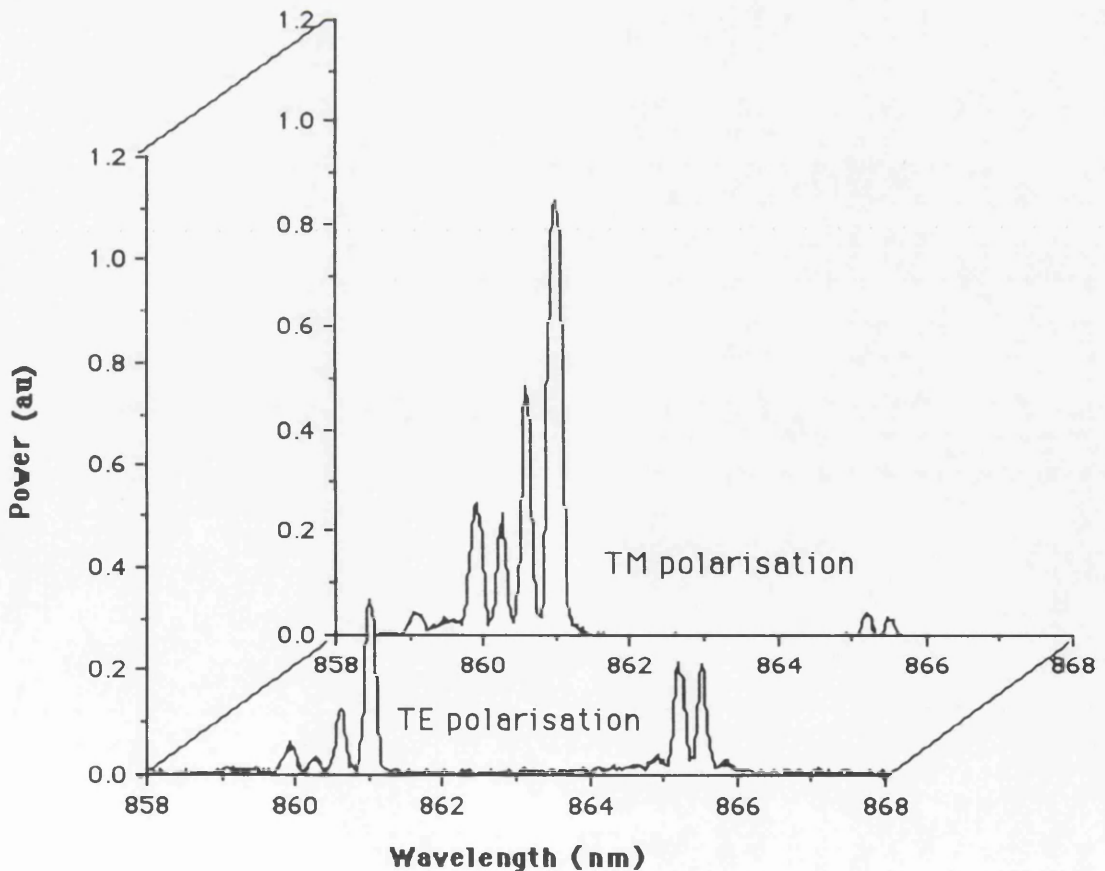


Figure 5.1.4: Optical spectrum for TE and TM polarisation of the CPM laser when 1.5V reverse bias is applied.

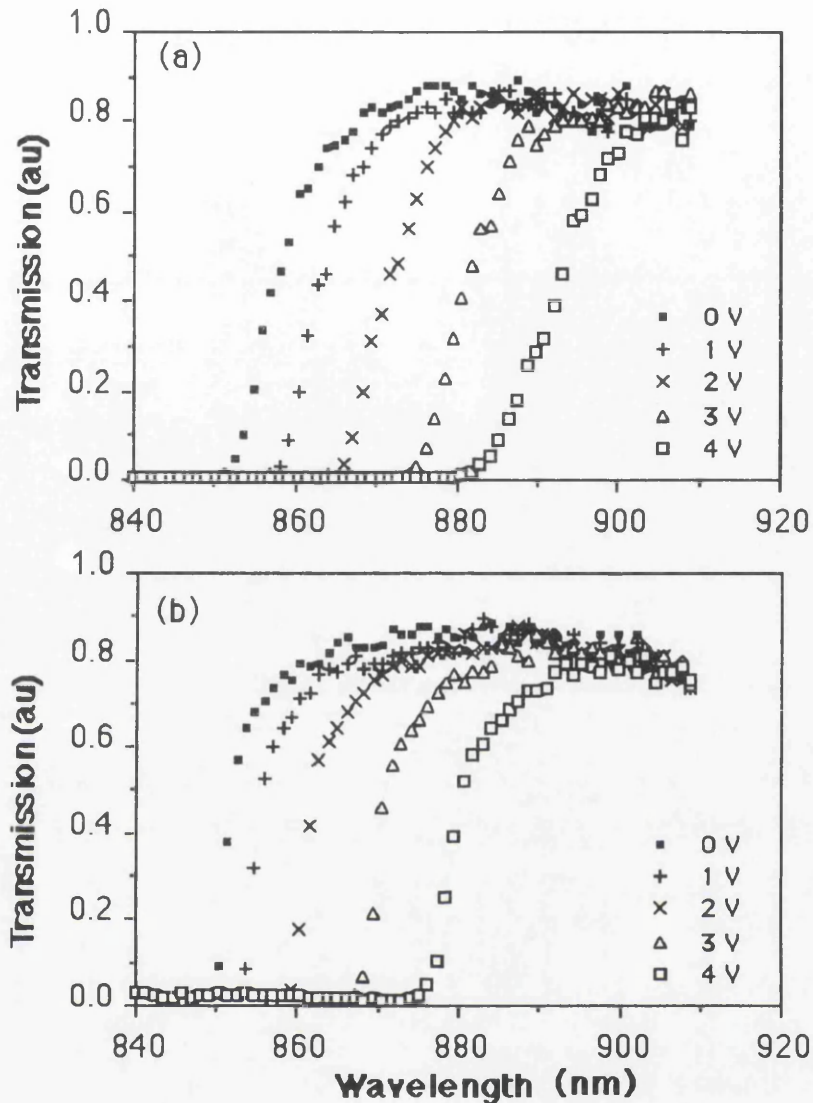


Figure 5.1.5: Spectra of transmitted light through quantum well waveguide as a function of applied reverse bias for (a) TE and (b) TM polarisation.

A full explanation of the above effect would require careful modelling. But in outline, a qualitative explanation is as follows: in a quantum well laser the heavy and light hole valence band degeneracy is removed due to the effects of confinement, and the laser operates preferentially in the heavy hole transition because of the higher density of states associated with the heavy hole and thereby larger gain for the heavy hole (TE polarised) transition. In the saturable absorber section of the CPM laser, the reverse bias produces an absorbing region with a polarisation dependent absorption as is well known from studies of the quantum confined Stark effect [8, 9] and is illustrated in figure 5.1.5. The losses introduced by the saturable absorber in the CPM laser are then polarisation, wavelength and intensity dependent in a complicated fashion which would require some detailed modelling to be understood. However, the general trend is

that the heavy hole operation is attenuated by the preferential TE absorption in the saturable absorber and this allows light hole and TM operation to take place in the laser.

The long term stability of these devices has not been fully investigated. Some simple tests have discovered that there is a change in the electrical characteristics of the saturable absorber after CPM operation of the device. After a short period (a few seconds) of CPM operation, the diode characteristics of the saturable absorber section are degraded permanently and afterwards, when the saturable absorber section is then forward biased, it does not provide gain. However, changes to the electrical characteristics cease after an initial “burn-in” period and can be avoided altogether if the reverse bias current is limited by a series resistance (although in the results presented here in this section the reverse bias current has not been limited).

These polarisation dependent effects could not be reproduced from another set of lasers fabricated afterwards. During tests of these new lasers, the previously observed change in the electrical characteristics of the saturable absorber could not be detected. Moreover, polarisation-bistability in lasers have been reported for InGaAsP/InP based materials [10]. In this case the TM gain is enhanced by stress in the active layer, which is introduced by lattice mismatch between epitaxial layer and substrate. Although lattice mismatch is usually very small for GaAs based material, some sort of defect on the substrate of that first particular sample might have caused some stress and contributed to the enhancement of TM polarisation gain in that laser. Therefore, further experimental work, as well as theoretical modelling, would be necessary to find out which of these three effects (dichroism of quantum wells or possible damage of saturable absorber or possible strain in active layer), or which combination of them, plays the major rule in the TE-TM polarisation effects observed here.

In conclusion to this section, the realisation and characterisation of a short wavelength (~860 nm) quantum well AlGaAs/GaAs monolithic colliding pulse mode-locked (CPM) laser has been described. The devices have mode locked operation repetition rates in the range 73-129 GHz and pulsewidths of 2 ps or less. The importance of the polarisation dependence of the saturable absorber and the gain section in the operation of a quantum well monolithic CPM is discussed.

5.2 - Multiple Colliding Pulse Mode-Locked Lasers

Semiconductor laser mode-locking at harmonics of the cavity round trip frequency allows the generation of high repetition rate train of pulses from longer cavities. It can be achieved in actively mode-locked lasers by suitable choice of the repetition frequency of the driving signal [11]. It has also been observed in extended cavity passive two-section mode-locked lasers [12, 13], where several harmonics were obtained depending on the gain section current, in a multi-stable behaviour.

The monolithic passive mode-locking scheme is attractive for achieving high repetition rates, above 100 GHz since it does not require the injection of a high frequency RF signal. Portnoi et al. first observed passive mode-locking at 200 GHz, by using ion implantation to form the saturable absorber section in a monolithic laser structure [14]. Chen et al. used a 250 μm long monolithic passive colliding pulse mode-locked (CPM) laser to obtain short pulses at 350 GHz [4]. CPM lasers usually have 2 counter propagating pulses circulating in the cavity which produce a train of pulses at a repetition rate that is twice the cavity mode space frequency, i.e. second harmonic of the repetition rate. Doubling of CPM repetition frequency has been observed in a passive monolithic ring laser [15], but again depending on the gain section current.

More recently a growing interest has been apparent in the generation of ultrashort pulses at ultrahigh repetition rates [16], reaching terahertz rates [17, 18]. Such high speed is achieved by inducing the laser to operate at harmonics of the fundamental inverse round-trip time of the monolithic cavity.

This section presents a modified CPM laser configuration which can generate 1, 2, 3 or 4 pulses in the cavity, giving the first, second, third or fourth harmonic of the repetition rate. The laser is flexible in the sense that its operation can be switched between 1, 2, 3 or 4 pulses depending on the bias (forward or reverse) applied to each of its 3 independent sections, changing the position and number of saturable absorbers in the cavity. In contrast to the lasers reported in references 12, 13 and 15 to 18, the multiple pulse operation here does not depend on the current applied to the gain section. The laser is an extension of the normal colliding pulse laser described in section 5.1 [6], which consists of a gain section with one saturable absorber placed in the centre. In the present laser more saturable absorber sections have been added. However, the basic type of operation is the same, pulses collide at each saturable absorber. This is the first observation of multiple colliding pulse mode-locked (MCPM) laser operation [19, 20]. A 400 μm long MCPM laser generates 1 ps pulses at 375 GHz, which is the fourth harmonic of the cavity round-trip frequency [21, 22].

Figure 5.2.1 shows the top view diagram of the MCPM laser, its longitudinal cross-section with the electrical connections for forward and reverse biasing, and a photograph of the actual device. The laser has a contiguously electrically connected gain section and 3 separated sections placed at every quarter of the cavity length. Each

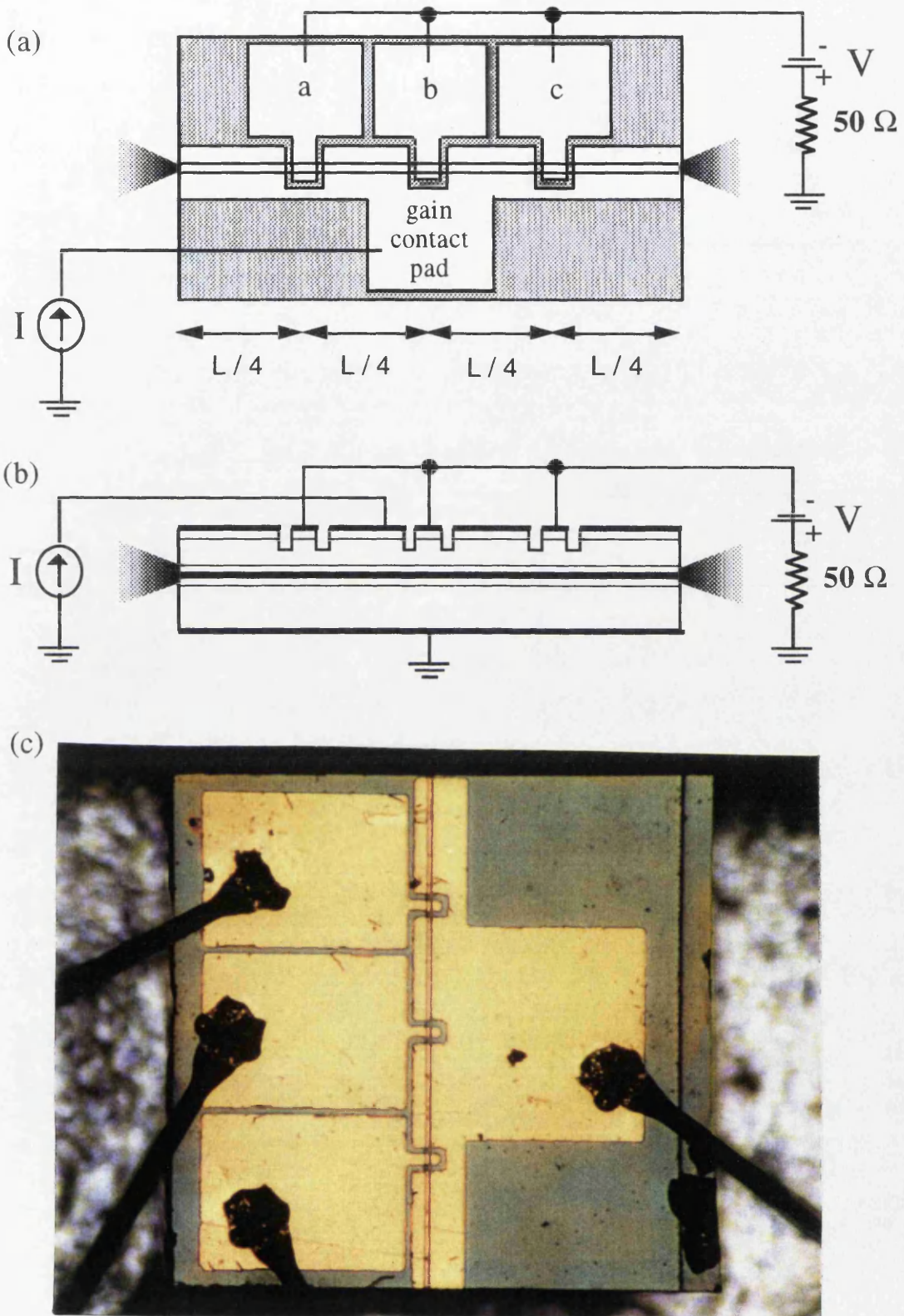


Figure 5.2.1: Top view diagram (a) and longitudinal cross-section on the waveguide (b) of the MCPM laser. The schematic electrical connections for forward and reverse biasing (for the case of having 3 absorbers in the cavity) are also shown in (a) and (b). Optical microscope photograph of a $600 \mu\text{m}$ long MCPM laser mounted and wire bonded (c).

of the 3 sections (labelled a, b and c on the diagram) is separately electrically addressable and when reverse biased it behaves as a saturable absorber, and when forward biased as a gain section. The device fabrication, as well as the semiconductor material structure, are described in Chapter 3.

The characterisation of the MCPM lasers is performed by measuring the time averaged optical spectra on an optical spectrum analyser and the linear cross-correlation trace, as described in Chapter 4. The linear cross-correlation method for time domain measurement uses a Michelson interferometer to scan a pulse through itself and its neighbours in a train of pulses, obtaining pulse width, repetition rate and coherence length of the laser [23]. This technique detects the mixing signal between light from each arm of the interferometer at a low speed photodetector and it does not employ second harmonic generation. The mixing technique employing a lock-in amplifier and 2 choppers (one in each arm of the interferometer) removes the dc level generated by the direct detection of light from each individual arm of the interferometer. Therefore only the interference signal is detected [23]. Although this technique has some limitations concerning pulse width measurement, it is attractive for characterisation of mode-locked semiconductor lasers since these devices generally generate low optical powers, which makes second harmonic generation (SHG) more difficult in practice. The limitation of the technique consists of its insensitivity to the effect of frequency chirp on pulses [19, 23]. Therefore measurements of time-bandwidth product could be misleading. However it is reasonable for these lasers because there has been no evidence of significant chirping from CPM lasers and measurements have generally indicated transform limited pulses [1-3]. A more detailed discussion about this technique is developed in Chapter 4.

The total cavity length of the laser tested is $600\ \mu\text{m}$ and each one of its 3 independent sections (a, b and c in figure 5.2.1) is $30\ \mu\text{m}$ long. The laser operates on CW regime and, when every section is forward biased, the threshold current is 30 mA. A current source is used to bias the gain sections, whereas a voltage source applies the reverse bias to the absorber sections. A $50\ \Omega$ resistor is used to limit the current flowing from the absorber sections preventing any possible damage to them. For the range of current applied to the gain section of the laser here (up to 100 mA), no temperature control is needed.

Mode locking can be achieved by reverse biasing one of the 3 sections (a, b or c in figure 5.2.1). If section a is reverse biased, providing saturable absorption, while sections b and c are forward biased, providing gain, the MCPM laser has one saturable absorber in the cavity and in this case it mode-locks at the repetition rate corresponding to the cavity round trip time. For the $600\ \mu\text{m}$ long laser it is 60 GHz, which is the first harmonic of the repetition rate. Since only one pulse is present in the cavity at a time, this mode of operation is called 1 pulse mode-locking. Figures 5.2.2-a and b show the

correlation trace and the optical spectrum for this type of operation when we apply -0.95 V to section a and 60 mA to the rest of the laser. The average width of the correlation trace pulses is 3 ps, obtained by measuring the width of each pulse shown in figure 5.2.2-a. Assuming in this case a hyperbolic secant pulse shape the deconvolution factor of 1.54 is used to obtain the actual pulse width [24], which is 2 ps FWHM. The same procedure will be applied to pulse width measurements thereafter. The longitudinal mode space measured in figure 5.2.2-b is 0.15 nm, which corresponds to the 60 GHz repetition rate obtained from figure 5.2.2-a. In contrast to the case of multimode operation discussed in Chapter 4, the coherence time of the laser observed in figure 5.2.2-a is much longer than the round-trip time of the cavity. The measurement of the coherence length is limited by the continuous scanning range of the interferometer, which is 15 mm (50 ps) in the experimental setup. But a non-continuous scan measurement, up to pulses 10 round-trips apart (150 ps), showed no noticeable change in pattern. This long coherence time compared to the round trip time (16.4 ps) and the photon lifetime (about 5 ps) is an indication of mode-locking operation. Due to symmetry similar results are obtained by reverse biasing section c and forward biasing sections a and b in figure 5.2.1.

Two pulse CPM operation is obtained when the central section of the laser (section b in figure 5.2.1) is reverse biased whereas the others (sections a and c) are forward biased by connecting them to the gain section. This configuration corresponds to standard CPM operation of lasers, which has one saturable absorber in the middle of the cavity [1, 6]. Figures 5.2.2-c and d show the cross-correlation and optical spectra for 2 pulse CPM operation when 0.37 V reverse bias is applied to section b and 54 mA is applied to the rest of the laser. It can be seen in figure 5.2.2-d that three longitudinal modes are apparent and the mode spacing is 0.3 nm which is twice the original cavity mode space (0.15 nm) and corresponds to a pulse repetition rate of 120 GHz. As discussed in section 5.1 this is the standard behaviour of a semiconductor CPM laser and it indicates that 2 pulses are circulating in the cavity and colliding in the saturable absorber. With only 3 modes locked it is difficult to fit a typical envelope shape to the optical spectra and the pulse shape can be close to a quasi-sinusoidal shape. But for the sake of simplicity it is assumed here and thereafter a hyperbolic secant pulse shape as well, which is the most commonly found in the literature for this type of device [1, 2]. From figure 5.2.2-c a deconvolved pulse width of 3 ps, at 120 GHz repetition rate is obtained.

The figures 5.2.2-e and f are obtained when the sections a and c are reverse biased with 0.74 V. The section b and the gain section are forward biased with 54 mA. In this configuration the laser has two saturable absorbers in the cavity. It can be seen in figure 5.2.2-f that in this case the separation of the longitudinal modes is 0.45 nm,

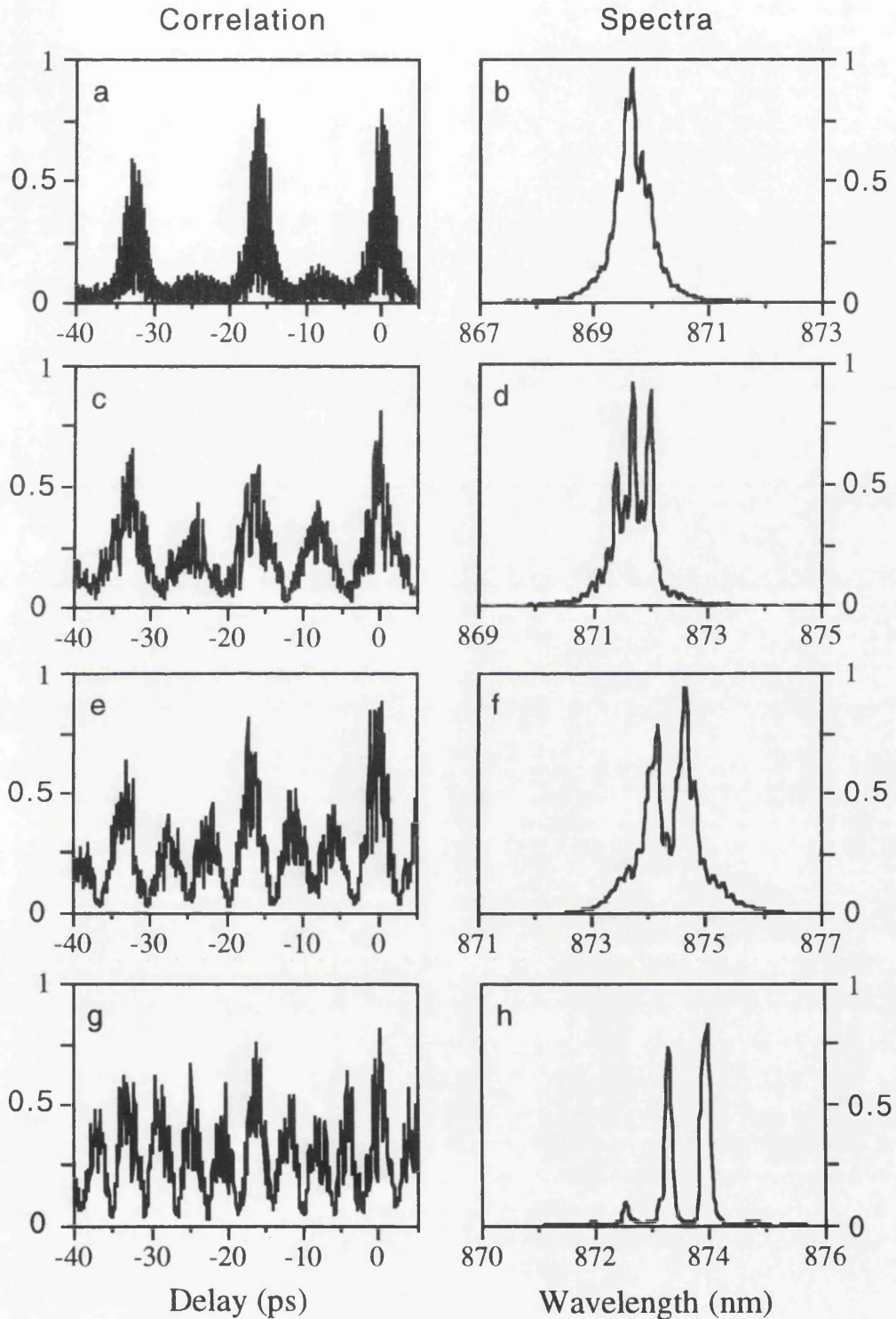


Figure 5.2.2: Linear correlation traces and optical spectra of a 600 μm long MCPM laser for different modes of operation: 1 pulse mode-locking (a and b); 2 pulse CPM operation (c and d); 3 pulse MCPM (e and f); 4 pulse MCPM operation (g and h). Vertical axes represent intensity in arbitrary units.

which is three times the original cavity mode space, corresponding to 180 GHz. Figure 5.2.2-e gives 2 ps pulse width and 180 GHz, which is the third harmonic of the repetition rate. As an extension of the 2 pulse CPM operation, this is explained by assuming that the laser is operating in a 3 pulse regime, where 3 pulses are present in the cavity, as illustrated in figure 5.2.3. Two pulses collide at every $1/3$ of the cavity length, while the other is $2/3$ of the cavity length distant from them, that is at the facet. Although the collision points do not correspond to the exact position of the saturable absorbers, the pulses are wide enough (2 ps pulsewidth is $150 \mu\text{m}$ long inside the laser) to overlap in the saturable absorber section. Therefore the pulses still collide in the absorber sections.

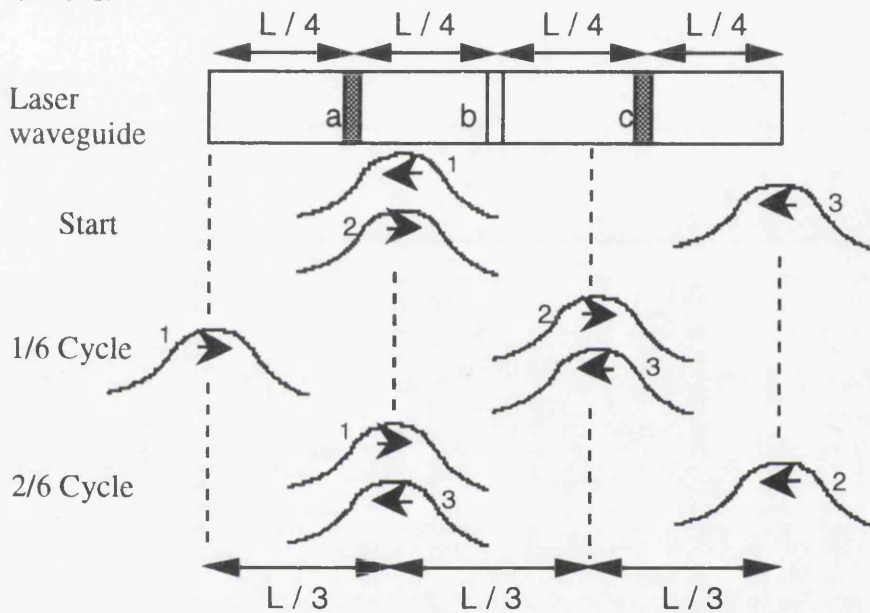


Figure 5.2.3: Illustration of the three pulse operation of the MCPM laser. Light (dark) areas in the laser waveguide indicate gain (saturable absorber a and c) sections.

Four pulse MCPM operation is achieved when the three sections (a, b, and c) are reverse biased. As a result, the laser has three saturable absorbers in the cavity. Figures 5.2.2-g and h show the cross-correlation and optical spectrum for 0.33 V reverse bias applied to the three sections, whereas the gain section is forward biased with 65 mA. The longitudinal mode separation is 0.6 nm which corresponds to a pulse repetition rate of 240 GHz, which is the fourth harmonic. The pulse width measured is 1.6 ps. This configuration has four pulses circulating in the cavity and they collide exactly in the saturable absorber sections, as illustrated in figure 5.2.4. Two of them collide with other two pulses in sections a and c, and after moving a quarter of the cavity length two pulses collide in the section b, while the other two pulses are at each facet of the laser. A shorter laser, $400 \mu\text{m}$ long with $15 \mu\text{m}$ saturable absorber sections, operating in 4 pulse mode generates 1 ps pulse width at 375 GHz repetition rate, as it is shown in figures 5.2.5-a and b.

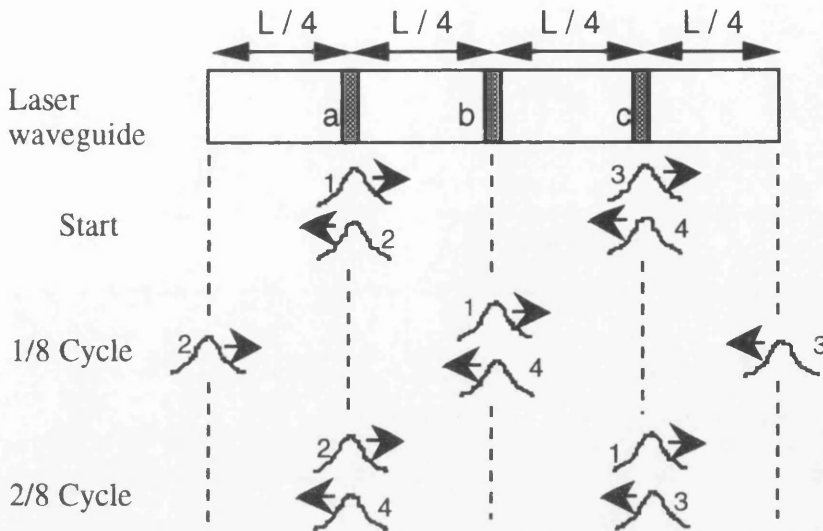


Figure 5.2.4: Illustration of the four pulse operation of the MCPM laser. Light (dark) areas in the laser waveguide indicate gain (saturable absorber a, b and c) sections.

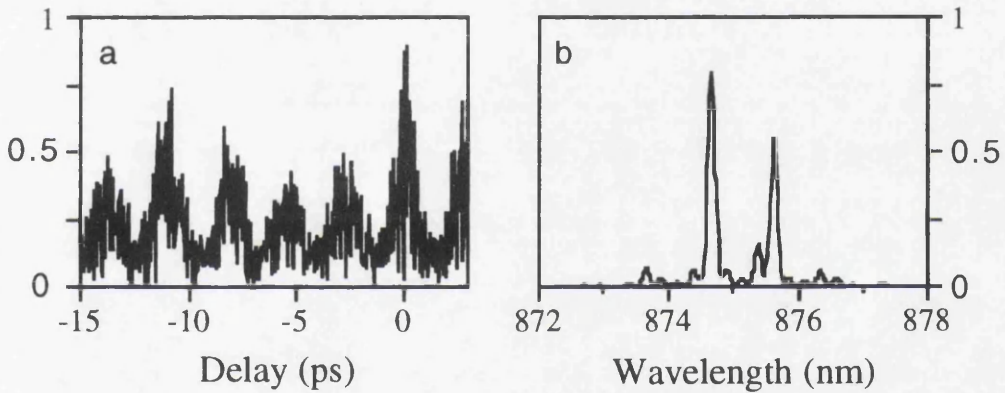


Figure 5.2.5: Linear correlation trace (a) and optical spectrum (b) of a 400 μm long MCPM laser for 4 pulse MCPM operation. The deconvolved pulse width is 1 ps and the repetition rate is 375 GHz. Vertical axes represent intensity in arbitrary units.

No change of harmonics (multistability) could be found in the devices studied here when the current is varied (up to 90 mA) for each laser configuration. It indicates that, in contrast to previous work [12, 13, 15-18], the multi-pulse operation, or in other words, the harmonic generation discussed here is due to the number and position of the saturable absorbers in the cavity and not the current level. It is corroborated by theoretical results from both frequency-domain and time-domain models, performed by E. A. Avrutin [22] (see Appendix 3).

Besides mode-locked, the laser can also operate single mode, multimode (free running, non-locked) and Q-switched, depending on the forward current and reverse bias applied to its sections. When every section of the laser is forward biased and it operates at currents not far beyond threshold, the laser emits in a single longitudinal mode. It is shown in figure 5.2.6-a for 60 mA pumping current. The side mode

suppression is larger than 25 dB (not measurable from the figure 5.2.6-a). Multimode operation occurs for currents very close to threshold and also for high currents, above the single mode operation region. Figure 5.2.6-b shows the optical spectrum for multimode operation when 35 mA is applied to the laser. Strong indications that the same laser device can also operate Q-switched were obtained from a fast photodetector and a RF spectrum analyser, where it could be observed that the laser can self-pulsate at about a few gigahertz repetition rate range, depending on the forward current applied to the gain section and the reverse bias applied to the absorber sections. The laser emits a broadened optical spectrum, typical of Q-switching [3], as can be seen in figure 5.2.7-c. Figure 5.2.7 also show optical spectra for single mode and 4 pulse mode-locked operation. It illustrates the change of mode of operation of the laser as a function of the applied bias to the saturable absorber sections. For a fixed gain section current of 80 mA, the laser spectrum changes from single mode to mode-locking and to Q-switching operation, as the absorber bias is decreased from +0.5 V to -0.4 V and to -1.66 V, respectively.

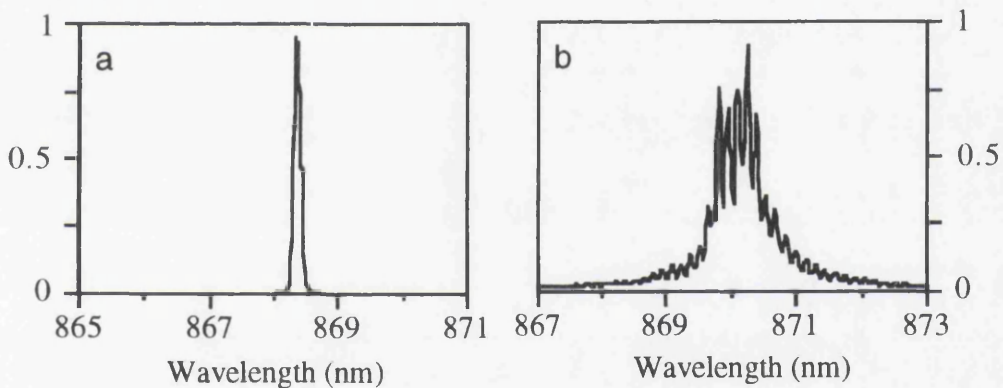


Figure 5.2.6: Optical spectrum of the MCPM laser when every section is forward biased with 60 mA (single mode) (a), and with 35 mA (multimode) (b). Vertical axes represent intensity in arbitrary units.

The range of stable mode-locking operation has also been studied. The ranges of current and absorber bias in which the laser operates in 4 pulse MCPM mode are shown in the light versus current curve of figure 5.2.8. The output optical power is measured as a function of the gain section current for different absorber biasing conditions. One can clearly see the increase of the threshold current of the laser as the absorber bias is decreased from 0V to -4V. It is due to the insertion of loss in the cavity, which comes from the increasing absorption in the absorber sections as a function of the applied reverse bias (see figure 5.1.5). The dark lines on the $L \times I$ curves show where stable 4 pulse mode-locking (at 240 GHz) is found. Up to 7 mW average power, corresponding to 25 mW peak power can be achieved. The pulse energy is 0.03 pJ. These values are very similar to the ones reported in the literature for this type of device [1, 2].

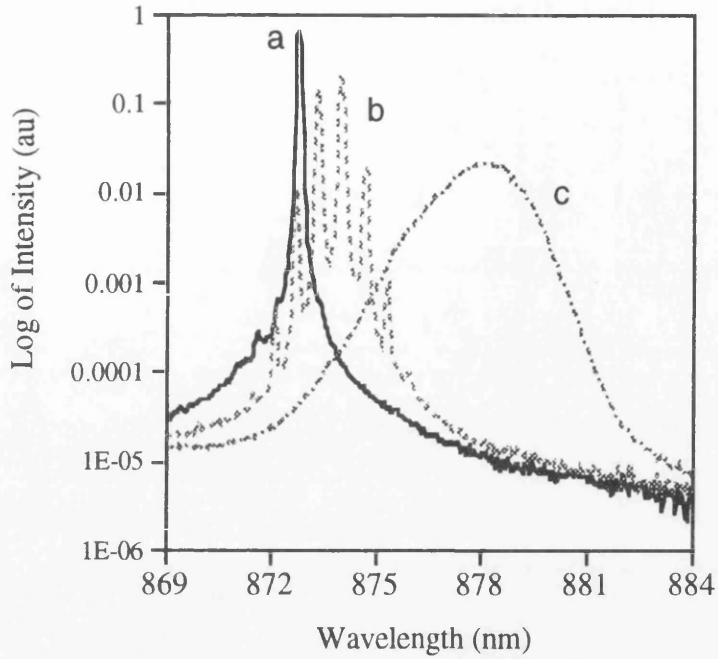


Figure 5.2.7: Optical spectra of the MCPM laser showing the change of mode of operation, from CW single mode (a) to 4 pulse mode-locking (b) and then to Q-switching (c), as the absorber sections are biased with +0.5 V (a), -0.4 V (b) or -1.66 V (c). The gain section current is fixed at 80 mA.

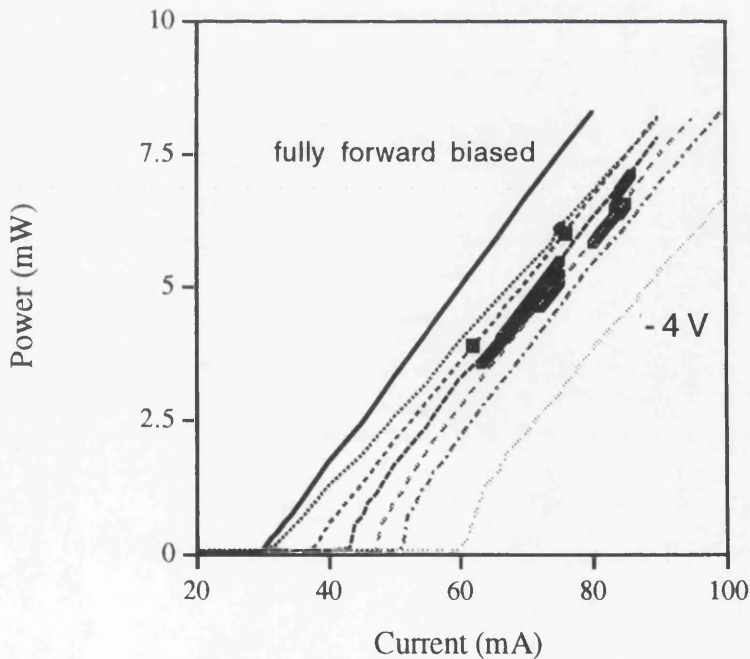


Figure 5.2.8: Laser output power versus gain section current ($L \times I$ curve) for the MCPM laser operating in 4 pulse mode for several absorber biasing conditions: all sections forward biased, 0V, -2.8V, -3V, -3.3V, -3.5V, -4V. The bias is set for zero current applied to the gain section of the laser. The range of mode-locking at 240 GHz is shown in dark lines.

The range of mode-locking has also been observed in a gain current versus absorber bias graph and it is shown in figure 5.2.9. In this graph the absorber bias is set at zero gain section current and we measure the change of the bias as the gain current is increased, which gives the dashed lines in figure 5.2.9. The lasing threshold and the areas of CW, mode-locking or self-pulsation operations are shown. Again the dark lines on the curves indicate where stable 4 pulse MCPM is found. In the $L \times I$ curves shown in figure 5.2.8, Q-switching occurs at lower currents than mode-locking, for a given reverse bias (not shown in figure 5.2.8), whereas figure 5.2.9 shows the area where Q-switching (self-pulsation) is found. A comprehensive study and characterisation of the Q-switching operation of these devices should be subject of future work.

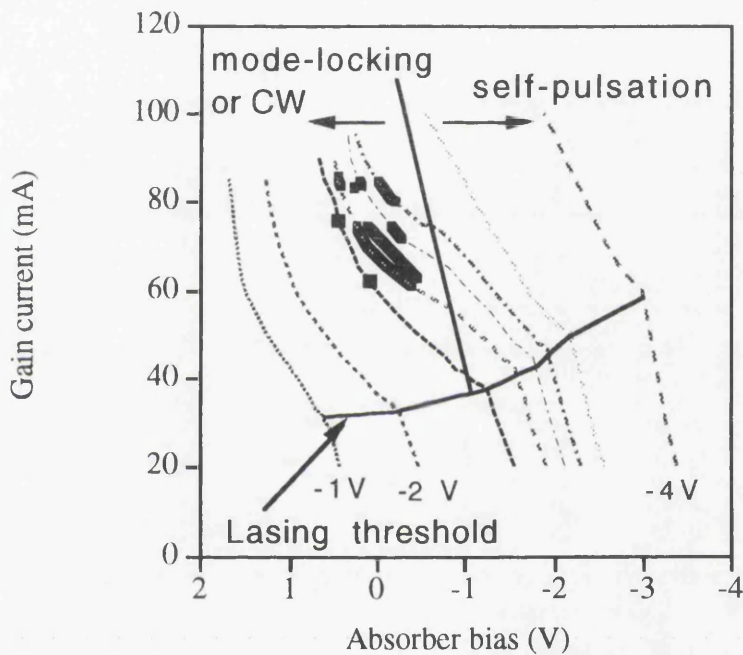


Figure 5.2.9: Variation of the absorber section bias with the gain section current for several initial values of the bias (-1, -2, -2.8, -3, -3.2, -3.3, -3.5 and -4V), which are set at zero current (shown with dashed lines). The first kink in the curves indicates the lasing threshold. The second kink marks the transition from self-pulsation to either CW or mode-locking operation. 4 pulse mode-locking operation at 240 GHz is indicated with dark lines.

Two main features differ this range of mode-locking from the ones found in the literature [1]. This range is rather small in current and reverse bias, and it shows two distinct areas where 4 pulse MCPM is observed. From figures 5.2.8 and 5.2.9 it is clear that there are two regions where mode-locking is found for each absorber bias curve, with initial values between -2.8 and -3.3V. A possible explanation for these features lies on the need of very fast absorption and gain recovery in order to sustain mode-locking at 240 GHz (4.1 ps period). In these mode-locked devices saturable absorption is achieved by applying a negative bias between the absorber section (a, b or c in figure 5.2.1) and the ground contact. This reverse biasing technique has been successfully

employed by a number of authors [1-7]. An electric field is applied perpendicular to the quantum wells, which induces a shift of the semiconductor band edge, known as quantum confined Stark effect (see figure 5.1.5) [8, 9]. Therefore the reverse bias introduces absorption in the laser sections, which is saturated by the intensity of the laser pulse travelling in the cavity by mostly band filling effect [8, 9, 25]. After the passage of the pulse the applied reverse bias acts sweeping out the generated carries from the absorber sections, helping the recovery to the unsaturated state. Pump and probe measurements of the absorption recovery time of such type of saturable absorber showed that the absorption recovers to a high absorption state in approximately 10 ps [26]. This recovery time allows mode-locking at repetition rates as high as 100 GHz, as predicted by Lau [27], but it seems unlikely that this mechanism alone would be responsible for mode-locking operation above 200 GHz. According to a number of authors [28-31], faster absorption bleaching and recovery mechanisms, with sub-picosecond relaxation times, should add to the relatively slow mechanism described above to sustain mode-locking at ultra-high repetition rates. This is also the conclusion from frequency and time domain models developed by E. A. Avrutin for the simulation of MCPM lasers [22] (see Appendix 3), where 0.5 ps recovery time was used. However it is still not clear which mechanisms are responsible for this fast dynamic behaviour and several different effects have been studied. Karin et al. found that spectral hole burning, carrier-carrier scattering and carrier heating by free carrier absorption and two-photon absorption give rise to a fast component (150 fs) of the recovery time of their saturable absorber [30, 31]. Besides these candidates, these fast dynamics might also be achieved with the help of the light and heavy hole excitonic non-linearities [25, 28]. The recovery time of excitonic absorption bleaching has been measured to be of approximately 300 fs in GaAs/AlGaAs multiple quantum well systems [32]. The two exciton peaks, corresponding to the light and heavy hole excitons, would give rise to the two distinct regions of mode-locking observed in figures 5.2.8 and 5.2.9. Mode-locking at 240 GHz would only be achieved for currents and reverse bias such that the lasing wavelength corresponds to an exciton peak of the quantum well saturable absorber. The previously reported ranges of mode-locking are for longer lasers, which generate lower repetition rates, at about 80 GHz [1]. They naturally have more relaxed requirements on fast dynamics of gain and absorption, which provokes the widening and merging of the two regions into a continuous one.

This conclusion is corroborated by figure 5.2.10, which shows the dependence of the lasing wavelength with the gain section current applied to the MCPM laser for different absorber sections bias. When the whole laser is forward biased the lasing wavelength increases with the increasing current at a rate of 0.65 \AA/mA . It is due to the temperature dependence of the semiconductor band-gap [33].

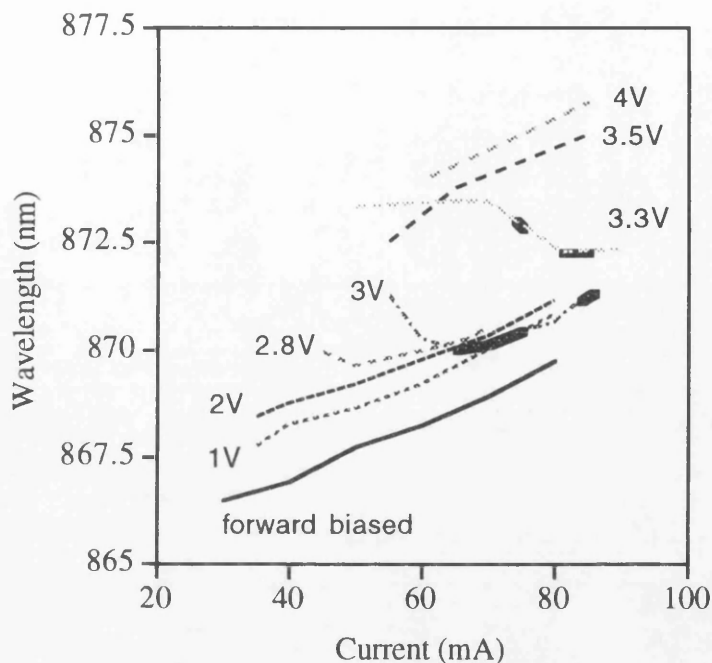


Figure 5.2.10: Lasing wavelength as a function of gain section current for different reverse bias applied to the saturable absorbers of the MCPM laser in 4 pulse configuration. Dark lines indicate where 4 pulse mode-locking at 240 GHz is found.

As the current is increased the temperature increases, decreasing the band-gap of the material, which causes the lasing wavelength to shift towards longer wavelength. For 1 and 2 V reverse bias applied to the absorber sections the lasing wavelength shifts in a similar manner to the one for fully forward bias condition. The pattern is substantially different for reverse biases between 2.8 and 3.3 V, where mode-locking at 240 GHz is found. In these cases the rate of shift is decreased or it even becomes negative. For higher reverse biases, 3.5 and 4 V, the pattern of the variation of lasing wavelength with current is again similar to the fully forward biased case. A possible explanation of these effects lies with the gain section lasing wavelength and absorber section reverse bias dependence with the injected current. The former was discussed before. The latter is due to finite ($2\text{ k}\Omega$) electrical isolation between gain and absorber sections. As the current in the gain section is increased, the reverse bias of the absorber section decreases because of current leak from the gain section to the absorber section. This effect can be seen in the dashed lines of figure 5.2.9. Therefore an increase of the current in the gain section causes a red shift of the lasing wavelength in the gain section and a blue shift of the absorption band edge in the absorber sections (see figure 5.1.5). Depending on the initial values of reverse bias and current, these opposing effects will tend to balance each other, which is the case for reverse biases between 2.8 and 3.3 V of figure 5.2.10. It corroborates with what was observed in figures 5.2.8 and 5.2.9, since mode locking is only found when the lasing wavelength is scanned through the

absorption band edge and consequently the exciton peaks of the absorber section. If too little reverse bias is applied initially, the red shift effect from the gain section is the dominant effect since the absorption band edge is too far behind the lasing wavelength. It is the case for 1 and 2 V of figure 5.2.10. In this case the laser does not operate mode-locked, as shown in figure 5.2.9. If too much reverse bias is applied to the absorber, lasing will occur at a wavelength lower than the absorption band edge and again the shifting behaviour will be dominated by the red shift of the gain section (which is the case for 3.5 and 4 V), up to the point when the band edge of the absorber is brought closer to the lasing wavelength (not observed for the currents used in figure 5.2.10). In this case the laser operates Q-switched, as shown in figure 5.2.9.

The difference of lasing wavelength between the two regions of mode-locking shown in figure 5.2.10, which is around 1 nm, does not correspond to the distance between the light and heavy hole excitons of the laser, estimated to be of around 4 to 5 nm. It is due to the opposite direction of the effects of gain (red shifting) and absorption (blue shifting) change in the lasing wavelength with increasing current.

In conclusion to this section, the operation of a monolithic multi-sectioned semiconductor laser has been described. The laser can be operated as either single mode, multimode, self pulsation (or Q-switched) and mode-locked in either 1, 2, 3 or 4 pulse operation. This device is a very versatile source of high repetition rate (up to 375 GHz) ultrashort pulses (around 1-3 ps) of light. The various modes of operation of the device have been experimentally investigated. Experimental indications of the presence of excitonic nonlinearities in its operation have been found and qualitatively discussed. The indications consist of the observation of two distinct regions where mode-locking is found in measurements of range of mode-locking. The two regions correspond to the contribution of fast bleaching and recovery of light and heavy hole excitons. These fast saturable absorption dynamics of quantum wells, measured in reference 32 to be of approximately 300 fs, may be responsible for the fast component of saturable absorption necessary for mode-locking operation at 240 GHz. A more comprehensive experimental as well as theoretical study of the contribution of excitonic nonlinearities for the ultra-high speed laser operation should be performed in order to obtain more quantitative conclusions on it.

5.3 - Monolithic CPM Ring Lasers

Semiconductor lasers in monolithic ring cavities are probably the most suitable laser configuration for applications in monolithic optoelectronic integrated circuits [34]. The ring cavity dispenses the use of facets for optical feedback and output coupling. The output coupling is provided from an extra waveguide by a simple Y-junction to the ring cavity [34], or a directional coupler [35], or a multimode interference (MMI) coupler [36]. The extra waveguide can then lead the laser beam to other optoelectronic devices in an integrated circuit without interfering with the laser operation.

Semiconductor lasers have been actively and passively mode-locked in external ring cavities [37, 38]. Monolithic ring lasers have also been successfully mode-locked, both in passive [15] and active regimes [39]. From the practical device fabrication point of view, monolithic mode-locked ring lasers have some particular characteristics, which give this configuration some advantages in relation to their linear Fabry-Perot cavity counterparts. Differently from Fabry-Perot (FP) cavities, the position of a saturable absorber in a ring cavity is not an important issue due to its inherent symmetry. Regardless of the position of the absorber section in the ring cavity the laser will operate in colliding pulse configuration, as long as there are two counter-propagating waves in the laser resonator. Another interesting aspect regards the repetition rate of the lasers. Since the cavity length is defined by photolithography, rather than by cleaving end facets like in FP cavities, the repetition rate of mode-locked ring lasers is better defined and would be more reproducible in mass-production. Moreover, because of the larger Q factor of the ring cavity, which comes from the lower loss from the output coupling, the ring laser is more suitable for implementation of long monolithic cavities than FP lasers. It means that with ring lasers it is easier to achieve lower repetition rates. Monolithic CPM ring laser operation has been demonstrated at 86 GHz [15]. 9 GHz repetition rate has been obtained from a monolithic CPM ring laser with non-absorbing passive sections [39].

This section reports on the design and characteristics of a monolithic CPM ring laser which has two saturable absorber sections and operates at 28 GHz repetition rate [40]. The realisation of this laser is a collaboration with Dr. T. Krauss from Glasgow University. The laser was fabricated in double quantum well GaAs/AlGaAs material. The 2 μm wide strip-loaded waveguide and MMI output coupler are formed by standard SiCl_4 dry etching. Detailed descriptions of wafer structure and fabrication technique for ring lasers are given in references 36, 40 and 41. After top metallisation (NiCr/Au), which defines the sections of the laser, a dry etch is performed to increase the electrical isolation between sections in a similar manner as described in Chapter 3. Figure 5.3.1 shows the top view of the CPM ring laser. The ring cavity configuration consists of two semi-circles of 400 μm radius, separated by two straight sections

300 μm long, in a "race-track" shape. The total length of the cavity is 3 mm. Each saturable absorber is 150 μm long, separated from the gain section by 10 μm long gaps. The MMI coupler is placed in one of the straight waveguide sections, to which the output waveguide is connected. This waveguide is designed to make a 4° angle with the perpendicular position at the laser output facet in order to reduce the optical feedback and possible disturbance of the ring laser operation. These tilted facets also avoid lasing action at the output waveguide, which effectively works as an amplifier section.

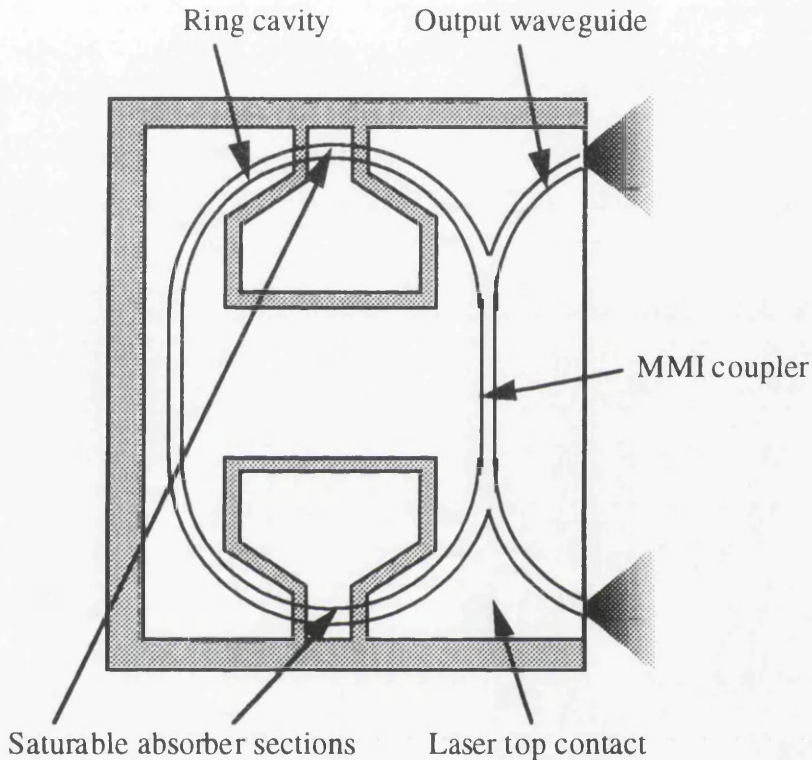


Figure 5.3.1: Schematic diagram of the monolithic CPM semiconductor ring laser. The ring cavity is not circular because of the MMI coupler. Gradients indicate laser output at waveguides.

The CW threshold current of the laser is 110 mA, which is low considering the total length of pumped waveguide (3 mm of laser and 1.5 mm of output waveguide) [40]. Optical spectra of the laser output have been obtained with a scanning Fabry-Perot interferometer. They revealed that when fully forward biased the laser emits in a single longitudinal mode, up to 10 mW CW output power. When the two saturable absorber sections are biased with -0.4 to -1.2 V the laser emits in 6 to 8 longitudinal modes, indicating that mode-locking might be taking place. The repetition rate is 28 GHz, given by the longitudinal mode separation [40]. Observation of CPM operation from the optical spectrum of the laser emission is more difficult in ring than in FP lasers. The typical doubling of longitudinal mode separation that occurs in a FP laser does not take place in a ring laser due to its cavity configuration. The round trip of a ring cavity is the same for CW and mode-locking emission. The confirmation of the mode-locking

operation of the laser with time domain measurements to obtain pulse width and repetition rate has not been performed yet.

When only one of the absorber sections is reverse biased and the other one is forward biased the laser operates at the same repetition rate but in a less stable mode-locking regime. The optical spectrum shows fewer modes, which indicates a longer pulse width. The two saturable absorbers in colliding pulse configuration in the cavity provide extra pulse shortening and stabilisation of the mode-locking operation of the laser.

In conclusion to this section, the design, fabrication and frequency domain characterisation of a monolithic CPM ring laser have been described. Evidence of mode-locking operation at 28 GHz repetition rate has been obtained from frequency domain measurements. The use of two saturable absorbers in colliding pulse configuration in the ring cavity showed improvements in the device operation. With two absorbers, the laser produces shorter pulses than with only one absorber section.

5.4 - CPM Bow-tie Lasers

High power, short pulse generation from semiconductor lasers has been sought for applications in free space and optical fibre communications, in diode pumped fibre and solid state lasers and amplifiers, and specially in nonlinear optical devices [42]. Such a compact, robust, reliable, low cost and low power consuming source of high peak power pulses would bring to the every-day-life the capabilities of the nonlinear optics, such as second harmonic generation and frequency conversion, ultrafast nonlinear switching and all-optical signal processing, among others. It would have a tremendous impact in ultra-high-bit-rate communication systems, high-density data storage, optical computing, material processing, marking and machining, and many others [42-44].

The recent development of a new type of device, the tapered-waveguide travelling-wave semiconductor laser amplifier, has contributed significantly to the achievement of high power CW laser output [43, 44]. The flared geometry of the device, narrow at the input (2-5 μm) and wide at the output (50-200 μm), can produce single transverse mode operation, lateral beam expansion and diffraction limited output beam with high gain coefficient [43, 45, 46]. The wider cross-section area at the output decreases the power density at the facet, which is the cause of catastrophic optical damage of the facets. These flared amplifiers, in conjunction with laser diodes in master oscillator power amplifier configuration, have produced 2 W CW output power in both discrete [47] and monolithically integrated [48] devices.

A tapered amplifier has been employed in conjunction with a passively mode-locked external extended cavity semiconductor laser to produce pulses of 4.2 ps duration at 2.5 GHz repetition rate with average powers of 296 mW, peak powers of 28.1 W and pulse energy of 118 pJ [49]. High power active mode-locking has also been realised with an external compound cavity containing a narrow stripe gain section, where a low DC bias and the RF signal is applied, and a tapered gain section to provide large amplification and high laser output powers [50]. This mode-locked laser generates 16 W peak power, with pulse energy of 450 pJ and pulse width of 12 ps at 500 MHz repetition rate. The average output power is 0.5 W.

A monolithic semiconductor laser employing tapered waveguides has been realised [51, 52]. The waveguide configuration of the device consists of two tapered waveguides joint at the narrow end, forming the so called bow-tie laser. With a reverse biased saturable absorber section in the middle of the device it has operated Q-switched [51], and passively mode-locked [52]. Under Q-switching operation the laser gave 100 pJ pulse energy and 15 ps pulse width, which implies a peak power of 6.6 W [51]. At mode-locked operation the device gave over 50 mW average power, with 0.65 pJ pulse energy, 5 ps pulse width and 130 mW peak power at 100 GHz repetition rate [52].

Although these figures represent improvements on previously reported monolithic device output powers, they are rather disappointing, specially considering that the current drive of the laser was pulsed, with 30 ns electrical pulses. The CW operation characteristics of these devices are yet to be shown.

This section is dedicated to the development of a monolithic colliding pulse mode-locked bow-tie laser similar to the one describe above for high power CW-mode-locked operation. Figure 5.4.1 shows the device diagram and an optical microscope photograph of the fabricated CPM bow-tie laser.

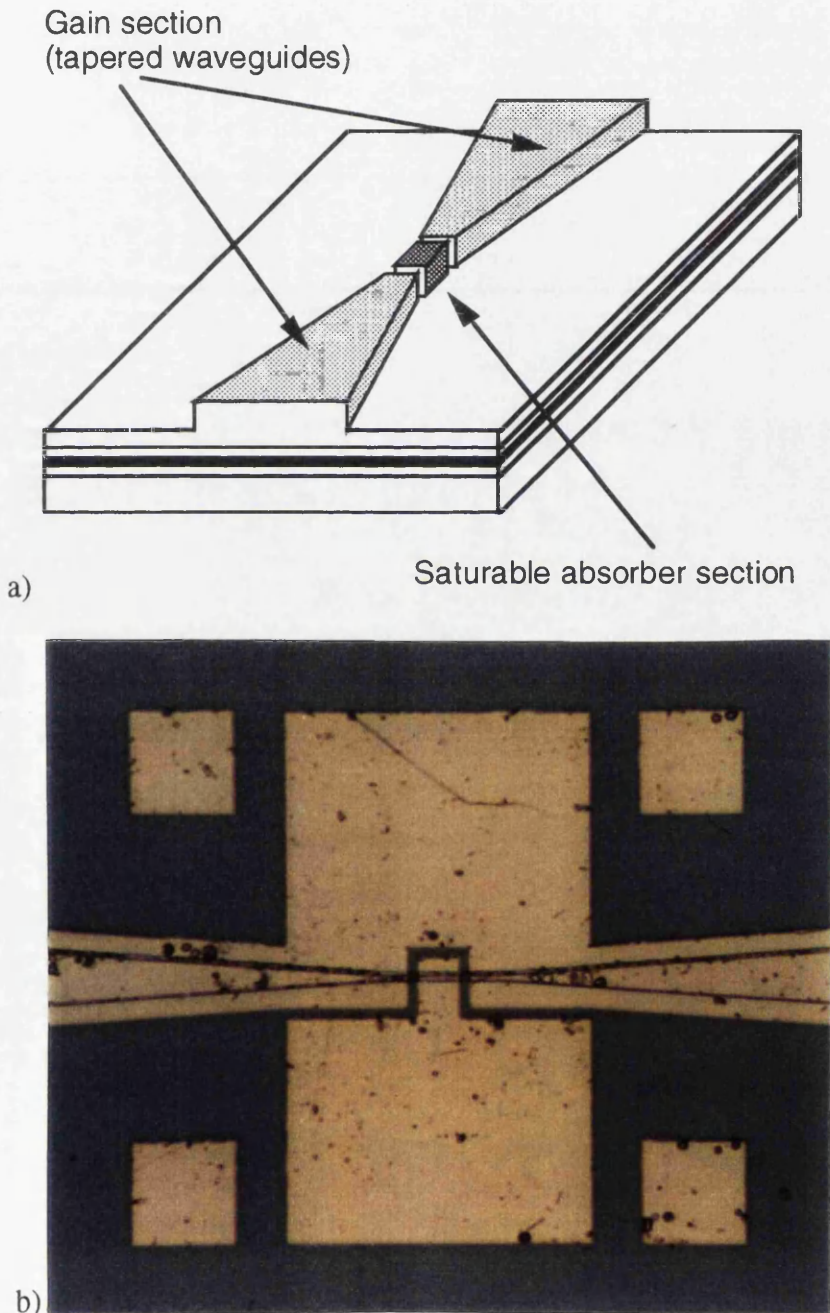


Figure 5.4.1: Schematic diagram in perspective (a) and optical microscope photograph (b) of a CPM bow-tie laser (the squares are $100 \times 100 \mu\text{m}$).

The semiconductor material structure and the fabrication procedure are described in details in Chapter 3. The narrow central part of the waveguide consists of a straight $3\ \mu\text{m}$ wide and $120\ \mu\text{m}$ long rib waveguide, from which the tapered waveguides follow with a half angle of 4 degrees. Two kinds of devices were fabricated. One of them with gain and saturable absorber contacts as shown in figure 5.4.1-b, to be mounted p-side-up, and another one with no electrical contact to the central absorber section. This one is designed to be mounted p-side-down to allow for more efficient heat sinking. Therefore in this device the saturable absorber section is left unbiased. The devices tested were 0.8 and 1 mm long, corresponding to waveguide width at facets of 50.5 and 64.5 μm , respectively. Under CW current pumping, the threshold current of the 1 mm long device mounted p-side-down is 0.25 A, corresponding to a threshold current density of $830\ \text{A}/\text{cm}^2$, at a stabilised heatsink temperature of 22°C . Pumped with 0.6 A the laser gives over 100 mW average power. Although the optical spectrum resembled the typical CPM features, with doubling of the longitudinal mode separation, the output power decreased very rapidly, changing the spectrum and the operating conditions. It is not believed to be an effect of inefficient heatsink since its temperature was kept constant at 22°C . From the expanded collimated laser beam, a constantly changing of transversal mode of the lasers was observed. After an initial single lobe (fundamental mode) operation the laser changes to 2 or 3 lobes as the output power drops. This mode changing behaviour persists until catastrophic failure occurs [53, 54]. It is believed that localised facet damage causes this mode instability and power drop, and leads to catastrophic failure of the lasers. Differently from the flared amplifiers, the facets of the lasers were not coated and they provide optical feedback to the laser. The feedback of light back to the waveguide tends to concentrate the optical intensity in the middle of the laser waveguide, not allowing it to expand as in amplifiers. The high power density at the uncoated facet causes facet oxidation and/or damage, which gives rise to the decrease in laser output power and induces the laser to switch to another transverse mode distribution within the wide facet area. The continuation of this process leads to the final laser failure. This process can be avoided all together if the output power of the laser is limited to about 20 mW.

In conclusion to this section it can be said that although this first attempt to realise high power CW operation of a CPM bow-tie laser has not been successful, the results obtained so far indicate that modifications on device structure should improve its performance and lifetime. The high-power short-pulse generation characteristics of the device cannot be studied until its reliability problems are solved. The main improvement would be the use of a reflection coating on laser facets to increase the power density limit at which facet damage occurs [53, 54]. Other modifications, like the decrease of the tapered waveguide half angle from 4 to 2 or 3 degrees and the decrease of the number of quantum wells of the material from 4 to 2 should decrease the

threshold current of the devices, decreasing the operating temperature and heatsink requirements, increasing device lifetime. These procedures would be particularly important for the realisation of long cavity (longer than 1 mm) lasers.

5.5 - Clock Recovery Device

The future (next millennium) demand for broad band services may require telecommunication networks to operate with Tb/s capacity. For such high bit-rate networks the conventional post-detection electronic processing circuitry would introduce an electronic "bottleneck" in the system due to its inherent speed limitations. To avoid it, all-optical signal processing schemes in the so called "transparent" networks are likely to be used [55, 56]. As part of this system, all-optical clock recovery must be realised to provide synchronisation in the time-division signal processing circuitry. The clock signal from which the data carrying signal was generated should be retrieved to be used in all-optical switching and/or all-optical data signal regeneration for further transmission through optical fibre [56, 57].

All-optical clock recovery has been demonstrated using a mode-locked fibre laser at a rate of 1 Gb/s, although the system is believed to be able to operate at 100 Gb/s [57, 58]. In this device the optical data signal is amplified by an erbium doped amplifier and launched into and out of part of a fibre ring laser through wavelength-dependent couplers. In the fibre the signal induces a periodic phase perturbation on the laser by cross-phase modulation. If the fibre cavity length corresponds to a round-trip equal to (or an integer multiple of) the signal period, then mode-locking occurs. Another coupler provides the mode-locked laser output, which is the recovered optical clock signal [57, 58]. Importantly, it was found that although the pulses from the data signal were far from being transform-limited, with significant time jitter, the mode-locked fibre laser produced transform-limited pulses with low jitter [57, 58]. This typical characteristic of mode-locked lasers makes them attractive for clock recovery applications.

All-optical clock recovery has also been achieved using self-pulsating semiconductor lasers with repetition rate ranging from 0.2 to 5 Gb/s [59, 60]. This approach involves the injection of the optical signal, from which the clock is to be recovered, into the waveguide of a self-pulsating diode laser. The signal, which contains frequency components of its generating clock signal, influences the saturable gain and absorption dynamics of the laser, synchronising its self-pulsation with the clock signal phase and frequency [60]. This technique is very flexible to bit-rate range of operation of the system since the self-pulsation frequency can be tuned to match the data frequency with the gain current and absorber bias applied to the laser, typically from 0.5 to 10 GHz. Although this typical operating frequency is high enough for near future application, it seems unlikely, however, that this technique will be able to reach the alleged Tb/s rates of the future applications due to inherent limitations of the self-pulsation process. Moreover, the generated pulses from these self-pulsating lasers are usually significantly chirped, being very far from a desirable transform-limited pulse.

These weaknesses tend to point to the monolithic mode-locked based clock recovery devices as the favourable technique for ultra-high repetition rate time-division multiplexed (TDM) telecommunication systems.

All-optical digital signal regeneration has been demonstrated by Nonaka et al. with a side-injection-light-controlled bistable laser diode (SILC-BLD) [61]. This device consists of a main waveguide laser for signal output and an orthogonally crossed sub-waveguide for signal input. This sub-waveguide in side-injection configuration guides the signal to a saturable absorber section in the main waveguide laser. By proper choice of the reverse bias applied to the saturable absorber section, the laser presents a hysteresis loop on its lasing threshold [62]. The injection of the data signal in the saturable absorber section switches the bistable laser on and off according to the digital data signal [61]. This device also performs wavelength conversion at the same time as signal regeneration [61, 63]. Although this device is attractive for performing the all-optical signal regeneration at once, skipping the clock recovery step, it has speed limitations. The maximum data signal frequency is limited to the relaxation frequency of the bistable laser [63] and the demonstration of signal regeneration has been limited to data signals at maximum rate of 1 Gb/s, so far [61]. Due to its limitation it is unlikely that this technique will be able to deal with signal rates far beyond a few tens of Gb/s.

This section is concerned with the design and fabrication of a monolithic semiconductor T-junction colliding pulse mode-locked (T-CPM) laser and the proposal of its application as an all-optical clock recovery device [64]. The device consists of a CPM laser which has an extra waveguide crossing the laser one in the saturable absorber section, as shown in figure 5.5.1. This extra waveguide in side-injection configuration guides the signal from which the clock is to be recovered to the saturable absorber section of the CPM laser, in a similar configuration to the SILC-BLD device discussed above. The side injection waveguide is electrically pumped to provide optical amplification on the signal before it reaches the absorber section. To achieve clock recovery this signal should contribute to the saturation of the absorber section of the CPM laser, synchronising its saturation with the injected data signal. If the CPM laser cavity length corresponds to a repetition frequency equal to (or an integer multiple of) the signal frequency, then mode-locking should occur and the T-CPM laser output would be the recovered clock signal. Therefore this device should be able to recover high speed clocks, above 100 GHz, with near transform limited pulses typical of mode-locked lasers.

Figure 5.5.1-a shows a diagram of the T-CPM laser with its 2 waveguides and 3 different sections, and figure 5.5.1-b shows a scanning electron micrograph of the fabricated device. The T-CPM laser is fabricated on a GaAs/AlGaAs four quantum well material. The strip-loaded waveguides are 3 μm wide and are fabricated by standard photolithography and SiCl_4 dry etching technique. The details of material structure and

fabrication technique are given in Chapter 3. The only difference in the fabrication of this device from CPM lasers is at the cleaving stage. Because of the waveguide configuration, every side of the device must be cleaved, rather than sawn, to ensure good facet profiles at waveguide ends.

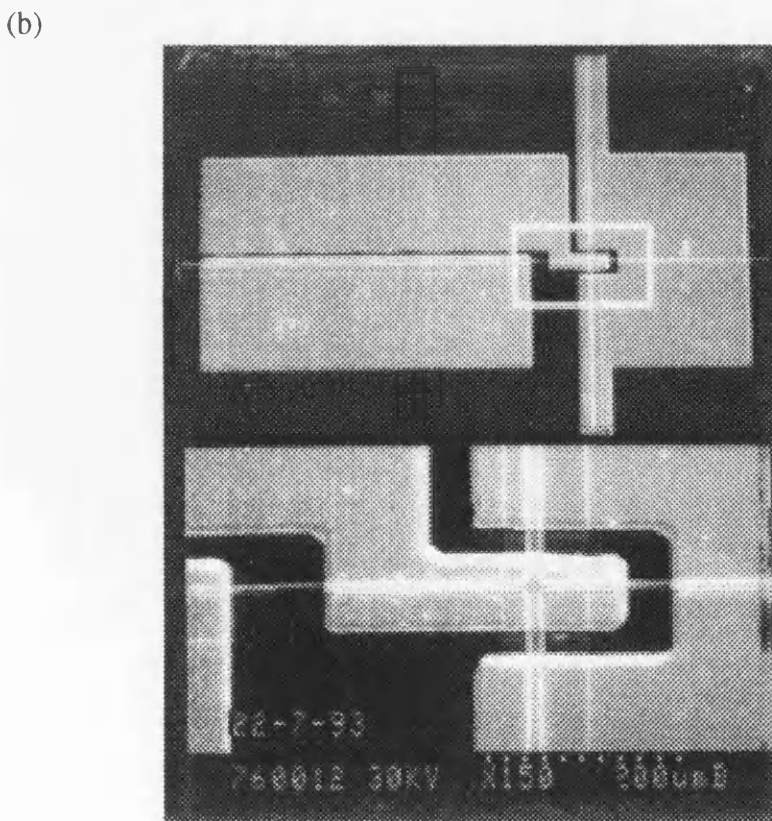
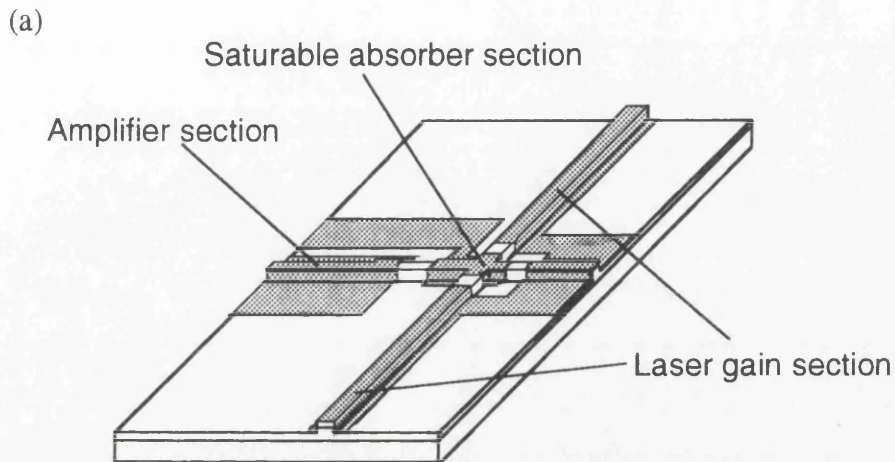


Figure 5.5.1: Diagram (a) and scanning electron micrograph (b) of the T-CPM laser.

As a first characterisation step, the CPM laser operation of the device is tested. Its laser cavity length is $430\ \mu\text{m}$, the saturable absorber section is $20\ \mu\text{m}$ long and the amplifier section is $380\ \mu\text{m}$ long. The separation gaps between sections are $10\ \mu\text{m}$ long. Figure 5.5.2 shows the optical spectrum of the T-CPM laser for a gain section current of $46\ \text{mA}$ and an absorber section reverse bias of $0.9\ \text{V}$. The threshold current of the laser is $30\ \text{mA}$. The separation between the two main modes is $0.44\ \text{nm}$, which is twice the ordinary longitudinal mode separation ($0.22\ \text{nm}$) of the $430\ \mu\text{m}$ long cavity. It indicates CPM operation, as described in section 5.1, at $175\ \text{GHz}$ repetition rate. The time domain characterisation technique was not available at the time of these measurements. Later S. D. McDougall obtained time domain characterisation of T-CPM lasers [64] with the linear cross-correlation technique described in Chapter 4. He also obtained a second harmonic autocorrelation trace of a T-CPM laser. Figure 5.5.3 shows the nonlinear autocorrelation trace (a) and the optical spectrum (b) of a $450\ \mu\text{m}$ long T-CPM laser operating in CPM regime. Figure 5.5.3-a and b also show a perfect Gaussian fit to the experimental data. He obtained a deconvolved pulsewidth of $1.05\ \text{ps}$ (deconvolution factor is 1.41 for Gaussian pulses) at $169\ \text{GHz}$ repetition rate, with a time-bandwidth product of 0.436, which is very close to the transform limited value of 0.441 for Gaussian pulses, indicating that the pulses are chip free [65].

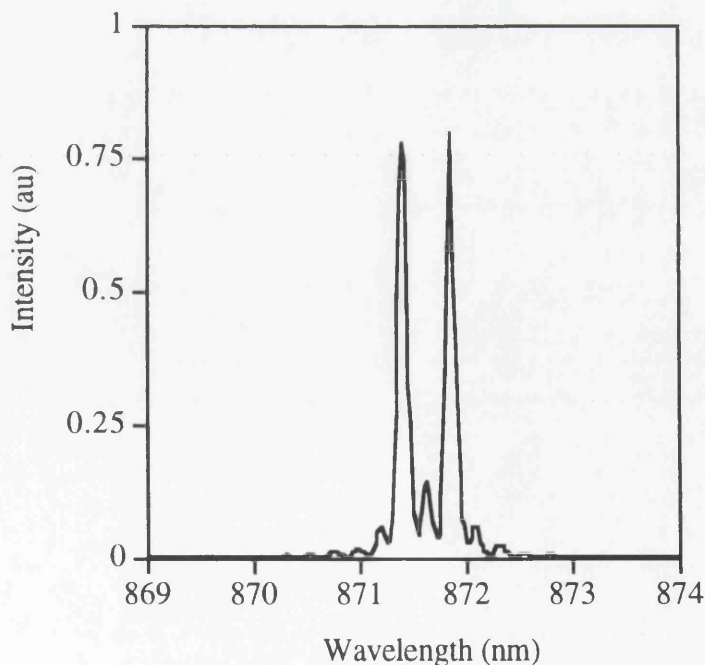


Figure 5.5.2: Optical spectrum of the T-CPM laser with no side-injected signal. Gain section current is $46\ \text{mA}$ and saturable absorber section reverse bias is $0.9\ \text{V}$.

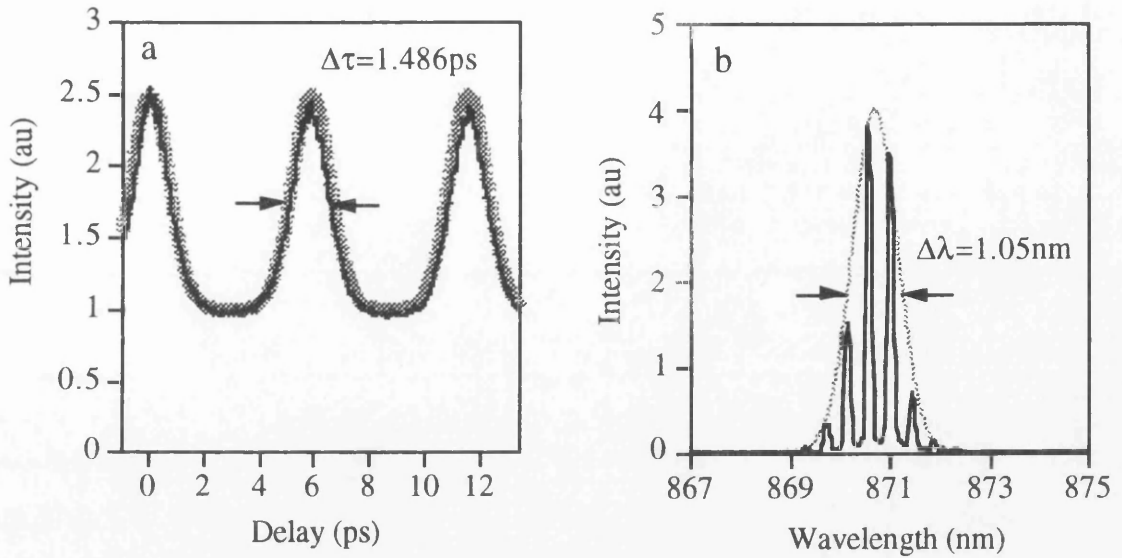


Figure 5.5.3: Second harmonic autocorrelation trace (a) and optical spectrum (b) of a 450 μm long T-CPM laser operating in CPM regime. Dark lines indicate experimental data and grey dashed lines represent a Gaussian fit to the pulse train and spectrum envelop (with permission of S. D. McDougall [65]).

The work towards the demonstration of all-optical clock recovery operation of this device has not been performed here. It will be the subject of a Ph.D. thesis by S. D. McDougall [65]. Therefore, in conclusion, this section describes the design and fabrication of a colliding pulse mode-locked laser based device which is intended to execute all-optical clock recovery at repetition rates above 100 GHz. Preliminary testing of the device showed standard CPM operation at 180 GHz. Lower repetition rates, for near future applications, may be achieved with the use of a monolithic extended cavity laser configuration fabricated by a quantum well intermixing technique [66, 67]. The use of long wavelength (1.3 and 1.5 μm) semiconductor material to fabricate the device is also a future goal, in order to make use of the full capability of optical fibres.

5.6 - Conclusions

This chapter comprised the description of the design and the characterisation of five different configurations of monolithic passive colliding pulse mode-locked lasers that have been fabricated. Firstly, in section 5.1, the results from a standard configuration of CPM laser are presented. These were the first published results on monolithic CPM quantum well laser at short wavelength, i. e. GaAs/AlGaAs based material. The obtained frequency domain evidence of mode-locking at repetition rates in the range of 73 to 129 GHz were confirmed by streak camera measurements. It also presented a previously unseen output laser polarisation dependence with the applied reverse bias to the absorber section of the laser. The generation of TE and TM polarised light from the CPM laser may have been caused by a combination of effects. Among other possible effects discussed in section 5.1, the dichroism of quantum well layers has been studied from polarisation dependent optical transmission spectra.

Section 5.2 was dedicated to the description of design and operation characteristics of a novel configuration of CPM laser. This multi-section device can have up to 3 monolithically integrated saturable absorber sections in the cavity, inducing the laser to operate at up to the fourth harmonic of the repetition rate, in what was described to be the multiple colliding pulse mode-locking (MCPM) regime. This was the first observation of geometry dependent change of harmonics in mode-locked lasers. The different regimes of operation of the MCPM laser were investigated, comprising single mode, multimode, Q-switched and first to fourth harmonic mode-locking, generating pulses of 1 ps width at up to 375 GHz repetition rate. From studies of the range of mode-locking at 240 GHz, it was found that the mode-locking occurs at two distinct regions of current and reverse bias. This previously unseen feature may represent an indication of the contribution of excitonic nonlinearities to the ultra-fast operation of the device. A more comprehensive study of these effects is necessary to confirm these indications.

Section 5.3 was concerned with the design and characterisation of a monolithic CPM ring laser which has two saturable absorbers in the cavity. Frequency domain measurements indicated mode-locking operation at 28 GHz repetition rate. The use of a second saturable absorber in the cavity has proved to improve the mode-locking operation of the device, obtaining shorter pulses and more stable operation. Time domain measurements are still to be carried out to obtain pulse width and confirmation of the repetition rate.

Section 5.4 presented an attempt to achieve high peak power CW-mode-locking operation from a CPM laser whose gain section waveguides are tapered, in the so called CPM bow-tie laser. The full characterisation of this device was not performed since it presented serious reliability problems concerning its high power CW operation. Over

100 mW average power under CW operation has been achieved, but very rapid device degradation and decrease of output power have been observed. Improvements on device design and fabrication, such as the use of reflecting coatings on the facets among others, are needed to avoid facet damage and extend the device lifetime.

Section 5.5 was dedicated to the design and development of a CPM laser based device which is intended to perform clock recovery at high repetition rates, above 100 GHz. This device consists of a standard CPM laser which has an extra waveguide in side-injection configuration. This extra waveguide amplifies and guides the optical signal from which the clock is to be recovered to the absorber section of the laser. Preliminary characterisation and tests showed that the CPM laser part of the device works as a standard CPM laser, as expected. The full characterisation of the device and the demonstration of clock recovery is currently a subject of research in the optoelectronics group at Glasgow University.

5.7 - References to Chapter 5

- [1] - Y. K. Chen and C. W. Ming, "Monolithic colliding-pulse mode-locked quantum-well lasers", *IEEE J. Quantum Electron.*, vol. 28, pp. 2177-2185, Oct. 1992
- [2] - D. J. Derickson, R. J. Helkey, A. Mar, J. R. Karin, J. G. Wasserbauer and J. E. Bowers, "Short pulse generation using multisegment mode-locked semiconductor lasers", *IEEE J. Quantum Electron.*, vol. 28, pp. 2186-2202, Oct. 1992.
- [3] - P. P. Vasil'ev, "Ultrashort pulse generation in diode lasers", *Optical and Quantum Electron.*, vol. 24, pp. 801-824, 1992.
- [4] - Y. K. Chen, M. C. Wu, T. Tanbun-Ek, R. A. Logan and M. A. Chin, "Subpicosecond monolithic colliding-pulse mode-locked multiple quantum well lasers", *Appl. Phys. Lett.*, vol. 58, pp. 1253-1255, Mar. 1991.
- [5] - C. Harder, J. S. Smith, K. Y. Lau and A. Yariv, "Passive mode locking of buried heterostructure lasers with nonuniform current injection", *Appl. Phys. Lett.*, vol. 42, pp. 772-774, May 1983.
- [6] - J. F. Martins-Filho, C. N. Ironside and J. S. Roberts, "Quantum well AlGaAs/GaAs monolithic colliding pulse mode-locked laser", *Electron. Lett.*, vol. 29, pp. 1135-1136, June 1993.
- [7] - P. P. Vasil'ev, V. N. Morozov, Y. M. Popov and A. B. Sergeev, "Subpicosecond pulse generation by tandem-type AlGaAs DH laser with colliding pulse mode locking", *IEEE J. Quantum Electron.*, vol. 22, pp. 149-151, Jan. 1986.
- [8] - S. Schmitt-Rink, D. S. Chemla and D. A. B. Miller "Linear and nonlinear optical properties of semiconductor quantum wells" *Advances in Physics*, vol. 38, no. 2, pp. 89-188, 1989.
- [9] - C. Weisbuch and B. Vinter, *Quantum semiconductor structures: fundamentals and applications*, Academic Press, 1991.
- [10] - A. Klehr, R. Müller, M. Voss and A. Bärowolf, "Gigahertz switching behavior of polarization-bistable InGaAsP/InP lasers under high-frequency current modulation", *Appl. Phys. Lett.*, vol. 64, pp. 830-832, Feb. 1994.
- [11] - G. Eisenstein, R. S. Tucker, U. Koren and S. K. Korotky, "Active mode-locking characteristics of InGaAsP - single mode fiber composite cavity lasers", *IEEE J. Quantum Electron.*, vol. 22, pp. 142-148, Jan. 1986.
- [12] - M. Kuznetsov, D. Z. Tsang, J. N. Walpole, A. L. Liao and E. P. Ippen, "Multistable mode locking of InGaAsP semiconductor lasers", *Appl. Phys. Lett.*, vol. 51, pp. 895-897, Sept. 1987.
- [13] - S. Sanders, A. Yariv, J. Paslaski, J. E. Ungar and H. A. Zaren, "Passive mode locking of a two-section multiple quantum well laser at harmonics of the cavity round-trip frequency", *Appl. Phys. Lett.*, vol. 58, pp. 681-683, Feb. 1991.

- [14] - E. L. Portnoi and A. V. Chelnokov, "Passive mode-locking in a short cavity diode laser", in *12th IEEE International Semiconductor Laser Conference*, Davos, Switzerland, 1990, pp. 140-141.
- [15] - J. P. Hohimer and G. A. Vawter, "Passive mode locking of monolithic semiconductor ring lasers at 86 GHz", *Appl. Phys. Lett.*, vol. 63, pp. 1598-1600, Sept. 1993.
- [16] - S. Arahira, S. Oshiba, Y. Matsui, T. Kunii and Y. Ogawa, "500 GHz optical short pulse generation from a monolithic passively mode-locked distributed Bragg reflector laser diode", *Appl. Phys. Lett.*, vol. 64, pp. 1917-1919, Apr. 1994.
- [17] - S. Arahira, S. Oshiba, Y. Matsui, T. Kunii and Y. Ogawa, "Terahertz-rate optical pulse generation from a passively mode-locked semiconductor laser diode", *Opt. Lett.*, vol. 19, pp. 834-836, June 1994.
- [18] - S. Arahira, S. Oshiba, Y. Matsui, T. Kunii and Y. Ogawa, "Generation of 1.54 THz pulse train by harmonic passive mode-locking in DBR lasers", in *14th IEEE International Semiconductor Laser Conference*, Maui, Hawaii, USA, Sept. 1994, paper M2.1, pp. 12-13
- [19] - J. F. Martins-Filho and C. N. Ironside, "Multiple colliding pulse mode-locked operation of a semiconductor laser", *Appl. Phys. Lett.*, vol. 65, pp. 1894-1896, Oct. 1994.
- [20] - J. F. Martins-Filho, E. A. Avrutin and C. N. Ironside, "Multiple colliding pulse mode-locking in a semiconductor laser: experiment and theory", in *CLEO/Europe*, Amsterdam, The Netherlands, Aug. 1994, paper CTuL3, pp. 158-159
- [21] - J. F. Martins-Filho, E. A. Avrutin and C. N. Ironside, "High repetition rate by multiple colliding pulse mode-locked operation of a semiconductor laser", in *14th IEEE International Semiconductor Laser Conference*, Maui, Hawaii, USA, Sept. 1994, paper M2.3, pp. 16-17
- [22] - J. F. Martins-Filho, E. A. Avrutin, C. N. Ironside and J. S. Roberts, "Monolithic multiple colliding pulse mode-locked quantum well lasers: experiment and theory", *IEEE J. Select. Topics in Quantum Electron.*, vol. 1, no. 2, Special Issue on semiconductor lasers, June 1995.
- [23] - K. N. Choi and H. F. Taylor, "Novel cross-correlation technique for characterisation of subpicosecond pulses from mode-locked semiconductor lasers", *Appl. Phys. Lett.*, vol. 62, pp. 1875-1877, Apr. 1993.
- [24] - J. P. Curtis and J. E. Carroll, "Autocorrelation systems for the measurement of picosecond pulses from injection lasers", *Int. J. Electron.*, vol. 60, no. 1, pp. 87-111, 1986.
- [25] - P. W. Smith, Y. Silberberg and D. A. B. Miller, "Mode locking of semiconductor diode lasers using saturable excitonic nonlinearities", *J. Opt. Soc. Am. B*, vol. 2, pp. 1228-1236, July 1985.

- [26] - D. J. Derickson, R. J. Helkey, A. Mar, J. R. Karin, J. E. Bowers and R. L. Thornton, "Suppression of multiple pulse formation in external-cavity mode-locked semiconductor lasers using intrawaveguide saturable absorbers", *IEEE Photon. Technol. Lett.*, vol. 4, pp. 333-335, Apr. 1992.
- [27] - K. Y. Lau, "Narrow-band modulation of semiconductor lasers at millimetre wave frequencies (>100 GHz) by mode locking", *IEEE J. Quantum Electron.*, vol. 26, pp. 250-261, Feb. 1990.
- [28] - H. A. Haus and Y. Silberberg, "Theory of mode locking of a laser diode with a multiple-quantum-well structure", *J. Opt. Soc. Am. B*, vol. 2, pp. 1237-1243, July 1985.
- [29] - J. C. Chen, H. A. Haus and E. P. Ippen, "Stability of lasers mode locked by two saturable absorbers", *IEEE J. Quantum Electron.*, vol. 29, pp. 1228-1232, Apr. 1993.
- [30] - J. R. Karin, R. J. Helkey, D. J. Derickson, R. Nagarajan, D. S. Allin, J. E. Bowers and R. L. Thornton, "Ultrafast dynamics in field-enhanced saturable absorbers", *Appl. Phys. Lett.*, vol. 64, pp. 676-678, Feb. 1994.
- [31] - A. V. Uskov, J. R. Karin, R. Nagarajan, J. E. Bowers and J. Mørk, "Ultrafast dynamics in waveguide saturable absorbers", in *14th IEEE International Semiconductor Laser Conference*, Maui, Hawaii, USA, Sep. 1994, paper P18, pp. 117-118, and J. R. Karin, A. V. Uskov, R. Nagarajan, J. E. Bowers and J. Mørk, "Carrier heating dynamics in semiconductor waveguide saturable absorbers", *Appl. Phys. Lett.*, vol. 65, pp. 2708-2710, Nov. 1994.
- [32] - W. H. Knox, R. L. Fork, M. C. Downer, D. A. B. Miller, D. S. Chemla, C. V. Shank, A. C. Gossard and W. Wiegmann, "Femtosecond dynamics of resonantly excited excitons in room-temperature GaAs quantum wells", *Phys. Rev. Lett.*, vol. 54, pp. 1306-1309, Mar. 1985.
- [33] - S. M. Sze, *Semiconductor Devices: Physics and Technology*, Wiley, 1985, Chapter 1.
- [34] - T. Krauss, P. J. R. Laybourn and J. Roberts, "CW operation of semiconductor ring lasers", *Electron. Lett.*, vol. 26, pp. 2095-2097, Dec. 1990.
- [35] - T. Krauss, P. J. R. Laybourn and R. M. De La Rue, "Directionally coupled semiconductor ring lasers", in *6th European Conference on Integrated Optics (ECIO)*, Neuchâtel, Switzerland, Apr. 1993, paper 7-6.
- [36] - T. Krauss, R. M. De La Rue, I. Gontijo, P. J. R. Laybourn and J. S. Roberts, "Strip-loaded semiconductor ring lasers employing multimode interference output couplers", *Appl. Phys. Lett.*, vol. 64, pp. 2788-2790, May 1994.
- [37] - J. McInerney, L. Reekie and D. J. Bradley, "Bandwidth limited picosecond pulse generation by hybrid mode-locking in a ring cavity GaAlAs laser", *Electron. Lett.*, vol. 21, pp. 117-118, Jan. 1985.
- [38] - C. F. Lin and C. L. Tang, "Colliding pulse mode locking of a semiconductor laser in an external ring cavity", *Appl. Phys. Lett.*, vol. 62, pp. 1053-1055, Mar. 1993.

- [39] - P. B. Hansen, G. Raybon, M. -D. Chien, U. Koren, B. I. Miller, M. G. Young, J. -M. Verdiell and C. A. Burrus, "A 1.54- μm monolithic semiconductor ring laser: CW and mode-locked operation", *IEEE Photon. Technol. Lett.*, vol. 4, pp. 411-413, May 1992.
- [40] - T. Krauss, J. F. Martins-Filho, C. N. Ironside, P. J. R. Laybourn and R. M. De La Rue, "Mode-locking in semiconductor ring lasers with two saturable absorbers", in *7th European Conference on Integrated Optics (ECIO)*, Delft, The Netherlands, Apr. 1995.
- [41] - T. F. Krauss, R. M. De La Rue, P. J. R. Laybourn, B. Vögele and C. R. Stanley, "Efficient semiconductor ring lasers made by a simple self-aligned fabrication process", *IEEE J. Select. Topics in Quantum Electron.*, vol. 1, no. 2, Special Issue on semiconductor lasers, June 1995.
- [42] - P. J. Delfyett, L. T. Florez, N. Stofell, T. Gmitter, N. C. Andreadakis, Y. Silberberg, J. P. Heritage and G. A. Alphonse, "High-power ultrafast laser diodes", *IEEE J. Quantum Electron.*, vol. 28, pp. 2203-2219, Oct. 1992.
- [43] - D. Welch, "New dawn beckons for semiconductor lasers", *Physics World*, pp. 35-38, Feb. 1994.
- [44] - D. F. Welch, "Progress in high power semiconductor lasers", in *14th IEEE International Semiconductor Laser Conference*, Maui, Hawaii, USA, Sep. 1994, paper M1.1, pp. 3-5.
- [45] - G. Bendelli, K. Komori and S. Arai, "Gain saturation and propagation characteristics of index-guided tapered-waveguide traveling-wave semiconductor laser amplifiers (TTW-SLA's)", *IEEE J. Quantum Electron.*, vol. 28, pp. 447-458, Feb. 1992.
- [46] - R. J. Lang, A. Hardy, R. Parke, D. Mehuys, S. O'Brien, J. Major and D. Welch, "Numerical analysis of flared semiconductor laser amplifiers", *IEEE J. Quantum Electron.*, vol. 29, pp. 2044-2051, June 1993.
- [47] - D. Mehuys, D. F. Welch and L. Goldberg, "2.0 W CW, diffraction-limited tapered amplifier with diode injection", *Electron. Lett.*, vol. 28, pp. 1944-1946, Oct. 1992.
- [48] - S. O'Brien, K. F. Welch, R. A. Parke, D. Mehuys, K. Dzurko, R. J. Lang, R. Waarts and D. Scifres, "Operating characteristics of a high-power monolithically integrated flared amplifier master oscillator power amplifier", *IEEE J. Quantum Electron.*, vol. 29, pp. 2052-2057, June 1993.
- [49] - A. Mar, R. Helkey, J. Bowers, D. Mehuys and D. Welch, "Mode-locked operation of a master oscillator power amplifier", *IEEE Photon. Technol. Lett.*, vol. 6, pp. 1067-1069, Sep. 1994.
- [50] - L. Goldberg, D. Mehuys and D. F. Welch, "High-power, mode-locked external-cavity tunable semiconductor laser", in *14th IEEE International Semiconductor Laser Conference*, Maui, Hawaii, USA, Sep. 1994, paper M2.2, pp. 14-15.

- [51] - K. A. Williams, J. Sarma, I. H. White, R. V. Penty, I. Middlemast, T. Ryan, F. R. Laughton and J. S. Roberts, "Q-switched bow-tie lasers for high energy picosecond pulse generation", *Electron. Lett.*, vol. 30, pp. 320-321, Feb. 1994.
- [52] - K. A. Williams, I. H. White, F. R. Laughton, J. Sarma, R. V. Penty, I. Middlemast, T. Ryan and J. S. Roberts, "Passive mode-locking of bow-tie lasers", in *CLEO/Europe*, Amsterdam, The Netherlands, Aug. 1994, paper CTuL2, pp. 158.
- [53] - G. H. B. Thompson, *Physics of Semiconductor Laser Devices*, Wiley, 1980, Chapter 1.
- [54] - R. G. Hunsperger, *Integrated Optics: Theory and Technology*, 3rd edition, Springer-Verlag, 1991, Chapter 12.
- [55] - M. J. Adams, P. E. Barnsley, J. D. Burton, D. A. O. Davies, P. J. Fiddymment, M. A. Fisher, D. A. H. Mace, P. S. Mudhar, M. J. Robertson, J. Singh and H. J. Wickes, "Novel components for optical switching", *BT Technol. J.*, vol. 11, no. 2, April 1993
- [56] - S. Shimada, K. Nakagawa, M. Saruwatari and T. Matsumoto, "Very-high-speed optical signal processing", *Proc. of the IEEE*, vol. 81, pp. 1633-1646, Nov. 1993.
- [57] - J. K. Lucek and K. Smith, "All-optical signal regenerator", *Optics Lett.*, vol. 18, pp. 1226-1228, Aug. 1993.
- [58] - K. Smith and J. K. Lucek, "All-optical clock recovery using a mode-locked laser", *Electron. Lett.*, vol. 28, pp. 1814-1816, Sept. 1992.
- [59] - P. E. Barnsley, H. J. Wickes, G. E. Wickens and D. M. Spirit, "All-optical clock recovery from 5 Gbit/s RZ data using a self-pulsating 1.56 μm laser diode", *IEEE Photon. Technol. Lett.*, vol. 3, pp. 942-945, Oct. 1991.
- [60] - P. Barnsley, "All-optical clock extraction using two-contact devices", *IEE Proc.-J*, vol. 140, pp. 325-336, Oct. 1993.
- [61] - K. Nonaka, Y. Noguchi, H. Tsuda and T. Kurokawa, "Digital signal regeneration with side-injection-light-controlled bistable laser diode", in *14th IEEE International Semiconductor Laser Conference*, Maui, Hawaii, USA, Aug. 1994, paper Th2.4, pp. 229-230.
- [62] - K. Nonaka, H. Tsuda, H. Uenohara, H. Iwamura and T. Kurokawa, "Optical nonlinear characteristics of a side-injection light-controlled laser diode with a multiple-quantum-well saturable absorber region", *IEEE Photon. Technol. Lett.*, vol. 5, pp. 139-141, Feb. 1993.
- [63] - H. Tsuda, K. Nonaka, K. Hirabayashi, H. Uenohara, H. Iwamura and T. Kurokawa, "Wide range wavelength conversion experiments using a side-injection light-controlled bistable laser diode", *Appl. Phys. Lett.*, vol. 63, pp. 3116-3118, Dec. 1993.
- [64] - S. D. McDougall, J. F. Martins-Filho and C. N. Ironside, "T-junction colliding-pulse mode-locked quantum-well laser for all-optical clock recovery", accepted to the

12th National Quantum Electronics Conference (QE-12), Southampton, UK, Sept. 1995.

[65] - S. D. McDougall, Ph.D. thesis, University of Glasgow, in preparation.

[66] - R. M. De La Rue and J. H. Marsh, "Integration technologies for III-V semiconductor optoelectronics based on quantum well waveguides", in *Integrated Optics and Optoelectronics*, K. -K. Wong and M. Razeghi, Eds. Los Angeles, CA:SPIE (Int. Soc. Opt. Eng.), pp. 259-288, Jan. 1993.

[67] - J. H. Marsh, S. I. Hansen, A. C. Bryce, R. M. De La Rue, "Applications of neutral impurity disordering in fabricating low-loss optical waveguides and integrated waveguide devices", *Optical and Quantum Electron.*, vol. 23, pp. S941-S957, 1991

Chapter 6: Summary and Conclusions

This chapter presents a summary of the more important aspects of mode-locked quantum-well lasers that have been studied in this thesis and gives the general conclusion to this project, as well as some prospects for future work.

Chapter 1 introduced the thesis into the context of the development of optoelectronics and optoelectronic integrated circuits. This introduction chapter gave a general outlook on quantum well structures and lasers, methods of short pulse generation from diode lasers including gain-switching, Q-switching and mode-locking, and their applications in telecommunications, optical computing and optoelectronic measurement systems.

Chapter 2 has reviewed the principles and the physics involved in the mode-locking process, with particular emphasis on passively mode-locked semiconductor lasers. The different methods, configurations and design considerations to achieve mode-locking in semiconductors have been discussed, specially for the passive colliding pulse configuration, which is the main subject of investigation in this thesis. The current trends in the development of monolithic mode-locked semiconductor lasers were presented as a prelude to the subsequent chapters. These trends are the pursuit of high peak power emission, ultra-high-speed operation (above 200 GHz) for future high capacity TDM systems, low speed operation (below 30 GHz) for near future applications and multi-functionality in multi-sectioned integrated devices.

The techniques for fabrication of monolithic mode-locked laser devices, from wafer scribing up to laser packaging, have been developed and were described in Chapter 3. It is a relatively elaborate fabrication process since it involves three photolithographic steps, two dry and five wet etching processes, and three metal and one dielectric layer deposition process, besides laser cleaving, mounting and wire bonding. Three important aspects of the design and fabrication of monolithic semiconductor mode-locked lasers should be highlighted here, which are the electrical isolation between sections, the adhesion of the top metallic contact to the silica and semiconductor material, and the final laser cleavage. The electrical isolation between sections depends on the doping level and thickness of the top contact and upper cladding layers, and the distance between sections. A poor isolation allows current leakage from the gain to the absorber section, decreasing the efficiency of the reverse bias on the absorber. In more general terms, a good electrical isolation between sections diminishes the interdependence of different sections of the device. The isolation can be improved by removing material from the gap between the section using an etching process. 1.5 k Ω isolation was found to be sufficient for the operation of the mode-locked semiconductor lasers.

The adhesion of the metallic contact to the silica as well as semiconductor materials is an important issue because it affects the electrical and mechanical properties of the contact, and it is specially important when wire bonding is needed. The adhesion depends on several factors including the sample cleanness, cleaning procedure, metallic alloy used as contact and post-evaporation procedure. As described in Chapter 3, to achieve the best performance of the metallic contacts several proceedings were taken, including the use of a deoxidising etch before contact evaporation, the use of a de-gas procedure before evaporation, the use of NiCr/Au p-type contact, and the use of other cleaning processes rather than with ultrasonic. Another important process that affects the contacts is thermal annealing. It was found that the usual temperatures used for annealing the contacts (above 250°C) deteriorate the adhesion of the metal to the silica layer underneath it. The annealed contact peels off when wire bonding is tried. However, electrical tests showed that the non-annealed lasers have a typical dynamic resistance of 20 Ω . Although lower resistances can be achieved with other contact recipes and annealing, the one used with no annealing seems to be the best compromise in terms of the electrical and mechanical properties of the contact. Future studies of new metallic contact recipes and other wire bonding processes should lead to improvements on the dynamic resistance and contact adhesion.

Accurate cleavage of the end facets of Fabry-Perot cavity mode-locked lasers is crucial for their operation, specially for CPM lasers. The cleavage defines the cavity length and therefore the repetition rate of a mode-locked laser. In CPM lasers it also defines the position of the absorber section in the cavity in relation to the facets, which affects the laser operation. The introduction of a cleavage marking technique, which determines the cleavage point and cavity length from marks defined by photolithography on the laser, along with the use of a special microscope set-up with top and side views of the scribe edge, represent a considerable improvement on reliability and accuracy of the laser cleaving process. It dispenses with the use of a micrometer for cavity length measurement and scribe positioning, which introduces the inaccuracy.

The fabrication technique developed for mode-locked lasers and described in Chapter 3 is simpler and of lower cost than for the buried heterostructure used by other authors, since it does not involve any regrowth process. The semiconductor material characterisation technique and the stripe-loaded waveguide structure used were also discussed in Chapter 3.

The testing and characterisation of the mode-locked lasers are performed in a test set-up which consists basically of an optical power metre, an optical spectrum analyser, and a linear correlation interferometer, and were described in Chapter 4. The linear cross-correlation method for time domain measurement uses a Michelson interferometer to scan a pulse through itself and its neighbours in a train of pulses,

obtaining pulse width, repetition rate and coherence length of the laser. This technique detects the mixing signal between light from each arm of the interferometer at a low speed photodetector and it does not employ second harmonic generation. The mixing technique employing a lock-in amplifier and 2 choppers (one in each arm of the interferometer) removes the dc level generated by the direct detection of light from each individual arm of the interferometer. Therefore only the pulse overlapping interference signal is detected. However, this linear method has limitations concerning pulsewidth measurements. The limitation of the technique consists of its insensitivity to the effect of frequency chirp on pulses. However it is reasonable for these lasers because there has been no evidence of significant chirping from monolithic CPM lasers, and measurements found in the literature have generally indicated transform limited pulses. Although the more commonly used method for short pulse characterisation is the nonlinear autocorrelation by second harmonic generation (SHG), the linear correlation is attractive for characterisation of mode-locked semiconductor lasers since these devices generally generate low optical powers, which makes SHG autocorrelation more difficult in practice. Besides, it is simpler and of lower cost to implement and easier to align. Moreover, a detailed study of short pulse structure is out of the scope of this work since it involves more sophisticated measurement schemes than correlation methods. Nevertheless the implementation of the SHG autocorrelation technique by S. D. McDougall in Glasgow University has recently shown that the pulses generated by monolithic passive CPM quantum well lasers are transform limited, corroborating the results from the linear correlation measurements.

Chapter 5 described the work performed on the design and the characterisation of the five different configurations of monolithic passive colliding pulse mode-locked lasers that have been fabricated. Firstly, the results from a standard configuration of CPM laser were presented. These were the first published results on monolithic CPM quantum well laser at short wavelength, i. e. GaAs/AlGaAs based material. The evidence of mode-locking at repetition rates in the range of 73 to 129 GHz obtained from frequency domain measurements was confirmed by streak camera measurements. It also presented a previously unseen output laser polarisation dependence with the applied reverse bias to the absorber section of this laser. The generation of TE and TM polarised light from the CPM laser may have been caused by a combination of effects, including the inherent dichroism of quantum wells under electric field, possible damage of the saturable absorber section due to high reverse current, and possible strain in the active layer caused by some defect induced lattice mismatch between epitaxial layer and substrate. Further experimental as well as theoretical work is necessary to find out which effects are responsible for the TE-TM polarisation emission observed.

Chapter 5 also described the design and operation characteristics of a novel configuration of CPM laser, the multiple colliding-pulse mode-locked (MCPM) laser.

The MCPM laser has a contiguously electrically connected gain section and 3 separated sections placed at every quarter of the cavity length. Each of the 3 sections is separately electrically addressable and when reverse biased it behaves as a saturable absorber and when forward biased as a gain section. Therefore, this multi-section device can have 1, 2, or 3 monolithically integrated saturable absorber sections in the cavity, inducing the laser to operate at the first up to the fourth harmonic of the repetition rate. This was the first observation of geometry dependent switchable change of harmonics in mode-locked lasers. The different regimes of operation of the MCPM laser were investigated, comprising single mode, multimode, Q-switched and first to fourth harmonic mode-locking, generating pulses of around 1 to 3 ps width at up to 375 GHz repetition rate. The laser is versatile in the sense that its operation can be switched depending on the electrical bias applied to each of its 3 independent sections, changing the position and number of saturable absorbers in the cavity. From studies of the range of mode-locking at 240 GHz, it was found that mode-locking occurs at two distinct regions of current and reverse bias. This previously unseen feature may represent an indication of the contribution of excitonic nonlinearities to the ultra-fast operation of the device. The indication is that the two regions correspond to the contribution of fast bleaching and recovery of light and heavy hole excitons. The fast saturable absorption dynamics of quantum wells, known to be of approximately 300 fs, may be responsible for the fast component of saturable absorption necessary for mode-locking operation at 240 GHz. A more comprehensive study of these effects is necessary to confirm these indications.

The third configuration of mode-locked laser described in Chapter 5 is a monolithic CPM ring laser. This ring laser has two saturable absorbers in colliding pulse configuration in the cavity. The ring cavity has a "race-track" configuration, with two semicircles where the two absorber sections are placed, and two strait sections, one of them having a MMI coupler to an output waveguide. Frequency domain measurements indicated mode-locking operation at 28 GHz repetition rate. The use of two saturable absorbers in colliding pulse configuration in the ring cavity showed improvements on the device operation. With two absorbers, the laser produces shorter pulses and more stable operation than with only one absorber section. Time domain measurements are still to be carried out to obtain pulse width and confirmation of the repetition rate.

Chapter 5 also presented an attempt to achieve high peak power CW-mode-locking operation from a CPM laser which gain section waveguides are tapered, in the so called CPM bow-tie laser. The double-tapered waveguide, narrow at the absorber section in the middle of the cavity and wider at the faces, should increase the saturation energy of the gain sections of the laser, allowing high power short pulse generation. The full characterisation of this device was not performed since it presented serious

reliability problems concerning its high power CW operation. Over 100 mW average power under CW operation has been achieved, but very rapid device degradation and decrease of output power have been observed. Indications of CPM operation at low powers from the optical spectrum of the laser emission were observed. However, improvements on device design and fabrication, such as the use of reflecting coatings on the facets among others, are needed to avoid facet damage and extend the device lifetime before high power CW CPM operation is to be achieved.

The last section of Chapter 5 was dedicated to the design and development of a CPM laser based device which is intended to perform clock recovery at high repetition rates, above 100 GHz. This device consists of a standard CPM laser which has an extra waveguide in side-injection configuration. This extra waveguide amplifies and guides the optical signal from which the clock is to be recovered to the absorber section of the laser. To achieve clock recovery this signal should contribute to the saturation of the absorber section of the CPM laser, synchronising its saturation with the injected data signal. Therefore the CPM laser output would correspond to the recovered clock signal. Preliminary characterisation and tests showed that the CPM laser part of the device works as a standard CPM laser, as expected. The full characterisation of the device and the demonstration of clock recovery is currently a subject of research in the optoelectronics group at Glasgow University.

Appendix 1: General Equations for the Linear Correlator

The complex electric field $E(t)$ of the laser output emitting into k longitudinal modes is written as:

$$E(t) = \sum_k \sqrt{P_k(t)} \cdot \exp[j\omega_k t + j\phi_k(t)] \quad (\text{A1})$$

where $P_k(t)$ is the light power and $\phi_k(t)$ is the phase of the k^{th} lasing mode emitting at the wavelength $\lambda_k = 2\pi c/\omega_k$. Therefore the output intensity of the laser is:

$$I(t) \propto P(t) = |E(t)|^2 \quad (\text{A2})$$

The output of an interferometer, where the signal is delayed in one of its arms by τ is:

$$E_T(t) = A[E(t) + E(t - \tau)] \quad (\text{A3})$$

where A is a constant (A is 0.5 for a Michelson interferometer). Therefore the output power is:

$$P_T(t, \tau) = A^2 \left\{ |E(t)|^2 + |E(t - \tau)|^2 + 2 \operatorname{Re}[E(t) \cdot E^*(t - \tau)] \right\} \quad (\text{A4})$$

The average power $\langle P_T(t, \tau) \rangle$, hence involves the first order correlation function of the field.

$$\langle E(t) \cdot E^*(t - \tau) \rangle = \int_{-\infty}^{\infty} E(t) \cdot E^*(t - \tau) dt = G^{(1)}(\tau) \quad (\text{A5})$$

$$\gamma_E(\tau) = \frac{\langle E(t) \cdot E^*(t - \tau) \rangle}{\langle |E(t)|^2 \rangle} \quad (\text{A6})$$

The classical coherence time is related to $\gamma_E(\tau)$ as:

$$t_c = \int_{-\infty}^{\infty} |\gamma_E(\tau)|^2 d\tau \quad (\text{A7})$$

Assuming a stationary emission of the laser, i.e.

$$\langle |E(t)|^2 \rangle = \langle |E(t - \tau)|^2 \rangle \quad (\text{A8})$$

the average transmitted power can be written as:

$$\langle P_T(t, \tau) \rangle = 2A^2 \langle |E(t)|^2 \rangle \{1 + \text{Re}[\gamma_E(\tau)]\} \quad (\text{A9})$$

Calculating $\gamma_E(\tau)$ using equations A6 and A1 one can obtain

$$\gamma_E(\tau) = \frac{\left\langle \sum_k \sqrt{P_k(t) \cdot P_k(t - \tau)} \cdot \exp[j\tau(\omega_o + k\Delta\omega) + j\Delta\varphi_k(t, \tau)] \right\rangle}{\left\langle \sum_k P_k(t) \right\rangle} \quad (\text{A10})$$

where $\omega_k = \omega_o + k\Delta\omega$, $k = \pm 0, \pm 1, \pm 2, \dots$, and $\Delta\varphi_k(t, \tau) = \varphi_k(t) - \varphi_k(t - \tau)$. The interference between different modes is not being considered since it yields very fast (≈ 100 GHz) oscillations in time, which wouldn't be detected by a photodetector.

Assuming that the amplitude is not time dependent (i.e. $P_k(t) = P_k(t - \tau) = P_k$), which only imply that amplitude noise is not being taken into account, one can obtain the expression

$$\gamma_E(\tau) = \frac{\exp[j\omega_o\tau] \cdot \sum_k P_k \cdot \exp[jk\Delta\omega\tau] \cdot \langle \exp[j\Delta\varphi_k(t, \tau)] \rangle}{\sum_k P_k} \quad (\text{A11})$$

Using equations A9 and A11 a general expression for the average output power can be obtained:

$$\langle P_T(t, \tau) \rangle = 2A^2 \left\{ \sum_k P_k + \cos(\omega_o\tau) \cdot \sum_k P_k \cdot \cos(k\Delta\omega\tau) \cdot \text{Re}\{\langle \exp[j\Delta\varphi_k(t, \tau)] \rangle\} \right\} \quad (\text{A12})$$

For the sake of comparison with the experimental results the equation A12 is written in the same form as the results are measured: with the dc level removed and then applying the absolute value to it, in arbitrary units, with $2A^2 = 1$.

$$\langle P_T(t, \tau) \rangle = \left| \cos(\omega_o\tau) \cdot \sum_k P_k \cdot \cos(k\Delta\omega\tau) \cdot \text{Re}\{\langle \exp[j\Delta\varphi_k(t, \tau)] \rangle\} \right| \quad (\text{A13})$$

To evaluate the mean value $\langle \exp[j\Delta\varphi_k(t, \tau)] \rangle$ in equation A13 the probability density distribution $p(\Delta\varphi)$ is required.

$$\langle \exp(j\Delta\varphi_k) \rangle = \int_{-\infty}^{\infty} p(\Delta\varphi_k) \cdot \exp(j\Delta\varphi_k) d(\Delta\varphi_k) \quad (\text{A14})$$

Since the phase changes $\Delta\varphi$ are introduced by a large number of independent noise events due to spontaneous emission, $\Delta\varphi$ may be considered to follow a Gaussian probability density distribution.

$$p(\Delta\varphi_k) = \frac{\exp(-\Delta\varphi_k^2/2\langle\Delta\varphi_k^2\rangle)}{\sqrt{2\pi\langle\Delta\varphi_k^2\rangle}} \quad (\text{A15})$$

Yielding from equation A14

$$\langle \exp(j\Delta\varphi_k) \rangle = \exp\left(-\frac{1}{2}\langle\Delta\varphi_k^2\rangle\right) \quad (\text{A16})$$

Assuming that the variance of the phase change increases in proportion to the delay difference $\langle\Delta\varphi_k^2\rangle \propto |\tau|$, i.e. the phase correlation decreases with increasing delay, and using the equation A7 for t_c one can obtain

$$\langle\Delta\varphi_k^2\rangle = \frac{2}{t_c}|\tau| \quad (\text{A17})$$

where t_c is the coherence time, the time at which the r.m.s. phase change $\sqrt{\langle\Delta\varphi_k^2\rangle} = \sqrt{2}$ radians. It implies that the spectral distribution of mode k has a Lorentzian line shape.

Therefore equation A16 is written as

$$\langle \exp[j\Delta\varphi_k(t, \tau)] \rangle = \exp(-|\tau|/t_c) \quad (\text{A18})$$

Appendix 2: References

A2.1 - Publications and conference contributions arising from this work

- J. F. Martins-Filho, E. A. Avrutin, C. N. Ironside and J. S. Roberts, "Monolithic multiple colliding pulse mode-locked quantum well lasers: experiment and theory", *IEEE Journal of Selected Topics in Quantum Electronics*, vol. 1, no. 2, pp. 539-551, Special Issue on semiconductor lasers, June 1995.
- J. F. Martins-Filho and C. N. Ironside, "Multiple colliding pulse mode-locked operation of a semiconductor laser", *Appl. Phys. Lett.*, vol. 65, pp. 1894-1896, Oct. 1994.
- J. F. Martins-Filho, C. N. Ironside and J. S. Roberts, "Quantum well AlGaAs/GaAs monolithic colliding pulse mode-locked laser", *Electron. Lett.*, vol. 29, pp. 1135-1136, June 1993.
- S. D. McDougall, J. F. Martins-Filho and C. N. Ironside, "T-junction colliding-pulse mode-locked quantum well laser for all-optical clock recovery", accepted to the *12th National Quantum Electronics Conference (QE-12)*, Southampton, UK, Sept. 1995.
- J. F. Martins-Filho, S. D. McDougall, E. A. Avrutin and C. N. Ironside, "Multiple colliding pulse mode-locked quantum well lasers for high repetition rate (up to 375 GHz) short pulse generation", in *IEE Colloquium on Towards Terabit Transmission*, Savoy Place, London, UK, 19 May 1995, Digest no. 1995/110, pp. 16/1-16/6.
- J. F. Martins-Filho and C. N. Ironside, "Multiple colliding pulse mode-locked quantum well lasers", in *Mini-Symposium on Solid State Lasers*, The Rank Prize Funds, Grasmere, England, Apr. 1995.
- T. Krauss, J. F. Martins-Filho, C. N. Ironside, P. J. R. Laybourn and R. M. De La Rue, "Mode-locking in semiconductor ring lasers with two saturable absorbers", in *7th European Conference on Integrated Optics (ECIO)*, Delft, The Netherlands, Apr. 1995.
- J. F. Martins-Filho, E. A. Avrutin and C. N. Ironside, "High repetition rate by multiple colliding pulse mode-locked operation of a semiconductor laser", in *14th IEEE International Semiconductor Laser Conference*, Maui, Hawaii, USA, Sept. 1994, paper M2.3, pp. 16-17
- J. F. Martins-Filho, E. Avrutin and C. N. Ironside, "Multiple colliding pulse mode-locked operation of a semiconductor laser: experiment and theory", in *Conference on Lasers and Electro-Optics Europe (CLEO/Europe'94)*, Amsterdam, The Netherlands, Aug. 1994, paper CTuL3, pp. 158-159

- J. F. Martins-Filho, C. N. Ironside and J. S. Roberts, "Frequency domain characterisation of CPM QW lasers", in *Semiconductor and Integrated Opto-electronics Conference (SIOE'93)*, Cardiff, Wales, Mar. 1993, paper 39

A2.2 - Alphabetical list of references to the thesis

- M. J. Adams, P. E. Barnsley, J. D. Burton, D. A. O. Davies, P. J. Fiddymment, M. A. Fisher, D. A. H. Mace, P. S. Mudhar, M. J. Robertson, J. Singh and H. J. Wickes, "Novel components for optical switching", *BT Technol. J.*, vol. 11, no. 2, April 1993
- G. P. Agrawal, "Effect of gain dispersion on ultrashort pulse amplification in semiconductor laser amplifiers", *IEEE J. Quantum Electron.*, vol. 27, pp. 1843-1849, June 1991
- G. P. Agrawal, *Nonlinear Fiber Optics*, Quantum Electronics: Principles and Applications Series, Academic Press, 1989.
- G. P. Agrawal and N. A. Olsson, "Self-phase modulation and spectral broadening of optical pulses in semiconductor laser amplifiers", *IEEE J. Quantum Electron.*, vol. 25, pp. 2297-2306, Nov. 1989.
- P. A. Andrekson, N. O. Olsson, J. R. Simpson, T. Tanbun-Ek, R. A. Logan, and M. Haner, "16Gbit/s all optical demultiplexing using four-wave mixing", *Electron. Lett.*, vol. 27, pp. 922-924, May 1991
- S. Arahira, Y. Matsui, T. Kunii, S. Oshiba and Y. Ogawa, "Optical short pulse generation at high repetition rate over 80 GHz from a monolithic passively modelocked DBR laser diode", *Electron. Lett.*, vol. 29, pp. 1013-1015, May 1993
- S. Arahira, S. Oshiba, Y. Matsui, T. Kunii and Y. Ogawa, "500 GHz optical short pulse generation from a monolithic passively mode-locked distributed Bragg reflector laser diode", *Appl. Phys. Lett.*, vol. 64, pp. 1917-1919, Apr. 1994.
- S. Arahira, S. Oshiba, Y. Matsui, T. Kunii and Y. Ogawa, "Terahertz-rate optical pulse generation from a passively mode-locked semiconductor laser diode", *Opt. Lett.*, vol. 19, pp. 834-836, June 1994.
- S. Arahira, S. Oshiba, Y. Matsui, T. Kunii and Y. Ogawa, "Generation of 1.54 THz pulse train by harmonic passive mode-locking in DBR lasers", in *14th IEEE International Semiconductor Laser Conference*, Maui, Hawaii, USA, Sept. 1994, paper M2.1, pp. 12-13
- Y. Arakawa and A. Yariv, "Theory of Gain, Modulation Response and Spectral Linewidth in AlGaAs Quantum Well Lasers", *IEEE J. of Quantum Elec.*, vol. 21, pp. 1666-1674, Oct. 1985.
- C. Baack, and G. Walf, "Photonics in future telecommunications", *Proc. of the IEEE*, vol. 81, pp. 1624-1631, Nov. 1993

- H. Bachert, P. G. Eliseev, M. A. Manko, V. P. Strahov, S. Raab and Chan Min Thay, "Multimode operation and mode-locking effect in injection lasers", *IEEE J. Quantum Electron.*, vol. 11, pp. 507-510, July 1975.
- P. Barnsley, "All-optical clock extraction using two-contact devices", *IEE Proc.-J*, vol. 140, pp. 325-336, Oct. 1993.
- P. E. Barnsley, H. J. Wickes, G. E. Wickens and D. M. Spirit, "All-optical clock recovery from 5 Gbit/s RZ data using a self-pulsating 1.56 μm laser diode", *IEEE Photon. Technol. Lett.*, vol. 3, pp. 942-945, Oct. 1991.
- D. A. Barrow, J. H. Marsh, E. L. Portnoi, "Q-switching pulses at 16 GHz from two-section semiconductor lasers", in *CLEO/Europe*, Amsterdam, The Netherlands, Aug. 1994, paper CTuE4, pp. 75.
- G. Bendelli, K. Komori and S. Arai, "Gain saturation and propagation characteristics of index-guided tapered-waveguide traveling-wave semiconductor laser amplifiers (TTW-SLA's)", *IEEE J. Quantum Electron.*, vol. 28, pp. 447-458, Feb. 1992.
- N. M. Bett, "An interferometric auto-correlator", M.Sc. Thesis, Glasgow University, 1990.
- D. J. Bradley and G. H. C. New, "Ultrashort pulse measurements", *Proc. of IEEE*, vol. 62, pp. 313-345, Mar. 1974.
- J. E. Bowers and Y. G. Wey, "High-speed photodetectors", *Handbook of Optics*, 2nd Edition, Edited by M. Bass, E. Van Stryland, D. Williams and W. Wolfe, Optical Society of America, 1994, Chapter 17.
- N. I. Cameron, G. Hopkins, I. G. Thayne, S. P. Beaumont, C. D. W. Wilkinson, M. Holland, A. H. Kean and C. R. Stanley, "Selective reactive ion etching of GaAs/AlGaAs metal-semiconductor field effect transistors", *J. Vac. Sci. Tech. B*, vol. 9, no. 6, pp. 3538-3541, 1991.
- H. C. Casey Jr and M. B. Panish, *Heterostructure Lasers, B*, Academic Press, 1978
- D. S. Chemla, D. A. B. Miller and P. W. Smith, "Nonlinear optical properties of multiple quantum well structures for optical signal processing", *Semiconductors and Semimetals*, vol. 24, Editor Raymond Dingle, Academic Press, 1987, Chapter 5.
- J. C. Chen, H. A. Haus and E. P. Ippen, "Stability of lasers mode locked by two saturable absorbers", *IEEE J. Quantum Electron.*, vol. 29, pp. 1228-1232, Apr. 1993.
- Y. K. Chen and C. W. Ming, "Monolithic colliding-pulse mode-locked quantum-well lasers", *IEEE J. Quantum Electron.*, vol. 28, pp. 2177-2185, Oct. 1992
- Y. K. Chen, M. C. Wu, T. Tanbun-Ek, R. A. Logan and M. A. Chin, "Subpicosecond monolithic colliding-pulse mode-locked multiple quantum well lasers", *Appl. Phys. Lett.*, vol. 58, pp. 1253-1255, Mar. 1991.
- Y. K. Chen, M. C. Wu, T. Tanbun-Ek, R. A. Logan and M. A. Chin, "Multicolor single-wavelength sources generated by a monolithic colliding pulse mode-locked quantum well laser", *IEEE Photon. Technol. Lett.*, vol. 3, pp. 971-973, Nov. 1991

- K. N. Choi and H. F. Taylor, "Novel cross-correlation technique for characterisation of subpicosecond pulses from mode-locked semiconductor lasers", *Appl. Phys. Lett.*, vol. 62, pp. 1875-1877, Apr. 1993.
- J. P. Curtis and J. E. Carroll, "Autocorrelation systems for the measurement of picosecond pulses from injection lasers", *Int. J. Electron.*, vol. 60, pp. 87-111, 1986.
- R. M. De La Rue and J. H. Marsh, "Integration technologies for III-V semiconductor optoelectronics based on quantum well waveguides", in *Integrated Optics and Optoelectronics*, K. -K. Wong and M. Razeghi, Eds. Los Angeles, CA:SPIE (Int. Soc. Opt. Eng.), pp. 259-288, Jan. 1993.
- M. Degenais, R. F. Leheny and J. Crow (Editors), *Integrated Optoelectronics*, Quantum Electronics: Principles and Applications Series, Academic Press, 1995.
- P. J. Delfyett, L. T. Florez, N. Stofell, T. Gmitter, N. C. Andreadakis, Y. Silberberg, J. P. Heritage and G. A. Alphonse, "High-power ultrafast laser diodes", *IEEE J. Quantum Electron.*, vol. 28, pp. 2203-2219, Oct. 1992.
- P. J. Delfyett, D. H. Hartman, and S. Zuber Ahmad, "Optical clock distribution using a mode-locked semiconductor laser diode system", *IEEE J. Lightwave Technol.*, vol. 9, pp. 1646-1649, 1991
- D. J. Derickson, R. J. Helkey, A. Mar, J. R. Karin, J. E. Bowers and R. L. Thornton, "Suppression of multiple pulse formation in external-cavity mode-locked semiconductor lasers using intrawaveguide saturable absorbers", *IEEE Photon. Technol. Lett.*, vol. 4, pp. 333-335, Apr. 1992
- D. J. Derickson, R. J. Helkey, A. Mar, J. R. Karin, J. G. Wasserbauer and J. E. Bowers, "Short pulse generation using multisegment mode-locked semiconductor lasers", *IEEE J. Quantum Electron.*, vol. 28, pp. 2186-2202, Oct. 1992.
- D. J. Derickson, R. J. Helkey, A. Mar, J. G. Wasserbauer, W. B. Jiang and J. E. Bowers, "Modelocked semiconductor lasers: short pulse, small package!", *Optics & Photonics News*, vol. 3, no. 5, pp. 14-20, May 1992
- D. J. Derickson, R. J. Helkey, A. Mar, J. G. Wasserbauer, Y. G. Wey, and J. E. Bowers, "Microwave and millimeter wave signal generation using mode-locked semiconductor lasers with intra-waveguide saturable absorbers", *IEEE Intern. Microwave Theory and Technol. Symposium*, Albuquerque, USA, 1992, paper V-2, pp. 753-756
- D. J. Derickson, P. A. Morton, J. E. Bowers and R. L. Thornton, "Comparison of timing jitter in external and monolithic cavity mode-locked semiconductor lasers", *Appl. Phys. Lett.*, vol. 59, pp. 3372-3374, Dec. 1991
- G. Eisenstein, R. S. Tucker, U. Koren and S. K. Korotky, "Active mode-locking characteristics of InGaAsP - single mode fiber composite cavity lasers", *IEEE J. Quantum Electron.*, vol. 22, pp. 142-148, Jan. 1986.

- L. Esaki, "A bird's-eye view on the evolution of semiconductor superlattices and quantum wells", *IEEE J. Quantum Electron.*, vol. 22, p. 1611-1624, Sep. 1986
- R. L. Fork, B. I. Greene and C. V. Shank, "Generation of optical pulses shorter than 0.1 psec by colliding pulse mode locking", *Appl. Phys. Lett.*, vol. 38, pp. 671-672, May 1981
- R. L. Fork, C. V. Shank, R. Yen and C. A. Hirlimann, "Femtosecond optical pulses", *IEEE J. Quantum Electron.*, vol. 19, pp. 500-505, Apr. 1983
- J. B. Georges, L. Buckman, D. Vassilovski, J. Park, M.-H. Kiang, O. Solgaard and K. L. Lau, "Stable picosecond pulse generation at 46 GHz by modelocking of a semiconductor laser operating in an optoelectronic phaselocked loop", *Electron. Lett.*, vol. 30, pp. 69-71, Jan. 1994
- L. Goldberg, D. Mehuys and D. F. Welch, "High-power, mode-locked external-cavity tunable semiconductor laser", in *14th IEEE International Semiconductor Laser Conference*, Maui, Hawaii, USA, Sep. 1994, paper M2.2, pp. 14-15.
- I. Gontijo, T. Krauss, J. H. Marsh, and R. M. De La Rue, "Postgrowth control of GaAs/AlGaAs quantum well shapes by impurity-free vacancy diffusion", *IEEE J. Quantum Electron.*, vol. 30, pp. 1189-1195, May 1994
- Hamamatsu streak camera, technical information and specifications, 1993.
- P. B. Hansen, G. Raybon, M. -D. Chien, U. Koren, B. I. Miller, M. G. Young, J. -M. Verdiell and C. A. Burrus, "A 1.54- μm monolithic semiconductor ring laser: CW and mode-locked operation", *IEEE Photon. Technol. Lett.*, vol. 4, pp. 411-413, May 1992.
- P. B. Hansen, G. Raybon, U. Koren, B. I. Miller, M. G. Young, M. Chien, C. A. Burrus, and R. C. Alferness, "5.5-mm long InGaAsP monolithic extended-cavity laser with a integrated bragg-reflector for active mode-locking", *IEEE Photon. Technol. Lett.*, vol. 4, pp. 215-217, Mar. 1992.
- C. Harder, J. S. Smith, K. Y. Lau and A. Yariv, "Passive mode-locking of buried heterostructure lasers with nonuniform current injection", *Appl. Phys. Lett.*, vol. 42, pp. 772-774, May 1983
- A. Hasegawa, *Optical Solitons in Fibres*, Second Edition, New York, Springer-Verlag, 1990.
- H. A. Haus, "Theory of mode locking with a fast saturable absorber", *J. Appl. Phys.*, vol. 46, pp. 3049-3058, July 1975, and H. A. Haus, "Theory of mode locking with a slow saturable absorber", *IEEE J. Quantum Electron.*, vol. 11, pp. 736-746, Sep. 1975
- H. A. Haus and Y. Silberberg, "Theory of mode locking of a laser diode with a multiple-quantum-well structure", *J. Opt. Soc. Am. B*, vol. 2, pp. 1237-1243, July 1985.
- R. Helkey and J. Bowers, "Mode locked semiconductor lasers", *Semiconductor Lasers: Past, Present and Future*, Edited by G. P. Agrawal, American Institute of Physics Press, 1993.

- R. J. Helkey, D. J. Derickson, A. Mar, J. G. Wasserbauer, J. E. Bowers and R. L. Thornton, "Repetition frequency stabilisation of passively mode-locked semiconductor lasers", *Electron. Lett.*, vol. 28, pp. 1920-1922, Sep. 1992
- P.-T. Ho, L. A. Glasser, E. P. Ippen and H. A. Haus, "Picosecond pulse generation with a CW GaAlAs laser diode", *Appl. Phys. Lett.*, vol. 33, pp. 241-242, Aug. 1978
- J. P. Hohimer and G. A. Vawter, "Passive mode locking of monolithic semiconductor ring lasers at 86 GHz", *Appl. Phys. Lett.*, vol. 63, pp. 1598-1600, Sept. 1993.
- R. G. Hunsperger, *Integrated Optics: Theory and Technology*, Third Edition, Optical Sciences Series, Springer-Verlag, 1991
- E. P. Ippen, D. J. Eilenberger and R. W. Dixon, *Picosecond Phenomena II*, edited by R. Hochstrasser, W. Kaiser, and C. V. Shank, pp. 21-25, Springer, New York, 1980
- M. N. Islam, C. E. Socolich, and D. A. B. Miller, "Low-energy ultrashort fiber soliton logic gates", *Opt. Lett.*, vol. 15, pp. 909-911, Aug. 1990
- K. Iwatsuki, K. Suzuki, S. Nishi, and M. Saruwatari, "80 Gb/s optical soliton transmission over 80 km with time/polarization division multiplexing", *IEEE Photon. Technol. Lett.*, vol. 5, pp. 245-248, 1993
- W. Jiang, M. Shimizu, R. P. Mirin, T. E. Reynolds and J. E. Bowers, "Femtosecond periodic gain vertical-cavity lasers", *IEEE Photon. Technol. Lett.*, vol. 5, pp. 23-25, Jan. 1993
- J. R. Karin, R. J. Helkey, D. J. Derickson, R. Nagarajan, D. S. Allin, J. E. Bowers and R. L. Thornton, "Ultrafast dynamics in field-enhanced saturable absorbers", *Appl. Phys. Lett.*, vol. 64, pp. 676-678, Feb. 1994.
- J. R. Karin, A. V. Uskov, R. Nagarajan, J. E. Bowers and J. Mørk, "Carrier heating dynamics in semiconductor waveguide saturable absorbers", *Appl. Phys. Lett.*, vol. 65, pp. 2708-2710, Nov. 1994.
- P. N. Kember, "Plasma deposition of insulators for semiconductor applications", *Plasma News, Oxford Plasma Technology*, no. 4, Sept. 1992.
- A. Klehr, R. Müller, M. Voss and A. Bärwolff, "Gigahertz switching behavior of polarization-bistable InGaAsP/InP lasers under high-frequency current modulation", *Appl. Phys. Lett.*, vol. 64, pp. 830-832, Feb. 1994.
- W. H. Knox, R. L. Fork, M. C. Downer, D. A. B. Miller, D. S. Chemla, C. V. Shank, A. C. Gossard and W. Wiegmann, "Femtosecond dynamics of resonantly excited excitons in room-temperature GaAs quantum wells", *Phys. Rev. Lett.*, vol. 54, pp. 1306-1309, Mar. 1985.
- T. Krauss, R. M. De La Rue, I. Gontijo, P. J. R. Laybourn and J. S. Roberts, "Strip-loaded semiconductor ring lasers employing multimode interference output couplers", *Appl. Phys. Lett.*, vol. 64, pp. 2788-2790, May 1994.
- T. F. Krauss, R. M. De La Rue, P. J. R. Laybourn, B. Vögele and C. R. Stanley, "Efficient semiconductor ring lasers made by a simple self-aligned fabrication process",

- IEEE J. Select. Topics in Quantum Electron.*, vol. 1, no. 2, Special Issue on semiconductor lasers, June 1995.
- T. Krauss, P. J. R. Laybourn and J. Roberts, "CW operation of semiconductor ring lasers", *Electron. Lett.*, vol. 26, pp. 2095-2097, Dec. 1990.
 - T. Krauss, P. J. R. Laybourn and R. M. De La Rue, "Directionally coupled semiconductor ring lasers", in *6th European Conference on Integrated Optics (ECIO)*, Neuchâtel, Switzerland, Apr. 1993, paper 7-6.
 - J. Kuhl, M. Serenyi and E. O. Göbel, "Bandwidth-limited picosecond pulse generation in an actively mode-locked GaAs laser with intracavity chirp compensation", *Optics Lett.*, vol. 12, pp. 334-336, May 1987
 - D. Kühlke, W. Rudolph and B. Wilhelmi, "Influence of transient absorber gratings on the pulse parameters of passively mode-locked cw dye lasers", *Appl. Phys. Lett.*, vol. 42, pp. 325-327, Feb. 1983
 - M. Kuznetsov, D. Z. Tsang, J. N. Walpole, A. L. Liao and E. P. Ippen, "Multistable mode locking of InGaAsP semiconductor lasers", *Appl. Phys. Lett.*, vol. 51, pp. 895-897, Sept. 1987.
 - R. J. Lang, A. Hardy, R. Parke, D. Mehuys, S. O'Brien, J. Major and D. Welch, "Numerical analysis of flared semiconductor laser amplifiers", *IEEE J. Quantum Electron.*, vol. 29, pp. 2044-2051, June 1993.
 - K. Y. Lau, "Narrow-band modulation of semiconductor lasers at millimeter wave frequencies (>100 GHz) by mode locking", *IEEE J. Quantum Electron.*, vol. 26, pp. 250-261, Feb. 1990
 - F. R. Laughton, J. H. Marsh, D. A. Barrow and E. L. Portnoi, "The two-photon absorption semiconductor waveguide autocorrelator", *IEEE J. Quantum Electron.*, vol. 30, pp. 838-845, Mar. 1994.
 - D. L. Lee, *Electromagnetic Principles of Integrated Optics*, Wiley, 1986.
 - C. F. Lin and C. L. Tang, "Colliding pulse mode locking of a semiconductor laser in an external ring cavity", *Appl. Phys. Lett.*, vol. 62, pp. 1053-1055, Mar. 1993
 - H. F. Liu, M. Fukazawa, Y. Kawai and T. Kamiya, "Gain-switched picosecond pulse (<10 ps) generation from 1.3 μm InGaAsP laser diodes", *IEEE J. Quantum Electron.*, vol. 25, pp. 1417-1425, June 1989.
 - W. A. Lopes, M. O. Morales, M. A. Rieffel, J. A. Giacoletti, J. T. Thorpe and L. A. Westling, "Intensity autocorrelation measurements of an AlGaAs diode laser", *Opt. Lett.*, vol. 18, pp. 820-822, May 1993.
 - J. K. Lucek and K. Smith, "All-optical signal regenerator", *Optics Lett.*, vol. 18, pp. 1226-1228, Aug. 1993.
 - A. Mar, R. Helkey, J. Bowers, D. Mehuys and D. Welch, "Mode-locked operation of a master oscillator power amplifier", *IEEE Photon. Technol. Lett.*, vol. 6, pp. 1067-1069, Sep. 1994.

- J. H. Marsh, S. I. Hansen, A. C. Bryce, R. M. De La Rue, "Applications of neutral impurity disordering in fabricating low-loss optical waveguides and integrated waveguide devices", *Optical and Quantum Electron.*, vol. 23, pp. S941-S957, 1991
- O. E. Martinez, R. L. Fork and J. P. Gordon, "Theory of passively mode-locked lasers including self-phase modulation and group-velocity dispersion", *Optics Lett.*, vol. 9, pp. 156-158, May 1984
- S. D. McDougall, Ph.D. thesis, University of Glasgow, in preparation.
- J. McInerney, L. Reekie and D. J. Bradley, "Bandwidth limited picosecond pulse generation by hybrid mode-locking in a ring cavity GaAlAs laser", *Electron. Lett.*, vol. 21, pp. 117-118, Jan. 1985.
- D. Mehuys, D. F. Welch and L. Goldberg, "2.0 W CW, diffraction-limited tapered amplifier with diode injection", *Electron. Lett.*, vol. 28, pp. 1944-1946, Oct. 1992.
- S. K. Murad, S. P. Beaumont and C. D. W. Wilkinson, "Selective and nonselective RIE of GaAs/AlGaAs in SiCl₄ plasma", *Microelectronic Eng.*, vol. 23, pp. 357-360, 1994.
- K. Naganuma, K. Mogi and H. Yamada, "General method for ultrashort light pulse chirp measurement", *IEEE J. Quantum Electron.*, vol. 25, pp. 1225-1233, June 1989
- R. Nagarajan, D. Tauber and J. E. Bowers, "High speed semiconductor lasers", *Intern. J. High Speed Electron. and Systems*, vol. 5, no. 1, pp. 1-44, 1994
- G. H. C. New, "The generation of ultrashort laser pulses", *Reports on Progress in Phys.*, vol. 46, pp. 877-971, 1983
- K. Nonaka, Y. Noguchi, H. Tsuda and T. Kurokawa, "Digital signal regeneration with side-injection-light-controlled bistable laser diode", in *14th IEEE International Semiconductor Laser Conference*, Maui, Hawaii, USA, Aug. 1994, paper Th2.4, pp. 229-230.
- K. Nonaka, H. Tsuda, H. Uenohara, H. Iwamura and T. Kurokawa, "Optical nonlinear characteristics of a side-injection light-controlled laser diode with a multiple-quantum-well saturable absorber region", *IEEE Photon. Technol. Lett.*, vol. 5, pp. 139-141, Feb. 1993.
- S. O'Brien, K. F. Welch, R. A. Parke, D. Mehuys, K. Dzurko, R. J. Lang, R. Waarts and D. Scifres, "Operating characteristics of a high-power monolithically integrated flared amplifier master oscillator power amplifier", *IEEE J. Quantum Electron.*, vol. 29, pp. 2052-2057, June 1993.
- H. Okamoto, "Semiconductor quantum well structure for optoelectronics - Recent advances and future prospects", *Jap. J. Appl. Phys.*, vol. 26, p. 315-330, Mar. 1987
- L. Olofsson and T. G. Brown, "On the linewidth enhancement factor in semiconductor lasers", *Appl. Phys. Lett.*, vol. 57, pp. 2773-2775, Dec. 1990
- M. Osinski and M. J. Adams, "Picosecond pulse analysis of gain-switched 1.55 μm InGaAsP lasers", *IEEE J. Quantum Electron.*, vol. 21, pp. 1929-1936, Dec. 1985.

- M. Osinski and J. Buus, "Linewidth broadening factor in semiconductor lasers - an overview", *IEEE J. Quantum Electron.*, vol. 23, pp. 9-29, Jan. 1987
- S. J. Pearton, "Dry Etching Techniques and Chemistries for III-V Semiconductors", *Mat. Res. Soc. Symp. Proc.*, vol. 216, pp. 277-290, 1991.
- K. Petermann, *Laser Diode Modulation and Noise*, Advances in Optoelectronics, Kluwer Academic Publishers, 1988, Chapters 7 and 8.
- K. Petermann and E. Weidel, "Semiconductor laser noise in an interferometer system", *IEEE J. Quantum Electron.*, vol. 17, pp. 1251-1256, July 1981.
- E. L. Portnoi and A. V. Chelnokov, "Characteristics of heterostructure lasers with a saturable absorber fabricated by deep ion implantation", *Sov. Tech. Phys. Lett.*, vol. 15, pp. 432-433, 1989
- E. L. Portnoi and A. V. Chelnokov, "Passive mode-locking in a short cavity diode laser", in *12th IEEE International Semiconductor Laser Conference*, Davos, Switzerland, 1990, pp. 140-141.
- E. L. Portnoi, V. B. Gorfinkel, D. A. Barrow, I. G. Thayne, E. A. Avrutin, J. H. Marsh, "Optoelectronic microwave-range frequency mixing in semiconductor lasers", *IEEE J. Selected Topics in Quantum Electron.*, vol. 1, no. 2, Special issue on semiconductor lasers, June 1995.
- K. L. Sala, G. A. Kenney-Wallace and G. E. Hall, "CW autocorrelation measurements of picosecond laser pulses", *IEEE J. Quantum Electron.*, vol. 16, pp. 990-996, Sept. 1980.
- R. A. Salvatore, T. Schrans and A. Yariv, "Pulse characteristics of passively mode-locked diode lasers", *Optics Lett.*, vol. 20, pp. 737-739, Apr. 1995
- S. Sanders, L. Eng, J. Paslaski and A. Yariv, "108 GHz passive mode locking of a multiple quantum well semiconductor laser with an intracavity absorber", *Appl. Phys. Lett.*, vol. 56, pp. 310-311, Jan. 1990
- S. Sanders, L. Eng, and A. Yariv, "Passive mode-locking of monolithic InGaAs/AlGaAs double quantum well lasers at 42 GHz repetition rate", *Electron. Lett.*, vol. 26, pp. 1087-1089, July 1990
- S. Sanders, T. Schrans, A. Yariv, J. Paslaski, J. E. Ungar and H. A. Zarem, "Timing jitter and pulse energy fluctuations in a passively mode-locked two-sections quantum-well laser coupled to an external cavity", *Appl. Phys. Lett.*, vol. 59, pp. 1275-1277, Sep. 1991
- S. Sanders, A. Yariv, J. Paslaski, J. E. Ungar and H. A. Zaren, "Passive mode locking of a two-section multiple quantum well laser at harmonics of the cavity round-trip frequency", *Appl. Phys. Lett.*, vol. 58, pp. 681-683, Feb. 1991.
- S. Schmitt-Rink, D. S. Chemla and D. A. B. Miller "Linear and nonlinear optical properties of semiconductor quantum wells" *Advances in Physics*, vol. 38, no. 2, pp. 89-188, 1989.

- T. Schrans, S. Sanders and A. Yariv, "Broad-band wavelength tunable picosecond pulses from CW passively mode-locked two-section multiple quantum-well lasers", *IEEE Photon. Technol. Lett.*, vol. 4, pp. 323-326, Apr. 1992
- A. J. Seeds, "Microwave optoelectronics", *Optical and Quantum Electron.*, vol. 25, pp. 219-229, 1993
- S. Shimada, K. Nakagawa, M. Saruwatari and T. Matsumoto, "Very-high-speed optical signal processing", *Proc. of the IEEE*, vol. 81, pp. 1633-1646, Nov. 1993.
- A. E. Siegman, *Lasers*, Oxford University Press, 1986.
- Y. Silberberg, P. W. Smith, D. J. Eilenberger, D. A. B. Miller, A. C. Gossard and W. Wiegmann, "Passive mode locking of a semiconductor diode laser", *Optics Lett.*, vol. 9, pp. 507-509, Nov. 1984
- K. Smith and J. K. Lucek, "All-optical clock recovery using a mode-locked laser", *Electron. Lett.*, vol. 28, pp. 1814-1816, Sept. 1992.
- P. W. Smith, Y. Silberberg and D. A. B. Miller, "Mode locking of semiconductor diode lasers using saturable excitonic nonlinearities", *J. Opt. Soc. Am. B*, vol. 2, pp. 1228-1236, July 1985
- M. S. Stix and E. P. Ippen, "Pulse shaping in passively mode-locked ring dye lasers", *IEEE J. Quantum Electron.*, vol. 19, pp. 520-525, Apr. 1983
- S. M. Sze, *Semiconductor Devices: Physics and Technology*, Wiley, 1985.
- G. H. B. Thompson, *Physics of Semiconductor Laser Devices*, Wiley, 1980.
- M. R. S. Taylor, *Fwave III: A vector E-M wave solver*, unpublished, 1993.
- W. T. Tsang, "Quantum Confinement Heterostructure Semiconductor Lasers", *Semiconductors and Semimetals*, vol. 24, Editor Raymond Dingle, Academic Press, 1987, Chapter 7.
- H. Tsuda, K. Nonaka, K. Hirabayashi, H. Uenohara, H. Iwamura and T. Kurokawa, "Wide range wavelength conversion experiments using a side-injection light-controlled bistable laser diode", *Appl. Phys. Lett.*, vol. 63, pp. 3116-3118, Dec. 1993.
- R. S. Tucker, U. Koren, G. Raybon, C. A. Burrus, B. I. Miller, T. L. Koch and G. Eisenstein, "40 GHz active mode-locking in a 1.5 μm monolithic extended-cavity laser", *Electron. Lett.*, vol. 25, pp. 621-622, May 1989
- A. V. Uskov, J. R. Karin, R. Nagarajan, J. E. Bowers and J. Mørk, "Ultrafast dynamics in waveguide saturable absorbers", in *14th IEEE International Semiconductor Laser Conference*, Maui, Hawaii, USA, Sep. 1994, paper P18, pp. 117-118
- J. A. Valdmanis and B. Mourou, "Subpicosecond electrooptic sampling: principles and applications", *IEEE J. Quantum Electron.*, vol. 22, pp. 69-78, Jan. 1986.
- J. P. Van der Ziel, W. T. Tsang, R. A. Logan, R. M. Mikulyak and W. M. Augustyniak, "Subpicosecond pulses from passively mode-locked GaAs buried optical guide semiconductor lasers", *Appl. Phys. Lett.*, vol. 39, pp. 525-527, Oct. 1981

- P. P. Vasil'ev, "Ultrashort pulse generation in diode lasers", *Optical and Quantum Electron.*, vol. 24, pp. 801-824, 1992.
- P. P. Vasil'ev, *Ultrafast Diode Lasers: Fundamentals and Applications*, Artech House Publishers, 1995.
- P. P. Vasil'ev, "Picosecond injection laser: A new technique for ultrafast Q-switching", *IEEE J. Quantum Electron.*, vol. 12, pp. 2386-2391, Dec. 1988.
- P. P. Vasil'ev, V. N. Morozov, Y. M. Popov and A. B. Sergeev, "Subpicosecond pulse generation by a tandem-type AlGaAs DH laser with colliding pulse mode locking", *IEEE J. Quantum Electron.*, vol. 22, pp. 149-151, Jan. 1986
- P. P. Vasil'ev and A. B. Sergeev, "Generation of bandwidth-limited 2 ps pulses with 100 GHz repetition rate from multisegment injection laser", *Electron. Lett.*, vol. 25, pp. 1049-1050, Aug. 1989
- A. G. Waber, M. Schell, G. Fischbeck and D. Bimberg, "Generation of single femtosecond pulses by hybrid mode locking of a semiconductor laser", *IEEE J. Quantum Electron.*, vol. 28, pp. 2220-2229, Oct. 1992.
- C. Weisbuch and B. Vinter, *Quantum semiconductor structures: fundamentals and applications*, Academic Press, 1991.
- D. Welch, "New dawn beckons for semiconductor lasers", *Physics World*, pp. 35-38, Feb. 1994.
- D. F. Welch, "Progress in high power semiconductor lasers", in *14th IEEE International Semiconductor Laser Conference*, Maui, Hawaii, USA, Sep. 1994, paper M1.1, pp. 3-5.
- K. A. Williams, J. Sarma, I. H. White, R. V. Penty, I. Middlemast, T. Ryan, F. R. Laughton and J. S. Roberts, "Q-switched bow-tie lasers for high energy picosecond pulse generation", *Electron. Lett.*, vol. 30, pp. 320-321, Feb. 1994.
- K. A. Williams, I. H. White, F. R. Laughton, J. Sarma, R. V. Penty, I. Middlemast, T. Ryan and J. S. Roberts, "Passive mode-locking of bow-tie lasers", in *CLEO/Europe*, Amsterdam, The Netherlands, Aug. 1994, paper CTuL2, pp. 158.
- S. Wolfram, *Mathematica: A System for Doing Mathematics by Computer*, Second Ed., Addison-Wesley, 1991.
- M. C. Wu, Y. K. Chen, T. Tanbun-Ek, R. A. Logan, M. A. Chin and G. Raybon, "Transform-limited 1.4 ps optical pulses from a monolithic colliding-pulse mode-locked quantum well laser", *Appl. Phys. Lett.*, vol. 57, pp. 759-761, Aug. 1990.
- A. Yariv, *Quantum Electronics*, 3rd edition, Wiley, 1989
- H. Yokoyama, H. Ito, and H. Inaba, "Generation of subpicosecond coherent optical pulses by passive mode locking of an AlGaAs diode laser", *Appl. Phys. Lett.*, vol. 40, pp. 105-107, Jan. 1982

- J. H. Zarrabi, E. L. Portnoi and A. V. Chelnokov, "Passive mode locking of a multistriple single quantum well GaAs laser diode with an intracavity saturable absorber", *Appl. Phys. Lett.*, vol. 59, pp. 1526-1528, Sep. 1991
- L. M. Zhang and J. E. Carroll, "Dynamic response of colliding-pulse mode-locked quantum-well lasers", *IEEE J. Quantum Electron.*, vol. 31, pp. 240-243, Feb. 1995
- P. S. Zory, Jr. (Editor), *Quantum Well Lasers*, Quantum Electronics: Principles and Applications Series, Academic Press, 1993.